POLITECNICO DI MILANO

Facoltà di Ingegneria Industriale

Corso di Laurea in

Ingegneria Energetica

INTEGRATION OF PRE-COMBUSTION CHEMICAL LOOPING PROCESS WITH IGCC PLANT FOR NEAR-ZERO CO_2 EMISSION

Relatore: Prof. Matteo Carmelo ROMANO

Co-relatore: Ing. Vincenzo SPALLINA

Tesi di Laurea di:

Fabio Curzio ARIENTI Matr. 800665

Anno Accademico 2013 - 2014

Ringraziamenti

Un primo ringraziamento va ai miei genitori, che mi hanno sempre incoraggiato e sostenuto economicamente in questo importante percorso della mia vita.

Un ringraziamento particolare va all' Ingegner Vincenzo Spallina, per l'importante opportunità da lui concessami nello svolgere il lavoro di tesi presso l'università tecnica di Eindhoven e per il supporto e i consigli che mi ha sempre dato.
Un grande ringraziamento va al Prof. Matteo Carmelo Romano per i suggerimenti e l'appoggio nell'elaborazione finale del lavoro di tesi.

Gli ultimi importantissimi ringraziamenti vanno ad una persona speciale (Giulia), a tutti gli amici di una vita (Compa, Gremis, Eddi, Lallo, Lietta, King, Nadia, Paglia, Stumpio, Tanita, Teo e la Vale, V33, il Corsaro), ai gumbagni e ai compagni di università (Marcellino, Frankone, Samu, Enzolotti, Marchino, Marco, Pietrone, Ale, Spi) e alle tante altre persone incrociate in questo periodo della mia vita (Beppe, la uida, Simo, Moretti, Germano, Ire, Lugaresi, Truce etc. etc.).

Summary

Most of the global energy demand, grown significantly in the recent past and foreseen to grow even more in the next decades, is satisfied by burning fossil fuels, whose combustion produces huge quantities of CO_2 emitted to the atmosphere.
Since the emission of CO_2 constitutes the major anthropogenic contribute to the increase of the greenhouse effect, which is commonly associated to global warming, there is a growing belief that the limitation of CO_2 emission is a vital challenge for the present century.
Emissions of CO_2 are mainly due to the combustion of fossil fuels, especially in large electric energy production plants. On a long term, the progressive substitution of power plants based on fossil fuels with renewable energies (wind, solar, hydro) is considered to be the most effective solution for emission reduction. On short to middle term, when fossil fuels are foreseen to remain our primary energy source, it is well accepted that Carbon Capture and Sequestration (CCS) can be an important measure.
Three different schemes of CO_2 capture are under development to produce energy from fossil fuels and obtain a separate stream of high purity CO_2 ready for storage: post-combustion, pre-combustion and oxy-combustion. For all of these schemes additional separation facilities are needed, leading to a significant efficiency penalty, with respect to the plant without CO_2 capture.

Among the different CO_2 capture solutions, a promising novel technology is the Chemical Looping (CL), where power production and CO_2 capture are intrinsically combined by the use of an intermediate oxygen carrier (metal oxides) that can alternatively be oxidized and reduced to enable the production of pure CO_2 undiluted with nitrogen.

The present work is centered on a specific type of Chemical Looping, the PeCLET process, which is integrated with a coal gasification-based power plant (IGCC), in order to capture CO_2 with limited energy penalty. PeCLET is the acronym of Pre-combustion & Chemical Looping Efficient Technology. The CL reaction process is accomplished in dynamically operated Packed Bed Reactors (PBRs). The metal oxide used in the reactors as Oxygen Carrier (OC) is alternatively oxidized by a stream of air and steam, to produce a H_2-rich and carbon free fuel diluted with Nitrogen and steam (fed to the gas turbine), and reduced by a syngas stream (fuel) to produce a pure CO_2 undiluted with nitrogen.
The main scope of the present work is to study the integration of the CL PeCLET process with an IGCC plant (IG-PCCL), to individuate the most important operating parameters and analyze their influence on the system, as well as to propose layout schemes of the entire plant.
Another important purpose is to evaluate the number of reactors needed in the process and their cycle of operation for different PeCLET process schemes.

The thesis is divided in seven chapters, whose contents are listed as follows:

1. A discussion on greenhouse gas effect on global warming and a description of the CO_2 capture schemes applied to power plants presently under development (post-combustion, pre-combustion, oxy-combustion).
2. An analysis of the Chemical Looping Combustion technology and its integration with the power plant, as well as a review of the characteristics of the applicable Oxygen Carriers..
3. A study of the Chemical Looping island of the PeCLET process as a function of different parameters, from which the Air-to-Steam ratio in the inlet stream to the oxidation reactor has come out as the most important parameter.
4. A study of the integration of the PeCLET Chemical Looping island with the Combined Cycle of an IGCC. Two possible plant schemes have been designed and analyzed: the "Base case plant" and the "HR plant". The Base case plant comes out to be the preferable plant choice at low air-to-steam ratio. At high air-to-steam ratio the alternative plant configuration (Heat Removal plant), has been proved as the only advisable choice..
   Both plant schemes are simulated by varying several parameters, in particular the air-to-steam ratio in the oxidation feed, the CL unit operating pressure and the gas turbine compressor ratio. The Combined Cycle is optimized in terms of efficiency.
5. A review of the characteristics of the iron based Oxygen Carriers applicable to the PeCLET scheme, analyzing the stoichiometry and the thermodynamics of the CL reactions. Furthermore, by using a 0D model of the reactors, the active fraction of the solid material (OC) is calculated in relation to the maximum temperature achieved in the packed beds.
6. Calculation of the overall volume and number of reactors necessary to accomplish the steps of the PeCLET cycle in both the Base case and HR case. A sequence of steps is also proposed for the management of the reactors work cycle.
7. Conclusions are drawn, comparing the two CL schemes (Base case and HR case) associated to the relevant OC. Both cases are then compared with the alternative CLC scheme (see item 2 above). The possible alternative of using the PeCLET scheme with natural gas as fuel is also presented.

The simulations of the CL island and the power plant schemes (in Chapter 1 and Chapter 4 of this work) have been carried out by the proprietary computer code GS (Gecos, 2013) developed by the GECOS group at the Department of Energy of Politecnico di Milano. The calculation code is designed according to a modular structure, allowing to calculate complex plant configurations.
The two proposed power plant schemes are based on different reactors work cycle strategies.
The Base case plant is based on a simple integration of the PeCLET process in the power plant. The reactor work cycle strategy includes oxidation by air and steam in order to produce a hydrogen flow fed finally to the GT, and the reduction of the syngas to produce CO_2 and H_2O.

The HR plant is operated with a different reactor work cycle, which includes an additional phase of heat recovery from the packed beds: the heat released in the CL unit by the oxidation reaction is used for pre-heating a stream of air exiting the GT compressor.
Both the schemes are conceived to achieve a full integration of the steam cycle between the Chemical Looping and the combined cycle to maximize the overall electrical efficiency.
During the simulations of the IG-PCCL the primary coal feed and the syngas produced by its gasification were kept constant in flow rate and composition. The size of turbo-machines is comparable with that of a conventional IGCC cycle: the simulated IG-PCCL produces a net electric power of 350 MWe with a coal thermal input equal to 860 MWth, which results in a net electrical efficiency slightly higher than 40%.

The most important operating parameter has come out to be the air-to-steam ratio in the feed of the CL oxidation reactor: when the CL unit is operated at a high air-to-steam ratio, the exothermicity of the PeCLET process is increased. The LHV of the inlet syngas is then allocated more on sensible heat (temperature of the outlet streams) than on hydrogen production.
The main characteristic of the air-to-steam ratio is therefore to establish the amounts of energy entering the CL unit that are converted into hydrogen production and sensible heat.
The thermodynamic analysis on the two power plant schemes has assessed that, at high air-to-steam ratio (when the hydrogen production is maximized with respect to the heat production) the HR plant is the only advisable choice, because, with the addition of the heat removal phase the heat released in the CL unit can be directly recovered in the GT and efficiency is optimized.
Instead, at low air-to-steam ratio, both the power plant configurations are feasible and with comparable net electrical efficiency. The net electrical efficiency achieved by the Base case plant and the HR plant was respectively 40.8% and 41.5%, very promising values compared with the alternative, the CLC.

Nevertheless, the integration scheme of the Base case plant is simpler and a lower number of reactors is needed, with a significant saving in the investment cost.
Hence, from the analysis the Base case plant emerged as the preferable choice for low air-to-steam ratio; its advantages are here below summarized:

- More simple plant integration: conceptually the PeCLET process can be inserted as it is in the IGCC plant.
- The connection between the CL reactors and the GT is less strict (no large flow rate of air GT compressed air is fed to the reactor and then back to the turbine). As example, the operating pressure of the CL unit and of the GT can be separately optimized. Significant decrease in the number of reactors needed in the process. This leads to a considerable potential reduction of the plant costs.

- The reduction reaction of the PeCLET process can be more easily carried out at high temperature, with the resulting advantage in the reaction kinetics.

Moreover, the air-to-steam ratio is substantially set by the choice of the Oxygen Carrier (OC) through the stoichiometry and the thermodynamics of the reactions involving the OC. The OC is therefore a key parameter not only for the feasibility of the CL reaction system, but also for the feasibility and the design of the entire power plant.
Due to the similarities of the PeCLET oxidation reactor with the steam-iron process, Fe-based OCs are considered as promising material. Two possible reductive states of iron were chosen in this work as starting metal oxide for the oxidation reactor: the Base case plant is operated with Fe, while the HR plant with FeO.

In conclusion, the coupling between Fe and the Base case plant has emerged as the better choice for the IG-PCCL plant, combining high efficiency and potentially limited investment cost.
Nevertheless all the configurations proposed in this work should be considered, since further deeper studies (not included in this work) on the reaction kinetics and on a 1D model of the reactors are needed, for a complete feasibility assessment of the system
Moreover, this work suggests that the OC research direction should be addressed towards the material which can guarantee a low air-to-steam ratio. In this way, a simpler and less expensive PeCLET process integration scheme would be obtained.

Riassunto esteso

La maggior parte della domanda globale di energia, cresciuta significativamente nel recente passato e che si prevede ancora più in aumento nelle prossime decadi, è soddisfatta attraverso l'utilizzo di combustibile fossile, la cui combustione produce ingenti quantità di anidride carbonica emessa nell'atmosfera.
Poichè le emissioni di anidride carbonica costituiscono il maggiore contributo antropogenico all'incremento dell'effetto serra, che è comunemente associato al riscaldamento globale, si consolida la convinzione che la limitazione all'emissione di anidride carbonica rappresenti una sfida vitale per il secolo in corso.
Le emissioni di anidride carbonica sono principalmente dovute all'utilizzo di combustibile fossile soprattutto nei grandi impianti di produzione di energia elettrica. A lungo termine la progressiva sostituzione di impianti power basati su combustibile fossile con impianti ad energia rinnovabile (eolico, solare, idroelettrico) è considerata la soluzione più efficace per la riduzione delle emissioni. A breve e medio termine, prevedendo che i combustibili fossili rimangano la nostra fonte di energia primaria, è comunemente riconosciuto che la cattura e lo stoccaggio dell'anidride carbonica (CCS) possa essere una misura importante.
Tre diversi schemi di cattura dell'anidride carbonica sono in via di sviluppo per produrre energia da combustibili fossili e separare una corrente di anidride carbonica pura pronta per lo stoccagggio: pre-combustione, post-combustione e oxy-combustione. Per questi schemi sono necessari sistemi di separazione addizionali che causano una significativa penalizzazione in efficienza rispetto agli impianti senza cattura.

Fra le diverse soluzioni per la cattura dell'anidride carbonica, una nuova e promettente tecnologia è il Chemical Looping (CL), nella quale la produzione di energia e la cattura dell'anidride carbonica sono intrinsecamente combinate mediante l'uso di un vettore di ossigeno intermedio (ossidi metallici) che può alternativamente essere ossidato e ridotto, in tal modo permettendo la produzione di anidride carbonica pura e priva di azoto.
La presente tesi è incentrata su una specifica tipologia di Chemical Looping (CL), il processo PeCLET, che viene integrato con un impianto power basato sulla gassificazione del carbone (IGCC) per catturare l'anidride carbonica con una ridotta penalizzazione energetica.
PeCLET è l'acronimo di Pre-combustion & Chemical Looping Efficient Technology. Il processo di reazione del CL è realizzato in Packed Bed Reactors (PBRs). L'ossido metallico usato nei reattori come vettore dell'ossigeno (OC) è alternativamente ossidato da una corrente di aria e vapore, per produrre un combustibile ricco di idrogeno e privo di carbonio, diluito con azoto e vapore e alimentato alla turbina a gas, e ridotto da una corrente di syngas per produrre anidride carbonica pura e priva di azoto.
Lo scopo principale di questa tesi è lo studio dell'integrazione del processo CL PeCLET con l'impianto IGCC (IG-PCCL), per individuare i parametri operativi più importanti ed

analizzarne l'influenza sul processo, così come per proporre diversi schemi dell'intero impianto.
Un altro importante scopo è la valutazione del numero dei reattori necessari e i loro cicli operativi per diversi schemi del processo PeCLET.
La tesi è divisa in sette capitoli di cui si elencano gli argomenti:

8. Discussione dell'effetto serra sul riscaldamento globale e descrizione degli schemi di cattura dell'anidride carbonica applicati ad impianti power ed al momento in via di sviluppo (post-combustione, pre-combustione e oxy-combustione).
9. Analisi della tecnologia Chemical Looping Combustion e sua integrazione con impianto power, oltre alla valutazione delle caratteristiche dei vettori di ossigeno applicabili.
10. Studio del Chemical Looping del processo PeCLET in funzione dei vari parametri, fra i quali il rapporto aria/vapore nella corrente entrante nel reattore di ossidazione è emerso come il più importante.
11. Studio dell'integrazione del Chemical Looping del processo PeCLET con il ciclo combinato del IGCC. Due schemi possibili sono stati concepiti ed analizzati.
    Il "Base case plant" e il "Heat Removal plant" ("HR plant"). Il primo è risultato preferibile per valori bassi del rapporto aria/vapore. Per valori alti di questo rapporto la configurazione alternativa (HR plant) è risultata l'unica soluzione raccomandata.
    Entrambi gli schemi vengono simulati variando diversi parametri, in particolare il rapporto aria/vapore nell'alimentazione al reattore di ossidazione, la pressione operativa del CL e il rapporto di compressione della turbina a gas. Il ciclo viene inoltre ottimizzato in termini di efficienza.
12. Studio delle caratteristiche del vettore di ossigeno a base ferro, applicabile allo schema PeCLET, analizzando la stechiometria e la termodinamica delle reazioni del CL. Inoltre, usando un modello 0D dei reattori, la frazione attiva del materiale solido del vettore di ossigeno viene calcolato in relazione alla massima temperatura raggiunta nei Packed Beds.
13. Calcolo del volume complessivo e del numero dei reattori necessari per realizzare le varie fasi del ciclo PeCLET per il Base case e per l'HR case. Viene inoltre proposta una sequenza di fasi per la gestione del ciclo operativo dei reattori.
14. Vengono presentate le conclusioni, paragonando i due schemi del CL (Base case e HR case) associati ai relativi vettori di ossigeno. Entrambi gli schemi sono quindi comparati con lo schema alternativo CLC (Chemical Looping Combustion, vedi punto 2).

Le simulazioni degli schemi del CL e dell'impianto power sono stati eseguiti attraverso il codice di calcolo GS (proprietario, Gecos 2013) sviluppato dal Gruppo Gecos nel

Dipartimento di Energia del Politecnico di Milano. Il codice di calcolo è basato su una struttura modulare che permette la simulazione di configurazioni di impianti complessi.

I due schemi proposti per l'impianto power sono basati su diverse strategie del ciclo operativo dei reattori. L'impianto Base case è basato sulla semplice integrazione del processo PeCLET nell'impianto power. La strategia del ciclo operativo del reattore prevede l'ossidazione con aria/vapore per produrre un flusso di idrogeno alimentato alla turbina a gas e la riduzione del syngas per produrrre anidride carbonica e vapore.
L'impianto HR è operato con un diverso ciclo operativo dei reattori che include una fase aggiuntiva per il recupero del calore dai Packed Beds: il calore rilasciato nel CL grazie alla reazione di ossidazione, è usato per pre-riscaldare una corrente di aria prelevata dal compressore della turbina a gas.
Entrambi gli schemi sono concepiti per ottenere la completa integrazione del ciclo vapore fra il Chemical Looping e il ciclo combinato, in modo da massimizzare l'efficienza elettrica complessiva.
Durante le simulazioni del IG-PCCL l'alimentazione primaria del carbone e il syngas prodotto nella gassificazione sono stati mantenuti costanti come flusso e composizione. La dimensione della turbina a gas è comparabile con quella di un ciclo IGCC convenzionale: l'impianto IG-PCCL produce una potenza elettrica netta di 350 MWe con una potenza termica del carbone pari a 860 MWth, che corrispondono ad una efficienza elettrica netta leggermente superiore al 40%.
Il parametro operativo più importante è risultato il rapporto aria/vapore nell'alimentazione al reattore di ossidazione: quando il CL è operato a valori elevati di questo rapporto, l'esotermicità del processo PeCLET è particolarmente alta. Il potere calorifico del syngas in ingresso viene quindi maggiromente allocato come calore sensibile (temperatura delle correnti in uscita) rispetto alla produzione di idrogeno.
La principale caratteristica del rapporto aria/vapore è quindi di determinare le quantità di energia che nel CL vengono convertite in produzione di idrogeno ed in calore sensibile.
Il risultato dell'analisi termodinamica è che, per valori elevati del rapporto aria/vapore l'impianto HR è l'unica soluzione raccomandabile perchè in questo schema il calore rilasciato nel CL può essere direttamente recuperato e l'efficienza della turbina a gas ottimizzata.
Per valori bassi del rapporto aria/vapore, invece, entrambe le configurazioni sono fattibili ed hanno efficienze elettriche nette comparabili: 40.8% per l'impianto Base case e 41.5% per l'impianto HR, entrambi valori promettenti rispetto alla alternativa con il CLC.

Comunque, lo schema di integrazione dell'impianto Base case è più semplice e richiede un numero inferiore di reattori, con un significativo risparmio sul costo di investimento. Dall'analisi emerge quindi che l'impianto Base case è preferibile per valori bassi del rapporto aria/vapore. I suoi vantaggi sono di seguito elencati:

- Integrazione di impianto più semplice: concettualmente il processo PeCLET può essere inserito tal quale nell'impianto IGCC.
- La connessione fra i reattori del CL e la turbina a gas è meno vincolante in quanto non è prevista l'alimentazione al reattore dell'aria compressa proveniente dalla turbina a gas, nè il suo ritorno dal reattore alla turbina a gas.
- Riduzione significativa del numero di reattori necessari nel processo rispetto all'impianto HR, che implica la potenziale notevole riduzione dei costi dell'impianto.
- La reazione di riduzione può avvenire più facilmente ad alta temperatura con conseguente vantaggio nella cinetica di reazione.

Inoltre il rapporto aria/vapore è sostanzialmente definito dalla scelta del vettore di ossigeno (OC) attraverso la stechiometria e la termodinamica delle reazioni che lo interessano. Il vettore di ossigeno è quindi il parametro chiave, non solo per la fattibilità delle reazioni del CL, ma anche per la fattibilità e la progettazione dell'intero impianto power.

In base alla similitudine del reattore di ossidazione PeCLET con i processi vapore-ferro, i vettori di ossigeno a base ferro sono considerati materiali promettenti. Due possibili stati di riduzione del ferro vengono scelti in questa tesi come ossidi metallici di partenza per il reattore di ossidazione: l'impianto Base case è operato con Fe, mentre l'impianto HR è operato con FeO.

In conclusione, la combinazione dell'impianto Base case con il vettore di ossigeno Fe è emersa come la migliore soluzione per l'impianto IG-PCCL, in grado di combinare alta efficienza e costo di investimento potenzialmente limitato.
Si evidenzia comunque che tutte le configurazioni proposte in questa tesi potrebbe essere ancora prese in considerazione, poichè ulteriori ed approfonditi studi (non facenti parte di questa tesi) sulla cinetica di reazione e su un modello 1D, sono necessari per una completa verifica della fattibilità del sistema.
Inoltre questa tesi suggerisce che sarebbe necessario indirizzare la ricerca sui vettori di ossigeno verso materiali che possano garantire un valore basso del rapporto aria/vapore. In questo modo si otterrebbe uno schema di integrazione del processo PeCLET più semplice e meno costoso.

Index

Abstract

The present work addresses the thermodynamic analysis of a coal gasification-based power plant (IGCC), integrated with the PeCLET process, a novel Chemical Looping (CL) technology applied to capture CO_2 with limited energy penalty. In this process, power production and CO_2.capture are intrinsically combined by the use of an intermediate oxygen carrier (metal oxide) that can alternatively be oxidized and reduced to enable the separate production of hydrogen rich gas and pure CO_2.undiluted with nitrogen.
The CL reaction process is accomplished in dynamically operated Packed Bed Reactors (PBRs). Iron oxides have been chosen as oxygen carrier.
The present work investigates two power plant schemes based on different reactors work cycle strategies. The schemes are conceived to achieve a full integration of the steam cycle with the Chemical Looping to maximize the overall electrical efficiency.
The performances of the plant are presented and compared with reference technologies. The calculated net electrical efficiency is around 41%, with a CO_2 capture efficiency of 97%.
A sensitivity analysis on the CL unit pressure, gas turbine compression ratio and air-to-steam ratio of the oxidation reactor feed, are carried out.
Moreover, for both PeCLET schemes the number of reactors is calculated and their cycle of operation defined.

Keywords: Chemical looping, PeCLET, CO_2 capture, IGCC

Introduction

Since the emission of CO_2 constitutes the major anthropogenic contribute to the increase greenhouse effect, which is commonly associated to global warming, there is a growing interest in limiting the CO_2 emission from the power plants based on the combustion of fossil fuels.

On a long term, the progressive substitution of power plants based on fossil fuels with renewables (wind, solar, hydro) and nuclear plants, is considered the most effective solution for emission reduction. On short to middle term period, when fossil fuels are foreseen to remain our primary energy source, it is well accepted that Carbon Capture and Sequestration (CCS) can be an important measure.

Among the different CO_2 capture solutions, a promising novel technology is the Chemical Looping (CL), where power production and CO_2 capture are intrinsically combined by the use of an intermediate oxygen carrier (metal oxides) that can alternatively be oxidized and reduced to enable the production of pure CO_2 undiluted with nitrogen.

The present work is centered on a specific type of Chemical Looping, the PeCLET process, which is integrated with a coal gasification-based power plant (IGCC) to capture CO_2 with limited energy penalty. PeCLET is the acronym of Pre-combustion & Chemical Looping Efficient Technology. The CL reaction process is accomplished in dynamically operated Packed Bed Reactors (PBRs). The metal oxide used in the reactors as Oxygen Carrier (OC) is alternatively oxidized by a stream of air and steam, to produce a H_2-rich and carbon free fuel diluted with Nitrogen and steam (fed to the gas turbine), and reduced by a syngas stream (fuel) to produce a pure CO_2 undiluted with nitrogen.
The main scope of the present work is to address the thermodynamic analysis of the integrated power plant. Two power plant schemes based on different reactors work cycle strategies are investigated. The schemes are conceived to achieve a full integration of the steam cycle between the Chemical Looping and the combined cycle to maximize the overall electrical efficiency.
Another important scope is to evaluate the number of reactors and their cycle of operation for both PeCLET schemes.

The thesis is divided in seven chapters, each containing the following topics:

1. A discussion on greenhouse gas effect on global warming and a description of the CO_2 capture schemes applied to power plants and presently under development (post-combustion, pre-combustion, oxy-combustion)
2. An analysis of the Chemical Looping Combustion technology and its integration with the power plant, as well as a review of the characteristics of the applicable Oxygen Carriers

3. A study of the Chemical Looping island of the PeCLET process as a function of different parameters, from which the Air to Steam ratio in the inlet stream to the oxidation reactor has come out as the most important parameter
4. A study of the integration of the PeCLET Chemical Looping island with the Combined Cycle of the IGCC. A Base case of the plant scheme is simulated, varying several parameters, in particular the steam to air ratio in the feed to the oxidation reactor. The Base case plant comes out to be more efficient at low air to steam ratio in the feed to the oxidation reactor. At high air to steam ratio it is proposed an alternative plant configuration, the Heat Removal (HR) plant, including an additional phase of heat recovery from the reactors to heat up a stream of air extracted from the gas turbine. For both the plant schemes a sensitivity analysis of the CL unit pressure, gas turbine compression ratio and air-to-steam ratio in the oxidation reaction feed is carried out
5. A review of the characteristics of the iron based Oxygen Carriers applicable to the PeCLET scheme, analyzing the stoichiometry and the thermodynamics of the CL reactions
6. A calculation of the overall reaction volume and number of reactors necessary to accomplish the steps of the PeCLET cycle in both the Base case and HR case. It is also proposed a sequence of steps for the reactors operation cycle. Furthermore, by using the 0D model of the reactors, the active fraction of the solid material (OC) is calculated.
7. Conclusions are drawn, comparing the two plant schemes (Base case and HR case) associated to the relevant OC. Both cases are compared with the CLC scheme (see point 2 above). In the conclusions it is also presented the possible alternative of using the PeCLET scheme with natural gas as fuel.

Chapter 1

CO_2 Capture

1.1 CO_2 Emission and Global Warming

There are strong indications that the human actions are affecting the climate of the Earth. This effect has been studied by the International Panel of Climate Change (IPCC).
In a comprehensive scientific framework they have summarized the evolution of the climate over very long time-scales and the observed deviations in more recent times. They have also interpreted both natural and man-made causes and their consequence on the greenhouse effect.
They have firstly concluded that "Warming of the climate system is unequivocal, as it is now evident for observations of increases in global average air and ocean temperature, wide-spread melting of snow and ice and rising global average sea level".
Furthermore, according to IPCC (Fourth Assessment Report), climate changes are likely to be the effect of human activities of changes (they mean more than 90% probability) and have prevailed on natural variations in especially the last 50 years. In this period the concentration of greenhouse gases has substantially increased (mainly carbon dioxide, methane, nitrous oxide and halocarbons) and now by far exceeds natural ranges encountered in the past.
Without significant changes in the energy policies, it is envisaged that the global emissions of anthropogenic greenhouse gases will continue to strongly increase , which may result in 2100 in a global average temperature rise ranging from 1.8 to 4°C (IPCC 2007b), with potential impacts, including sea level rise, more extreme weather conditions and the extension of species.
For this reason there is a common thought that stringent measures shall be taken to mitigate climate change by reducing the anthropogenic emissions of greenhouse gases.
Among the various greenhouse gases, the most significant contribute to the increased greenhouse effect is due to carbon dioxide.
Emissions of CO_2 are mainly due to the combustion of fossil fuels, especially in large energy production plants.
Therefore, on the short term, the saving in energy production and energy consumption may lead to significant reductions of CO_2 emissions.
On a long term, the progressive substitution of power plants based on fossil fuels with renewable energies (wind, solar, hydro) is considered the most effective solution.
Yet the transition is expected to be a long process and the use of fossil fuels to remain predominant for several decades, especially in relation to the bad public image of nuclear plants and the very long time needed for the development of fusion technology.
Thus, for the time being, the use of fossil fuels remains important. In this situation, it is nowadays well accepted that Carbon Capture and Sequestration (CCS) is the most

promising short/medium term technology and a feasible solution for the reduction of anthropogenic CO_2 emissions.

1.2 CO_2 Capture

Three different schemes are proposed to produce energy from fossil fuels and obtain a separate stream of high purity CO2:

- Post-combustion capture: the carbon dioxide is removed after the combustion of the primary fuel in air.
- Pre-combustion: the carbon contained in the fuel is separated as carbon dioxide before the combustion, via chemical reactions and carbon dioxide absorption.
- Oxy-combustion: the fuel is burnt with oxygen instead of air, so that the flue gas is composed of steam and carbon dioxide only and the carbon dioxide is easily separated through the condensation of the steam.

For all of these schemes additional separation facilities are needed, leading to a significant energy penalty with respect to the plant without CO_2 capture. The three schemes are described in the following sections.

1.2.1 CO_2 capture post-combustion scheme

The scheme is represented in the following Figure 1.1:

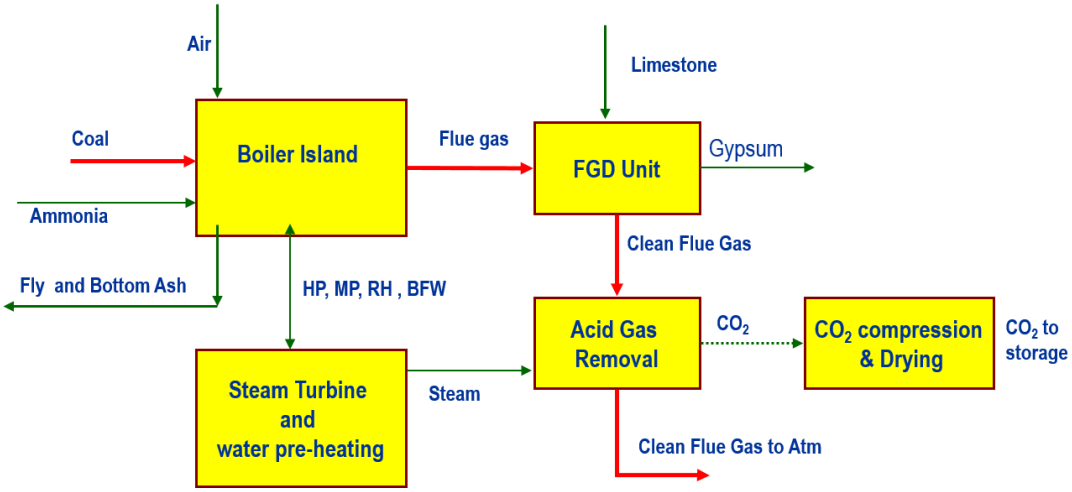

Figure 1.1: Scheme of a USC plant fed by coal with post combustion CO_2 capture.

This scheme envisaged the absorption of the CO_2 from the flue gas produced by the combustion of the fossil fuel. Due to the low pressure of the flue gas and the modest concentration of the CO_2 in the flue gas, it is preferable to apply a chemical absorption using an amine. The principle of this technology is to make carbon dioxide react with an alkaloammine (e.g. monoethanolamine (MEA)) in an absorption column.

The absorption liquid is regenerated in a stripper at the maximum temperature allowed by the stability of the amine (to favor desorption of the CO_2 from the amine).
The most important challenges of this process are the huge regeneration energy input and the sensitivity of the absorption liquid for oxygen and water present in the flue gas.
The stream exiting regenerator top is a CO_2 rich stream from which water is separated for condensation. CO_2 stream can be further dehydrated, if necessary, and compressed.
Other interesting technologies to capture carbon dioxide from the flue gas are based on absorption by an ammonia solution, or solid solvents, or cryogenic separation and membrane processes.
For the short term, post combustion seems an interesting option for CO_2 capture. A lot of research and development is in progress on several technologies, to reduce the energy consumption and improve the solvent stability, or reduce the membrane costs.

1.2.2 CO_2 capture pre-combustion scheme

The scheme is represented in the following Figure 1.2:

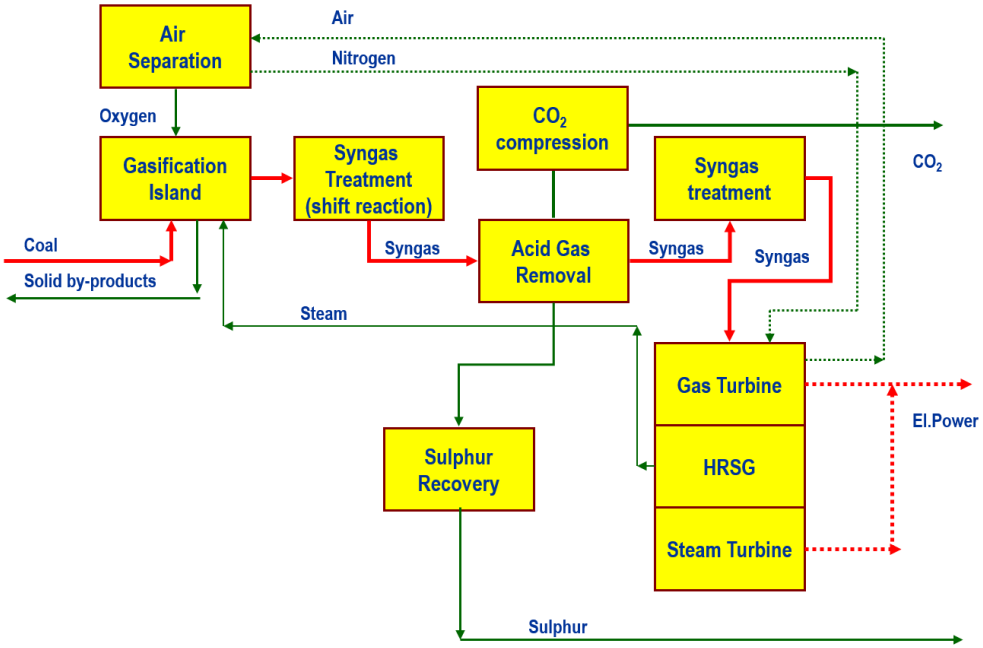

Figure 1.2: Scheme of the IGCC plant fed by coal with pre-combustion CO_2 capture.

The concept of this scheme is to transfer the heating value of the original fossil fuel to a syngas rich of hydrogen, so that the downstream combustion of the syngas produces a flue gas stream without CO_2.
Pre-combustion capture is often conceived in combination with an Integrated Gasification Combined Cycle (IGCC) plant, having solid (coal) or liquid (heavy oil) feed stocks. It could be applied also to a reforming process fed, for example, with natural gas.
The scheme represented in (Figure 1.5) is relevant to an IGCC with CO_2 capture.

The syngas, a mixture of carbon monoxide and hydrogen, is produced in the gasification unit. The CO present in the syngas is converted into H_2 and CO_2 in the water gas shift reactors. The resulting converted syngas is separated into a CO_2-rich stream, which can be compressed and stored, and a hydrogen-rich stream that is combusted in the gas turbine of the power plant to generate power and heat The separation is achieved in an absorption process normally utilizing a physical solvent, that is efficient in CO_2 removal thanks to the high pressure of the syngas system.
All the technologies used in the IGCC scheme with pre-combustion capture of CO_2 are commercially proven, and this is an advantage with respect to the other two capture schemes. The drawbacks of the pre-combustion are the complication of the scheme and the associated cost.

1.2.3 CO_2 capture oxy-combustion scheme

The principle of oxyfuel combustion is to enable the fuel combustion by oxygen only, in order to obtain steam and CO_2 only as flue gas. By separating water by condensation a stream of CO_2 is ready for compression and storage.
Some inert gas (nitrogen and argon) is present in a quantity depending on the purity of the oxygen produced in the Air Separation Unit (ASU), normally fixed at 98%.
Inert gas content is normally kept below 4% vol, to avoid problems in the transport and storage systems, due to the separation of these gases from the main stream.
The scheme of the oxy combustion is shown in the following Figure 1.3:

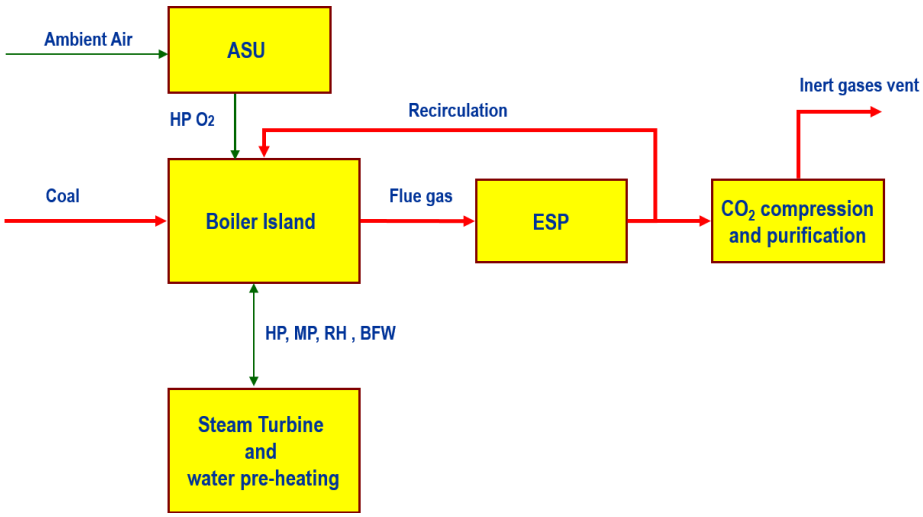

Figure 1.3: Scheme of a USC fed by coal with oxy combustion.

Due to the absence of nitrogen, in the combustion chamber of the boiler the temperature could increase a lot jeopardizing the resistance of the materials. A substantial recycle of flue gas back to the boiler is provided to avoid this effect, in order to create conditions similar to those encountered in the usual air combustion.

Another beneficial effect of the recycle is the dilution of the SOx in the Flue Gas Desulphurization (FGD) system and the consequent relaxation of the corrosion issues associated to the sulfuric acid condensation.
One of the important challenges of the oxyfuel combustion is the minimization of the energy of the ASU consumption, which is huge in relation to the energy produced in the oxyfuel power plant. This consumption is even higher for higher CO_2 purity.
So the rate success of this technology could increase in the future, should novel technologies for air separation be developed, requiring less energy, such as the ASU based on membranes.

1.3 CO_2 Storage

Once produced with the methods described in 2, it is necessary to dispose the CO_2 either permanently (sequestration) or at least for a long period (storage).
The most promising option is the geological storage, whose principles are shown in the following Figure 1.4:

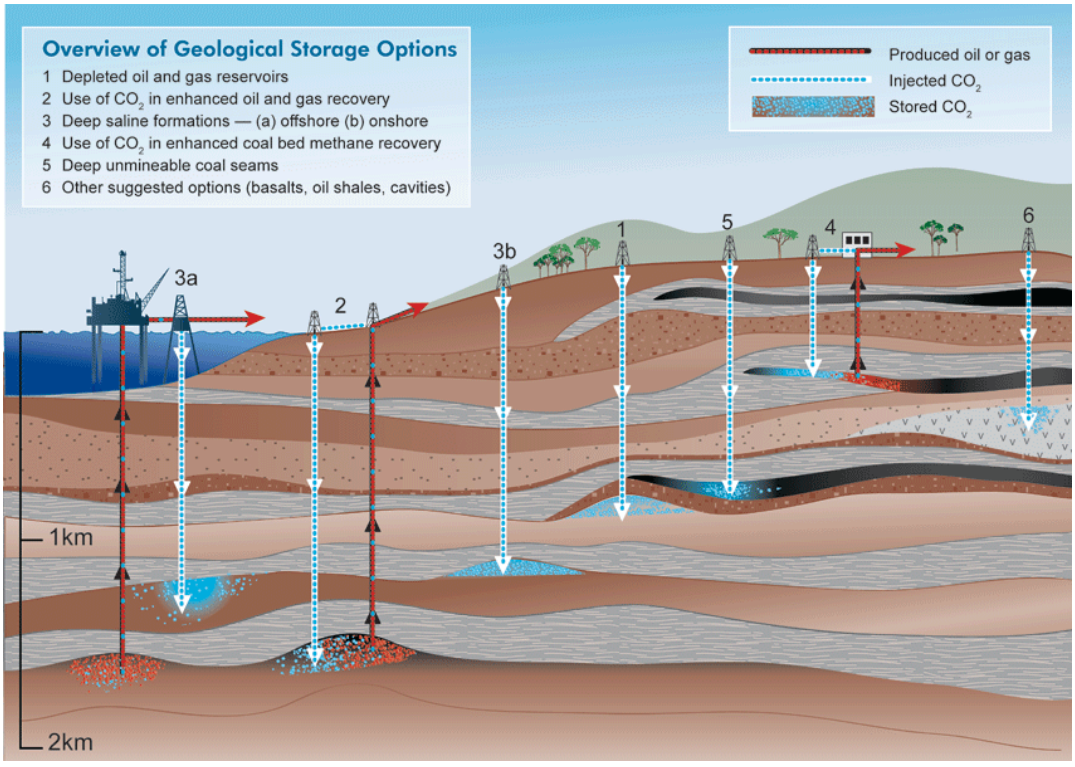

Figure 1.4: Principles of geological CO_2 storage

The accumulation of carbon dioxide in the earth geological layers is a very long natural process which has created the formation of mineral carbonates. The idea is to create artificial storages of carbon dioxide by injecting into geological media the CO_2 captured with different technologies.

From an economic point of view is the use of carbon dioxide is interesting to promote the extraction of fossil fuel from almost depleted gas fields (Enhanced Gas Recovery (EGR)) and oil fields (Enhanced Oil Recovery (EOR)), or from unminable coal seams (Enhanced Coal Bed Methane Recovery (ECBMR)).
The fraction of carbon dioxide that can be used for these purposes is relatively small (IPCC 2005, although is increasing). Therefore the most important options for sequestration are the depleted gas and oil fields and deep saline aquifers.
Saline aquifers are rock formations saturated with water where huge quantities of salts are dissolved, covered with an impermeable layer. The carbon dioxide would be injected into these spaces at about 1000 meters below ground, which have a considerable geological stability.
Another option for CO_2 sequestration is the oceanic storage, but it is believed that its public acceptance is doubtful, in view of possible damage to the marine ecosystems.

Chapter 2

Chemical Looping Combustion

2.1 Technology Description

Chemical Looping Combustion (CLC) is a novel promising technology for the integration of low CO_2 emissions with lower energy penalties. CLC is based on the use of an Oxygen Carrier (OC) which is alternatively oxidized and reduced by reacting with an Air stream and a fuel stream (Figure 2.1). These conversions take place in two different reactors, the fuel reactor and the air reactor, that are operated in a loop: in the first reactor the fuel is converted into CO_2 and H_2O by reducing a Metal Oxide from his oxidative state; in the second reactor the oxygen carrier is oxidized to his original form by reacting with the oxidant stream (i.e. air).
The outputs of this process are an exhaust stream undiluted with nitrogen, so that CO_2 can be easily captured after water condensation, and an O_2-depleted air.

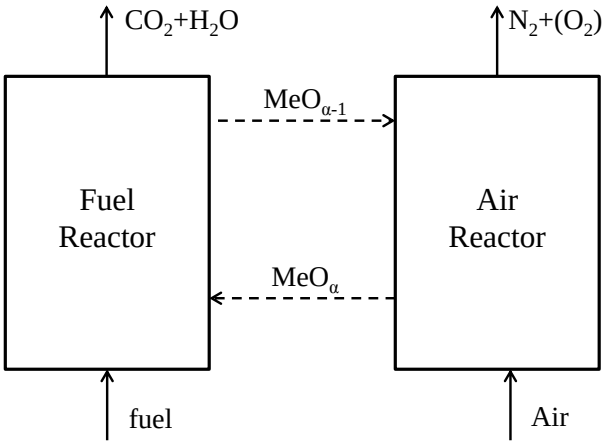

Figure 2.1: Schematic of CLC process

The oxidation reaction is always exothermic and the heat generated is used for power production, while the metal reduction can be both exothermic and endothermic depending on the fuel composition and the oxygen carrier.
The generic reactions that occur are:

$$MeO_{\alpha-1} + \frac{1}{2}O_2 \rightarrow MeO_{\alpha} \tag{2.1}$$

$$MeO_{\alpha} + H_2 \rightarrow MeO_{\alpha-1} + H_2O \tag{2.2}$$

$$MeO_{\alpha} + CO \rightarrow MeO_{\alpha-1} + CO_2 \tag{2.3}$$

$$\left(2x+\frac{y}{2}\right)MeO_{\alpha}+C_xH_y \rightarrow \left(2x+\frac{y}{2}\right)MeO_{\alpha-1}+xCO_2+\frac{y}{2}H_2O \quad (2.4)$$

From the stoichiometry above it can be observed that the sum of these reactions brings to the stoichiometry of the typical combustion.

2.1.1 Integration with power plant

In this configuration the Chemical Looping reactors basically replace the combustor of the gas turbine (Figure 2.2): the compressor feeds high pressure air to the Air Reactor (AR) where exothermic metal oxidation reactions occur. The heat generated is mainly stored as sensible heat in the O_2-depleted air which leaves the CL island at high temperature and is subsequently expanded in the gas turbine.

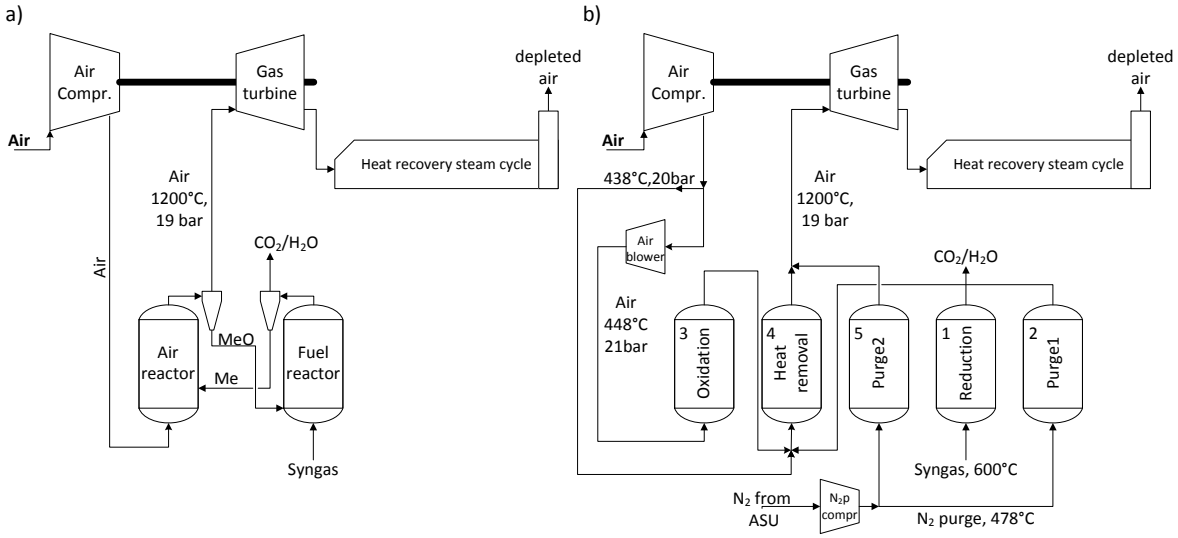

Figure 2.2: Simplified plant scheme with circulating fluidized bed (a) and packed bed (b).

The net electrical efficiency of a combined cycle is strongly affected by the turbine inlet temperature (TIT). Hence the hot stream produced in the CL system and sent to the gas turbine has to be at an adequately high temperature [2], [3]. In the case studied by Spallina et al. (2013, [4]) the TIT was fixed at 1200°C for achieving higher efficiency. In this CLC scheme the maximum temperature is strictly connected to the OC thermal stability, there is therefore strong incentive to increasing it.

A clean gaseous fuel feeds the Fuel Reactor (FR) where it is oxidized by the OC, producing a CO_2/H_2O flow without Nitrogen dilution, suitable for CO_2 storage after cooling, water condensation and final compression. Depending on the configuration, a fraction of the heat produced in the CL island is also stored as sensible heat in this exhaust flow; so different strategies have been proposed for the efficient recovery: the high pressure CO2-rich stream cooled down by producing additional steam for the Heat Recovery Steam Cycle (HRSC) [2] or expanded down to atmospheric pressure before cooling, water condensation and recompression [3].

On the other hand, the FR can be fed with clean gaseous fuel such as Natural Gas or Syngas, but also a direct solid fuel oxidation can be realized. Lot of research has been devoted to the study of the direct solid chemical looping combustion in order to extend the technology of interconnected fluidized bed reactors to the use of solid fuels (such as coal, petcoke, biomass). Coal can be therefore converted in a CLC process in two ways: in the first case is gasified and oxidized in the FR, in the second is fed directly to the FR. Two different options have been proposed for the latter process (Figure 2.3): chemical looping with oxygen uncoupling (CLOU) and the in-situ gasification CLC (iG-CLC). The first process is based on the use of an oxygen carrier which is first reduced by releasing O_2 in the gas phase and then the gaseous oxygen reacts with the fuel [5]: using the CLOU mechanism is possible to overcome the low reactivity which is associated to the char gasification stage because the char can directly reacts with the $O_{2(g)}$. The iG-CLC process consists of feeding coal with H_2O and CO_2 (that acts as fluidization agents) [6]: the solid fuel is first devolatilized and char gets gasified producing H_2 and CO; the volatile matter and the syngas is then oxidized reacting with the OCs like in the CLC with gaseous fuels.
In this work, all the cases studied and mentioned are referred to the use of syngas from coal gasification.

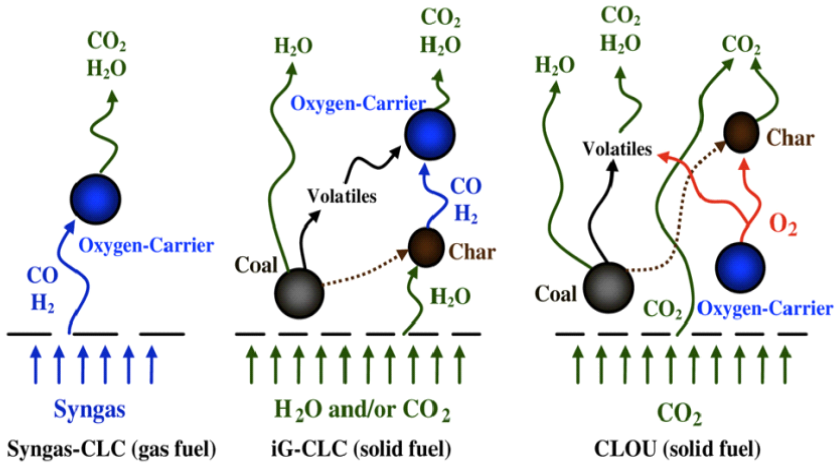

Figure 2.3: Different mechanism to convert coal with a CLC process.

2.2 Oxygen Carrier

The choice of the Oxygen Carrier is extremely important, because it affects the performance and the feasibility of the entire process; the CLC technology can be successfully used only if the metal oxide is properly selected and designed. In general, the OC should have the following properties:

- High oxygen capacity, in order to decrease the quantity of material that has to be used in the system. If the fraction of oxygen in the metal oxide is high,

the same stream of oxidant can be supplied with a reduced amount of metal particles.

- High selectivity towards CO_2 and H_2O, in order to fully convert the fuel in the reduction phase.
- Long-term stability during the repeated cycle operation. The OC should not loose his reactivity and his material losses have to be minimized, in order to obtain good performance and lower associated costs.
- High melting point, in order to accomplish the process at high temperature, as it is requested to maximize the efficiency of the power plant.
- Low attrition rate and good resistance to agglomeration, in order to reduce the possibility of a bed defluidization.
- Very low carbon deposition activity. When this phenomenon occurs, the CO2 capture rate decreases because, during the subsequently oxidation phase, carbon dioxide is formed and released into the atmosphere. The formation of metal component that would deactivate the material is another risk of the carbon deposition. The OC has to show also resistance to contaminants that might be present in the fuel.
- Low cost and low environmental impact.

The oxygen carrier is usually mixed with an inert matter that can guarantee better diffusion inside the particles (increasing the porosity), improve the thermal-mechanical properties and increase the heat capacity. The most common OC families are based on Nickel, Iron, Copper, Manganese or some mixed metal oxides. Alumina (Al_2O_3), Titanium Oxide (TiO_2), $MgAl_2O_4$, SiO_2, Zirconia (ZrO_2), Bentonite, Sepiolite are the most studied inert matter for the CL process. A list of the main properties of the OC is presented in Table 2.1.

2.2.1 Nickel-based

The Nickel-oxide is a high reactivity material with a high oxygen content. It can be used in high temperature operations such as a large scale power plant, due to his melting point of 1455°C. The selectivity is good, but in the range of 98/100%; it decreases with temperature. Although this material shows a high fuel conversion, the presence of not complete oxidation products leads to thermodynamic limitations. The reduction is exothermic, when the material reacts with syngas, and endothermic with methane.
The pure NiO shows low reaction rate, due to his poor porosity. This is an issue of all the pure MeO used as OC; so lot of researches were carried out looking for a good support material. One of the best possibilities is the use of Alumina (Al_2O_3). High thermal stability, mechanical resistance and better kinetic are typical improvements. When Alumina is used as support material, $NiAl_2O_4$-Spinel can be formed, provoking a decrease in the reactivity. One possible solution is to use directly this spinel as inert: NiO particles over $NiAl_2O_4$ support have demonstrated to be very reactive. The Mg or Ca addition on this support material leads to the formation of $MgAl_2O_4$ and $CaAl_2O_4$ which were proved as good OC for the conversion of fuel and high thermal stability [7].

In the end this material shows great potentiality for the large scale power plant application, but it has also some drawbacks: the costs are relatively high and the material is considered to be toxic.

2.2.2 Iron-based

Iron is a real valid alternative because it is cheap and common in nature. The high melting point (1565°C) makes it suitable for the power plant. Iron can be present in several phases, from the most oxidized to the less:

a) Ematite, Fe_2O_3
b) Magnetite, Fe_3O_4
c) Wustite, FeO
d) Pure iron, Fe

Problems of selectivity arise when this material is further reduced than Fe_3O_4 to FeO and even more to Fe. If the process is stopped at the Magnetite level of reduction, the oxygen capacity involved is limited. For this reason studies has being carried out to overcome this problem: a full conversion of fuel could be reached by adding Alumina or Titanium to the metal oxide, using Al_2O_3 $MgAl_2O_4$ or TiO_2 as inert matter, because the porosity of the particles increases and therefore gas-solid reaction are enhanced.
The latter option is very interesting. Ilmenite ($FeTiO_3$) is a natural material that can be extracted from pits in Norway, South Africa and Australia. It can be used directly as OC in the reactor because it contains already the inert matter (TiO_2) and the reacting metal oxide (FeO). The oxidation is strongly exothermic and reduction is slightly endothermic. Before the use it has to be activated in a process that increases the porosity and reactivity.
Ilmenite has been demonstrated as very good oxygen carrier for converting syngas, but not methane. It is therefore a very suitable solution for the combined cycle power plant integrated with a coal gasification and the subsequently CLC [4], [8].

2.2.3 Copper-based

Copper, together with Iron and Nickel, is one of the most studied OC for the CLC applications. The selectivity is very high and, with both syngas and methane, a full conversion of the fuel is achieved. It is a fast reacting material and his cost is very cheap in comparison with Nickel. All the reactions, including the reduction, are exothermic. Copper can be present in several phases: the most oxidized is CuO and then Cu_2O and Cu.
This oxygen carrier is also applicable for the CLOU concept: CuO is formed in the air rector, while in the fuel reactor, where higher temperature is reached, oxygen is released and Cu_2O is formed [9].
Despite the good properties this material showed a critical issue: the melting temperature is low (1085°C) and so its use in the power plant application is compromised, at least when high temperature process is required.

2.2.4 Manganese-based

As the Iron and Copper based OC, this material is of interest due to its low cost and not toxicity issue. Five state of oxidation can be present: Mn, MnO, Mn_3O_4, Mn_2O_3, MnO_2. The most oxidative state is the MnO_2, but it decomposes at 500°C. After this temperature the stable phase is Mn_2O_3, but for temperature higher than 850/900°C only Mn_3O_4 is stable. Hence, for the CLC applications, only the reactions between MnO and Mn_3O_4 could been used, with the critical issue of the low oxygen carrier capacity.

2.2.5 Other oxygen carriers

Cobalt is not often applied and studied due to its cost (higher than Nickel) and environmental issues. Several phases can be present, Co, CoO, Co_3O_4. For temperature lower than 900°C the Co_3O_4 phase is not stable anymore and then CoO becomes the only possible oxidative state. This material can also be used for the CLOU process exactly around this temperature taking advantage from the thermodynamic equilibrium of these two species.

$CaSO_4$/CaS is a low-cost material with high oxygen capacity, but slow reaction kinetics were measured. Also the side reaction could occur, where CaO and SO_2 are formed [9].

In the last years studies on mixed oxygen carrier have been carried out with the aim of unifying the advantages and reducing the drawbacks. The main targets are:

- Improve the stability and reactivity of the particles
- Increase the conversion of the fuel
- Improve the mechanical resistance
- Reduce the cost and the presence of toxic material (such as Nickel)

Many different combinations (such as Cu/Fe Cu/Ni Fe/Ni Co/Ni Fe/Mn) have been proposed but, until now, they do not have result in large scale plant application.

material type	Weight content in the particle (%.wt)	support type	Fuel type	Process	Temperature range tested (°C) [10]	Selectivity to CO_2/H_2O * (800-1000°C) [11], [12]	Oxygen Carrier pair considered	Melting points °C, [11]	Oxygen ratio, R_0 (not considering support)	Reaction enthalpy at 1000°C** (kJ/mol reactant gas) [13], [11]					Metal cost ($/ton metal) [14]
										CO	H_2	CH_4	C	O_2	
Ni based	18-100%	α-Al_2O_3,γ-Al_2O_3, Al_2O_3, $NiAl_2O_4$, $NiAl_2O_4$-MgO, $MgAl_2O_4$, Bentonite, ZrO_2-MgO	CH_4, C_2H_6, C_3H_8, H_2, CO, syngas, CH_4+H_2S	CLC/CLR	450-1200	>98.9% (Ni)	NiO/Ni	1455°C	0.214	-47	-15	134	75	-468	15'000
Cu based	12-15%	α-Al_2O_3,γ-Al_2O, $MgAl_2O_4$	CH_4, H_2, CO, syngas, C_xH_y, CH_4+H_2S	CLC	300-1000	100% (Cu)	CuO/Cu	1085°C	0.201	-134	-101	-212	-99	-296	7'000
Cu based	15-80%	Al_2O_3,γ-Al_2O, Sepiolite, $MgAl_2O_4$, Bentonite, ZrO_2, TiO_2, SiO_2	CH_4, coke, char, N_2, CO_2	CLOU	850-985	100% (Cu)	CuO/Cu_2O	1235°C	0.112	-151	-119	-283	-135	-260	7'000
Fe based	20-100%	Al_2O_3, Bentonite	CH_4, PSA-offgas, biomass	CLC	430-1000	100% (Fe_3O_4) 54-78% (FeO)	Fe_2O_3/Fe_3O_4	1565°C	0.033	-42	-10	154	84	-479	200
Mn based	40%	ZrO_2-MgO	syngas	CLC	810-1000	100% (MnO)	Mn_2O_3/MnO	1347°C	0.101	-102	-70	-85	-36	-359	<200
Mn based	80%	SiO_2	CH_4	CLOU	800-1000	100% (MnO)	Mn_2O_3/Mn_3O_4	1347°C	0.034	-192	-160	-446	-217	-179	<200
Ilmenite ($FeTiO_3$)	100%	-	coal, petcoke, syngas	CLC	813-1030	almost 100%	Fe_2O_3/FeO***	1565°C	0.100	-4.7	27.5	304	158	-554	<200

Table 2.1: List of material properties used for CLC.

* = the species between brackets are the reduced components

** = the dependency of the reaction enthalpy on the temperature is small.

*** = different components containing iron, titanium and oxide can be considered, like Fe_2TiO_5, $FeTiO_3$. In that case, the reaction enthalpy is a bit different.

2.2.6 Carbon deposition & sulfur tolerance

In the CLC system the carbon deposition can become a very relevant issue, with two main effects: firstly, the presence of carbon solid on the oxygen carrier in the subsequent oxidation phase will result in the production of carbon dioxide, thus decreasing the CO_2 capture efficiency [15]. This might be tolerated if the amount of carbon deposition is limited, mainly because the CO_2 capture efficiency obtained in this case would be comparable with that of common CCS technologies.
An additional effect of the carbon deposition is that the morphology of the oxygen carrier particles may change, which could affect the stability of the material in the long run.
From the study it is concluded that, when additional oxygen atoms are added to the system, the pure carbon presence at equilibrium decreases. In conclusion the carbon deposition can be suppressed by either the addition of pure steam or the recirculation of a part of the exhaust flow (mainly formed by H_2O and CO_2) [15]. The latter solution is more suitable for the power plant application, because it leads to less energy losses.

When the fuel contains sulfur, typically H_2S and COS, in the fuel reactor gaseous SO_2, sulfates and sulfites could be formed. This phenomenon can lead to deactivation of the oxygen carrier and possible formation of SO_2 in the following oxidation cycle.
Hence, in the case of integration with a power plant, the fuel containing sulfur should be previously treated in the AGR system.
The Nickel-based oxygen carrier shows a predisposition to the formation of sulfides, while better behavior can be seen with the use of Copper and Iron.

2.3 Use of Interconnected Fluidized Bed Reactor (IFBR) or Packed bed Reactor (PBR)

The alternated oxidation and reduction reactions of the CLC process can be achieved in different ways. The most studied way is based on the use of Interconnected Fluidized Bed Reactor (IFBR) (Figure 2.4.a), where the oxygen carrier particles are recirculated between the fuel and the air reactors. In this configuration the metal oxide is reduced with syngas in the fuel reactor and a continuous H_2O/CO_2-rich flow is produced. Then, the gas turbine can be fed with the high temperature O_2-depleted air, produced in the air reactor after the oxidation of the oxygen carrier. Since the gas turbine cannot be fed with a flow containing fines, a gas-solid separation unit (the cyclone) and subsequent filters for trim removal have to be provided.
In this configuration, the temperature difference between the two reactors is kept low by the continuous recirculation of the particles from one bed to the other one. The temperature difference depends on the solids circulation and on the thermal behavior of the reduction reaction, which is usually slightly exothermic when syngas is used.
The operability of IFBR under atmospheric pressure at different scales was already proved, but his applicability in large plants at elevated pressure, has not been yet demonstrated.

The most critical issue of this concept is the solid recirculation that has to be kept constant and the gas-solid separation through the cyclones and filters, at the high pressure and temperature that are needed when this process is integrated with a combined cycle.

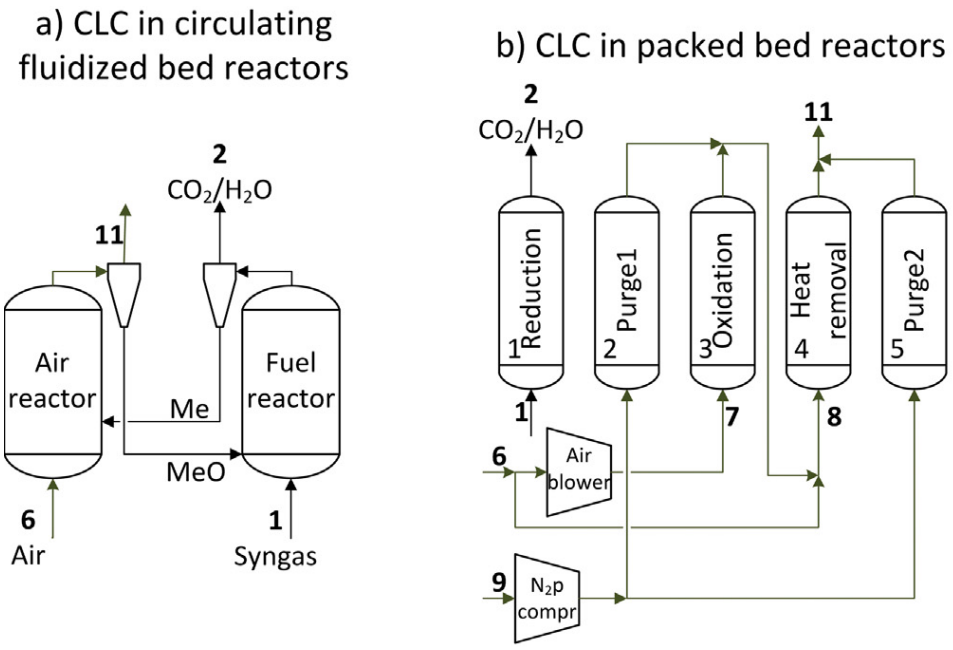

Figure 2.4: Scheme of the circulating fluidized bed (a) and the packed bed configuration (b)

These problems can be overcome by the use of the dynamically operated **Packed Bed Reactor** (**PBR**) (Figure 2.4.b), in which the solid is kept stationary and the oxygen carrier is alternately exposed to oxidizing and reducing conditions, by switching the gas flows among different beds. Since the solid circulation is not needed anymore, pressurized conditions do not present any critical issue. Furthermore the gas-solid separation is easier or not needed at all, because the risk of fine formation is minimal due to the larger particles that are used in this bed to avoid excessive pressure drops.

The operation of PBR for CL technology application is intrinsically dynamic. As it will be more widely described in the (74), the formation of a reaction front and a heat front, with different velocities, occurs (Figure 2.5).

The reaction front divides the bed into two zones: the initial part (nearby the reactant inlet) where the metal oxide has already reacted, and the final one still filled with unreacted material. The heat front divides the bed into two portions at different temperature. The integration of PBR with a power plant is possible because the reaction front is usually faster than the heat front. In this way the heat released during the oxidation reaction is retained in the bed, and can be exploited for the production of a flow at constant high temperature and mass flow rate, during the subsequent heat removal phase.

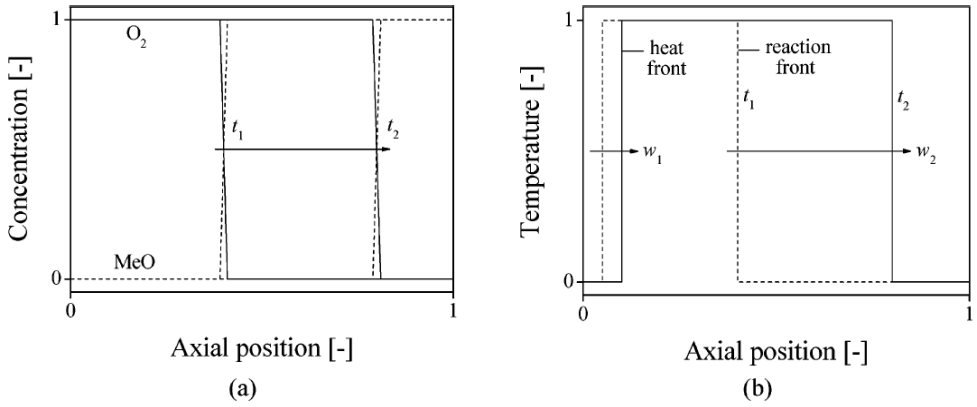

Figure 2.5: Schematic representation of the evolution of dimensionless axial concentration (a) and temperature (b) profiles in PBRs.

Furthermore the solid temperature profile at the beginning of each phase depends on the operation of the previous one. When a gaseous stream is fed to the reactor, the temperature of the initial part of the bed tends to be close to the inlet gas temperature because the solid is continuously in contact with a stream at constant (moderate) temperature. If the temperature of the inlet gas is not high enough, the oxygen carrier will not react with a sufficiently fast kinetics with the gaseous stream in the following phase and the process cannot proceed in a stable and continuous way [4].

The work strategy is different from the one of the IFBR, a sequence of steps is required. It's important to underline that the power island needs the hot stream to be produced at constant temperature and mass flow rate to preserve the following expander from sudden thermal stress and fluid-dynamic instability. Multiple reactors operating in parallel and an adequate heat management are therefore needed. A possible operation strategy (strategy "A") is depicted here below:

a) Oxidation: the reduced beds are fed with air to oxidize the metal oxide. The heat released during this operation is mostly retained in the bed because the reaction front is usually faster than the heat front. In this way the outlet O_2-depleted air is not at very high temperature and is usually mixed with compressed air. Then it is fed to the reactors which are working in the subsequent heat removal phase.
b) Heat removal: in this step the heat retained in the bed after the oxidation phase is removed and high temperature flow is produced to feed the gas turbine.
c) Purge: in order to avoid the mixing of fuel and air during the reactors switch, a purge phase with N_2 is needed. In fact a contact between air and fuel could cause safety issue and also a decrease in the performance because the fuel would not be oxidized by the oxygen carrier.
d) Reduction: after the previous two steps the bed is still oxidized and can be fed with syngas in order to be reduced.

In this strategy "A" (OX-HR-purge-RED-purge) the reduction is accomplished at relatively low temperature after the heat removal step, but it is possible also to carry it out at higher temperature directly after the oxidation phase in the case of low reactivity of the oxygen carrier. With this changing in the operations order (strategy "B": OX-purge-RED-HR) the

heat removal has to be done with a Nitrogen flow because this step is now carried out when the bed is reduced (**Errore. L'origine riferimento non è stata trovata.**6). It is important to underline that the kinetics of the reduction is very sensitive to the solid composition and temperature.

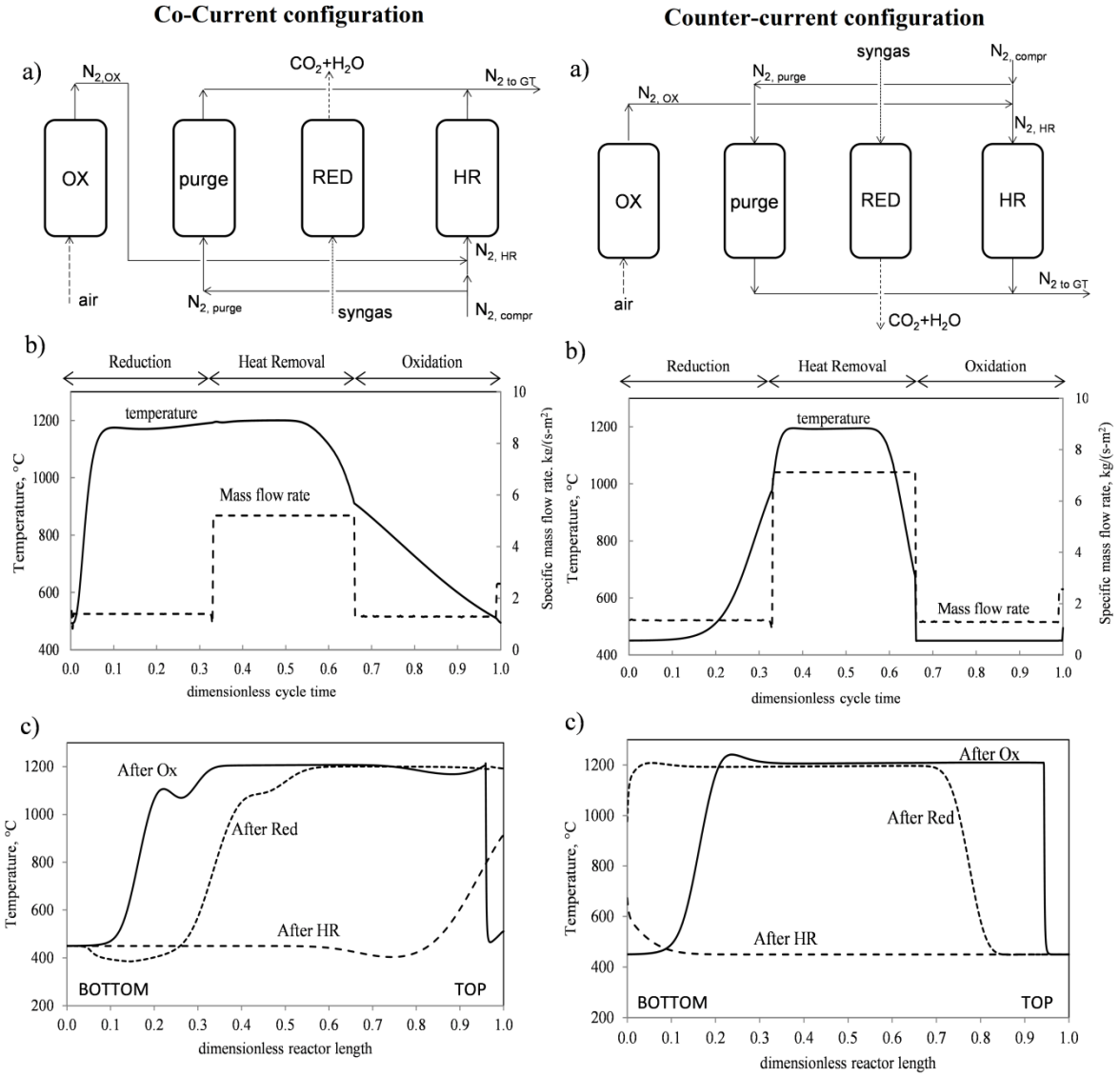

Figure 2.6: STRATEGY B: (a) Schematic of the configuration (b) gas conditions at the reactor outlet (c) Solid profile temperature of the reactor after the steps.

As it was widely discussed in Spallina et al. [16] two possible schemes, shown in (Figure 2.66) for the strategy "B", can be used for the reactor feeding:

a) Co-current feeding (Figure 2.66, Left): all the streams are fed to the same reactor end. When the operations are carried out following the strategy B, the exhaust flow come out from the reactor at very high temperature (around the maximum temperature of the bed, the same as the heat removal step).

b) Counter-current feeding (Figure 2.66, Right): The reduction and the heat removal streams are fed to the opposite end of the reactor with respect to the oxidation one. In case "B", the CO_2/H_2O flow is released at a lower temperature and so a higher fraction of the heat is stored in the bed for the following heat removal step.

Despite the good properties and simplicity of this solution, the Packed Bed Reactors have some relevant challenges to be solved for assessing their feasibility:

- High temperature valves are needed at the outlet of the CL island to switch the gas stream and distribute them to the right downstream sections. These valves are expected to be high cost components.
- The processes involved are intrinsically dynamic and the unsteadiness of the temperature of the outlet flow is a critical issue that has to be solved with an accurate heat management strategy. As we said before, special attention should be paid to the temperature at which the reduction is carried out.
- An almost complete solid conversion has to be reached in order to use all the capacity of the reactors.
- The reactions kinetics have to be fast enough to avoid fuel slip.

A comparison between the performance of PBR and IFBR in a power plant integrated with a CLC of syngas (IG-CLC) was carried out by Hamers et al. [17]. The process efficiency for both the solutions was fairly the same, 41-42%. Hence, the reactor selection will not be based on the process efficiency, but on the availability, operability and cost of high temperature and high pressure reactor systems. These systems are still under development and both present pros and cons [17].

2.4 Conclusions

The advantages of the CLC are herewith summarized:

a) Low Energy penalties for the CO_2 capture due to the intrinsic capability of this technology in capturing the CO_2. This leads to lower SPECCA [1] index, in comparison with other conventional CCS technology. As showed in Spallina et al. [4], the IGCC plant based on the CLC combustion (IG-CLC) showed a SPECCA of 1.3 $MJ_{LHV}/kg_{CO2,}$ vs. 3.4 MJ_{LHV}/kg_{CO2} of the pre-combustion capture system with solvents in the IGCC scheme. A very interesting efficiency was therefore reached: in the IG-CLC case it approaches 41%, 3.4-5.7 percentage points higher than benchmark IGCCs with CO2 capture.

[1] SPECCA: Specific Primary Energy Consumption for CO_2 avoided. In every CCS technology, energy losses due to the CO_2 capture process and therefore drop of the global efficiency, occur. The SPECCA index quantifies this energy losses, comparing the CCS power plant performance with the benchmark correspondent technology without CO_2 capture. It is expressed in the form of: MJ_{LHV}/kg_{CO2}.

b) High CO_2 capture efficiency and CO_2purity. In the IG-CLC plant studied in [4], a 96% of CO_2 capture efficiency was achieved. The CO_2 stream was pure at 96.5%, but a 98.2% CO_2 purity can be reached by increasing the purity of the oxygen from 95% to 98.5% with a minor effect on the complete plant efficiency (a slight increase in the ASU consumption occurs) [18].
c) There is no production of Nitrogen oxide, because the combustion process is occurs at relatively low temperature.

Besides these good properties, this technology shows some critical issues:

a) When a Chemical Looping process is integrated in a power plant, very high temperature and medium-high pressure streams are needed for achieving good efficiency. This becomes a critical technological issue for the IFBR, for what concerns the solid recirculation and gas-solid separation, and also a cost issue for the PBR, relevant to the high temperature valves system that is needed to switch properly the reactor feeds.
b) In the PBR, the variability of temperature and mass flow rate of the stream coming out from the reactor, can become a problem for the following expander and has to be carefully managed.
c) Oxygen carrier: the Chemical Looping process can be successfully used only when the oxygen carrier shows good performance in the selectivity, conversion, kinetics and thermal-mechanical stability over a long term use. This aspect represents a continuous challenge for the chemical and the material engineering.

Chapter 3

PeCLET Process

3.1 PeCLET Concept

The research work that is carried out in this thesis is centered on the PeCLET process: a novel and promising technology in the application of the chemical looping system in a power plant with pre-combustion CO_2 capture. PeCLET is the acronym of Pre-combustion & Chemical Looping efficient Technology. It is based on the use of packed bed reactors; the main output of the CL unit is a H_2-rich and carbon free fuel diluted with Nitrogen and steam, ready for use in the gas turbine combustor.
It is considered a promising technology because it shows some advantages in comparison with the CLC: the production of a hydrogen rich stream, instead of a very high temperature flow that feeds directly the gas turbine expander, makes the CL unit more flexible and not strictly dependent on the gas turbine operating conditions. Furthermore the process is carried out at high pressure and moderate temperature (600°C-800°C) and hence high temperature valves, reactor and piping system are not needed anymore, with a decrease in the costs [19].

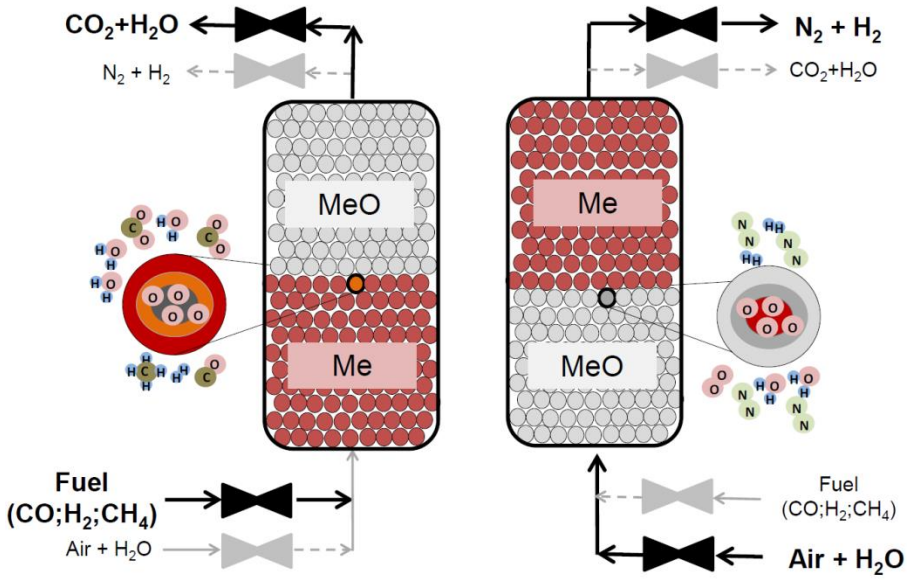

Figure 3.1: The concept of the PeCLET process, image from [19].

The schematic concept of this process is shown in Figure 3.1, based on the use of two reactors, the Oxidation Reactor (OR) and the Fuel Reactor (FR). The latter is operated in the same way as the CLC case. It can be fed with syngas or natural gas, properly treated

and cleaned. Inside the bed, the MeO is reduced to Me by reacting with the fuel, that is oxidized. A stream of CO_2/H_2O without nitrogen dilution is produced, so that the carbon dioxide can be easily captured after water condensation. With the progress of the chemical conversions, the reaction front goes up through the reactor. When the upper end of the FR has been reached, a total conversion of the solid is achieved, and the bed is entirely reduced to Me. At this point the feeds are switched, and the same reactor starts working as an OR.
In the PeCLET process, the oxidation reactor operates quite differently from the CLC case. It is fed with a mixture of steam and sub-stoichiometric air. The Me is therefore oxidized by reacting with the steam in the H_2O-splitting reaction to form hydrogen, and with the oxygen from air to complete the oxidation. In the H_2O-splitting reaction, the steam, in contact with a proper metal oxide, tends to be split into O and H_2.
The output of this reactor (OR) is a hydrogen flow diluted with nitrogen and unreacted steam, and can be used as fuel for a combined cycle plant or as input for the ammonia production process (*Sec. 3.1.3* Use of the PeCLET process for NH_3 production).

A CL process for the hydrogen production conceptually similar to the PeCLET process has been already proposed by Chiesa et al. [20]. As depicted in Figure 3.2, three different interconnected fluidized bed reactors (AR, FR and a Steam Reactor SR) and three different stages of iron oxidation are considered. The complete solid oxidation is accomplished in two steps: the FeO is firstly oxidized to Fe_3O_4 by steam in the SR producing hydrogen ("Steam-Iron process"); large steam excess is needed to achieve an acceptable metal oxidation. Then, in the AR Fe_2O_3 is formed by the reaction between Fe_3O_4 and the oxygen from air. The chemical loop is completed with the reduction of the Fe_2O_3 to FeO in the FR by natural gas.
The outlet streams of this process are a H_2-rich gas containing steam, an exhaust gas produced by the oxidation of the natural gas and a hot O_2-depleted air stream coming out from the AR after solid separation.

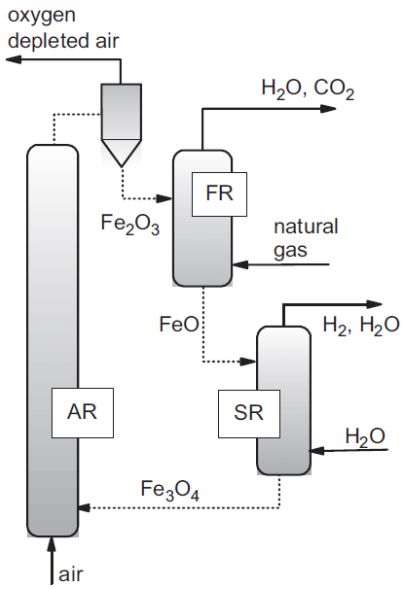

Figure 3.2: Conceptual scheme of the "three reactors CL process for hydrogen production".

3.1.1 Oxygen Carrier

The oxygen carrier (OC) is an extremely important component because it affects the performance and the feasibility of the entire PeCLET process. The main properties of a good OC for a successful use in the CL technology were listed in Chapter 1. As for the chemical looping combustion, the OC has to provide fast kinetics and good conversion during the reduction operation but, in the case of PeCLET process, it has to be selected and designed also to accomplish a proper conversion during the oxidation phase, by reacting with O_2 and H_2O for the production of hydrogen [19]. In this perspective, more research on the OC behavior has to be carried out, in order to achieve good performance for both the oxidation and the reduction reactions.

This concept shows similarities with the steam-iron process; therefore the Fe-based OC is a promising choice for the PeCLET technology, but also perovskite-based material is of interest [21]. The first option has been already studied with good results by Chiesa et al. [20] for the production of hydrogen only with the use of three reactors and three oxidation states of the Iron: the FeO was oxidized to Fe_3O_4 in the steam reactor in order to produce H_2, then the maximum oxidation state Fe_2O_3 was reached in the air reactor before the reduction to FeO state with natural gas is accomplished.

Preliminary experimental studies on a small scale reactor have been also carried out by Spallina et al. [19], in order to verify the feasibility of this process. Fe and FeO states of reduction were reached in different experiments, assessing the possibility to use both wustite and pure iron as reductive state.

In the following Figure 3.3 the resulting compositions of the oxidation cycle at different temperature are shown (feed gas composition: 0.55 H_2O and 0.45 air, molar basis).

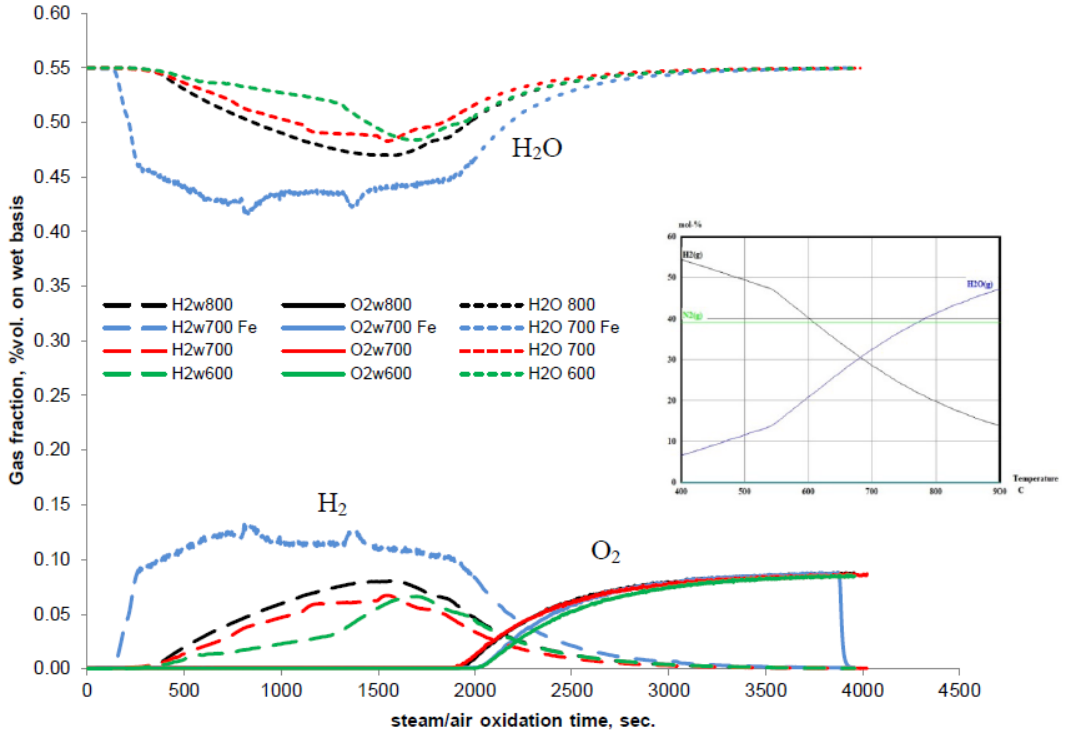

Figure 3.3: Syngas ($H_2/N_2/H_2O$) composition at the reactor outlet during the oxidation.

On the right hand side is also shown the equilibrium composition expected (y-axis at different operating temperature (x-axis) when feeding the same gas. An additional experiment (blue line in Figure 3.3) has been carried out by reducing the Fe_2O_3 to Fe by feeding a mixture of H_2 and N_2 and the oxidation has been carried out at 700°C.

The ΔT that was registered in the bed during the oxidation phase was less than the CLC case. This is due to the heat released by the oxidation reaction with H_2O-splittting which is not as exothermic as the oxidation with air, and confirms that the temperature rise of the PeCLET concept is a combination of both CLC and steam-iron process.

In this work, due to its capacity of reacting with steam and for the good properties listed in Chapter 1, iron was chosen as base for the oxygen carrier. In particular the two possible reductive states (Fe, FeO) are considered.

3.1.2 Integration of the PeCLET concept in a power plant

This work aims at developing the process and evaluating the performance of the PeCLET concept integrated with a combined cycle fed with the syngas provided by a coal gasification and cleaning unit. In Figure 3.44 the configuration of this process is shown and compared with the current benchmark technologies: the pre-combustion CO_2 capture in the IGCC plant and the CLC.

The today's solution includes the typical gasification unit for syngas production and is based on the use of two Water Gas Shift (WGS) reactors (high temperature and low temperature) and of a CO_2 separation unit based on the exploitation of absorption columns. It is clearly seen in the picture that this process needs more conceptual stages and

components than the two solutions based on the CL technology and above all it is strongly penalized in the efficiency by the heavy consumption of steam in the solvent regeneration section of the CO_2 absorption unit. The CL technologies presents instead a lower number of conversion/separation reactors with the intrinsic advantage of lower energy losses. This leads to a higher value of SPECCA for both the CL configurations.
In the PeCLET case, after the syngas production and cleaning, the fuel is fed to the fuel reactor where a CO_2/H_2O-rich flow at medium-high temperature is produced. This stream has to be cooled down by producing steam before the water can be condensed and the CO_2 captured. The heat of this stream is therefore recovered in the steam cycle.
On the other side of the unit, the sub-stoichiometric air is compressed to the oxidation reactor pressure and mixed with the steam which is usually taken from the end of the HP section of the combined cycle steam turbine. The output of the oxidation reactor is then a hydrogen flow already diluted with nitrogen and with the H_2O not reacted (the steam will be always fed with an excess). This aspect fits perfectly the use of the hydrogen fuel in the combined cycle, where it needs to be properly diluted to limit the temperature in the diffusive combustor of the gas turbine in order to limit the NO_X production [16,17].
The OC affects strongly the air-to-steam feed ratio, because it sets a minimum value of this ratio, as it will be discussed in the following section (*Sec. 3.2.2* Air-to-Steam ratio in the feed). Provided that you remain above this minimum value, an optimized H_2-N_2-H_2O composition can be achieved by varying the air and steam mass flow rate which feed the oxidation reactor.

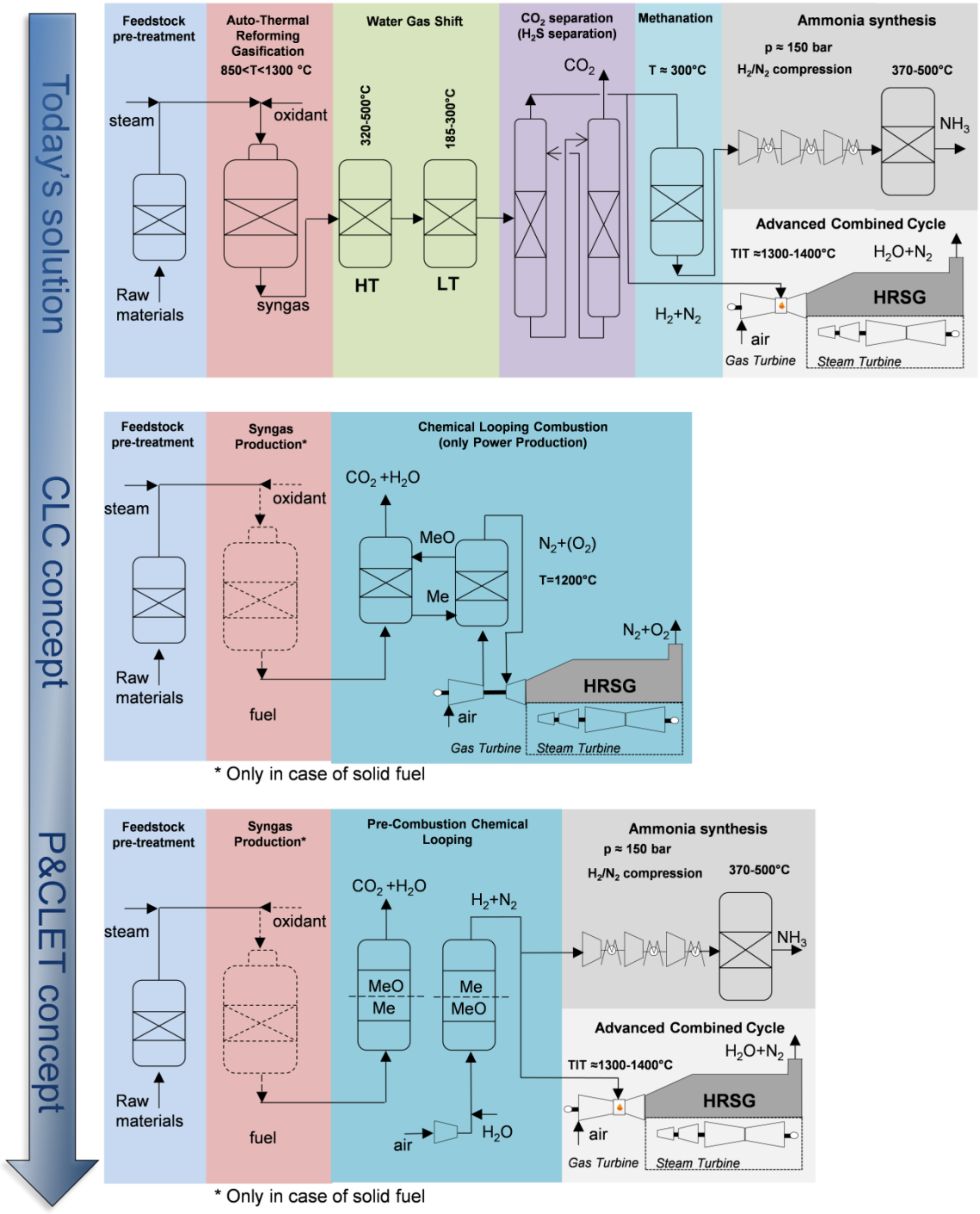

Figure 3.4: Comparison of CO2 pre-combustion capture and CLC configurations with the P&CLET concept, image from

The main advantage of the PeCLET process is that the CL unit and the thermodynamic cycle are less operating-condition-linked in comparison with the CLC process because a hydrogen fuel is produced instead of a very high temperature stream that feeds directly the gas turbine expander. The reactors are therefore more flexible and less dependent on the

operating conditions of the gas turbine which, therefore, can be operated at the optimum conditions and achieve its best performance.
Another advantage of the PeCLET process is that the CL island can be operated at higher pressure resulting in lower reactor volume (and consequently a lower investment cost) and less power consumption for the CO_2 compressor train.
Furthermore, the maximum temperature of the thermodynamic cycle (which is the most important parameter for the gas turbine efficiency) is not limited anymore by the resistance of the OC, because the production of a hydrogen rich fuel allows the use of advanced H_2-fuelled gas turbine which can reach the maximum achievable TIT in relation to the technological development, and work with the optimized compression ratio.

3.1.3 Use of the PeCLET process for NH_3 production

The ammonia production is nowadays accomplished with a pre-combustion CO_2 capture concept based on the use of several reactors and separation/conversion steps, which lead to efficiency penalties.
The PeCLET concept shows potentiality also for this process, because a H_2/N_2 gas mixture with the required composition can be directly produced in the CL island and fed to the ammonia synthesis unit (Figure 3.4).
Using a proper steam to air ratio in the oxidation stage, it is indeed possible to produce the hydrogen flow with H/N equal to 3, as it is required for the ammonia synthesis, without any other separation/conversion step.

3.2 Simulation of the chemical looping island

The goal of the entire work is the design and performance assessment of a power plant fed with coal and based on the integration of the PeCLET concept with the IGCC technology. The internal mechanism of the reactor, the kinetics and the real solid temperature profile will not be investigated in this study.
The aim of this first part of the work is to carry out an analysis on the CL island in an energy perspective. Hence, by varying key parameters of this process, results about the temperatures, compositions and performances of this unit will be presented. The all integration will be instead discussed in the next Chapter (*Chapter 4*).
The simulations have been carried out by the proprietary computer code GS (Gecos,2013) described in the 4.2 Base case plant0).

3.2.1 Simulation scheme

Before explaining the simulation scheme of the PeCLET concept, it is important to underline that, when a boundary as the one depicted in Figure 3.5 is considered, the entire process can be described by the use of only gaseous reactants without considering the loop reactions in which the metal oxide is involved. This fact has been already demonstrated in

(*Chapter 1*) for the CLC concept, where the global reaction of the process corresponded to the combustion of the fuel with air.
Similarly, in the PeCLET case the sum of the real gas-solid reactions that occur in the packed-beds, results in a system of two reactions: the syngas oxidation by O_2 from air, and the Water Gas shift (WGS). Hence, in this equivalent system adopted for the simulation, the reactant atoms are C-H-O only, and the same overall energy and material balance of the real gas-solid reactions can be obtained.
A direct example of this mechanism will be shown in 78, concerning the stoichiometry of the iron-based OC case.
Conceptually, the fuel reacts with oxidant stream (air + H_2O) and is converted into H_2 rich stream and CO_2/H_2O. In terms of heat reaction, the system is affected by two main reactions:

a) Oxidation Reaction: the sub-stoichiometric O_2 oxidizes part of the reactive components of the syngas.

$$CO + \frac{1}{2}O_2 \rightarrow CO_2 \qquad \Delta H^0_{298} = -283\ kJ/mol \tag{3.1}$$

$$H_2 + \frac{1}{2}O_2 \rightarrow H_2O \qquad \Delta H^0_{298} = -242\ kJ/mol \tag{3.2}$$

b) Water Gas Shift (WGS): the steam reacts with the CO of the syngas producing hydrogen.

$$CO + H_2O \rightarrow CO_2 + H_2 \qquad \Delta H^0_{298} = -41\ kJ/mol \tag{3.3}$$

Within this reactions, the final streams composition are calculated: in case of low amount of air, most of the OC which is reduced by the fuel is oxidized reacting with H_2O producing (H_2). On the other hand, if the amount of O_2 is high, the system behaves more similarly as in the CLC concept. In term of heat of reactions, the lower is the amount of O_2 in the system, the lower is the final temperature of the gas streams (which is supposed to be same for simplicity and due to the lack of a specific model for the assessment of reactor behavior).

As it will be described in Sec. 3.2.2 Air-to-Steam ratio in the feed, the steam is fed in excess in order to achieve the entire conversion of the metal oxide during its reaction with the H_2O. This means that all the hydrogen that could be stoichiometrically obtained from the H_2O is effectively produced. To get this result in the simulation, the WGS has been pushed to the complete conversion of CO, overcoming the thermodynamic limit. This approach results in the correct outlet composition without altering the overall energy balance.
Furthermore the outlet composition changes by varying the air-to-steam ratio in the feed: in particular, when this ratio is increased, more pure oxidation reaction occurs and consequently more sensible heat is released and less H_2 is produced. A deeper analysis of this parameter is carried out in the next sections (*Sec. 3.2.2* Air-to-Steam ratio in the feed *and 3.2.3* Presentation of the results).

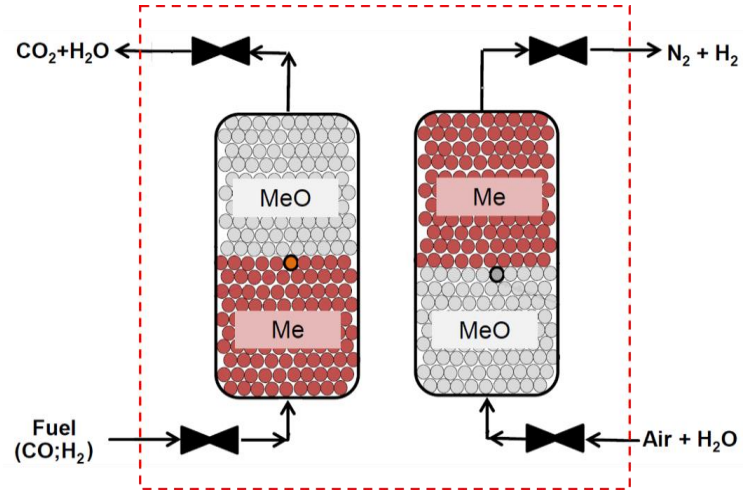

Figure 3.5: CL simulation boundary layer.

The conceptual simulation scheme of the PeCLET process is shown in the following figure (Figure 3.66). Syngas and Air-steam flows are both conceptually split into two streams: one with reactive elements and the other with inert elements. In the center it is represented the "Reactive Mixer", which only the reactive components enter. Then each not reactive stream is mixed adiabatically with the correspondent flow resulting from the reaction: N_2 with the hydrogen stream and CO_2-H_2O present in the syngas with the exhaust flue gas. The H_2O in the CO_2-H_2O stream (exiting the oxidation/reduction splitter) corresponds to the same number of moles of the H_2 present in the syngas. The remaining part of steam entering this splitter is sent to the oxidant flow because it corresponds to the H_2O not reacted in the oxidation reactor.

At the end of the CL unit a heat exchanger that equalizes the temperature of the two output streams is provided.

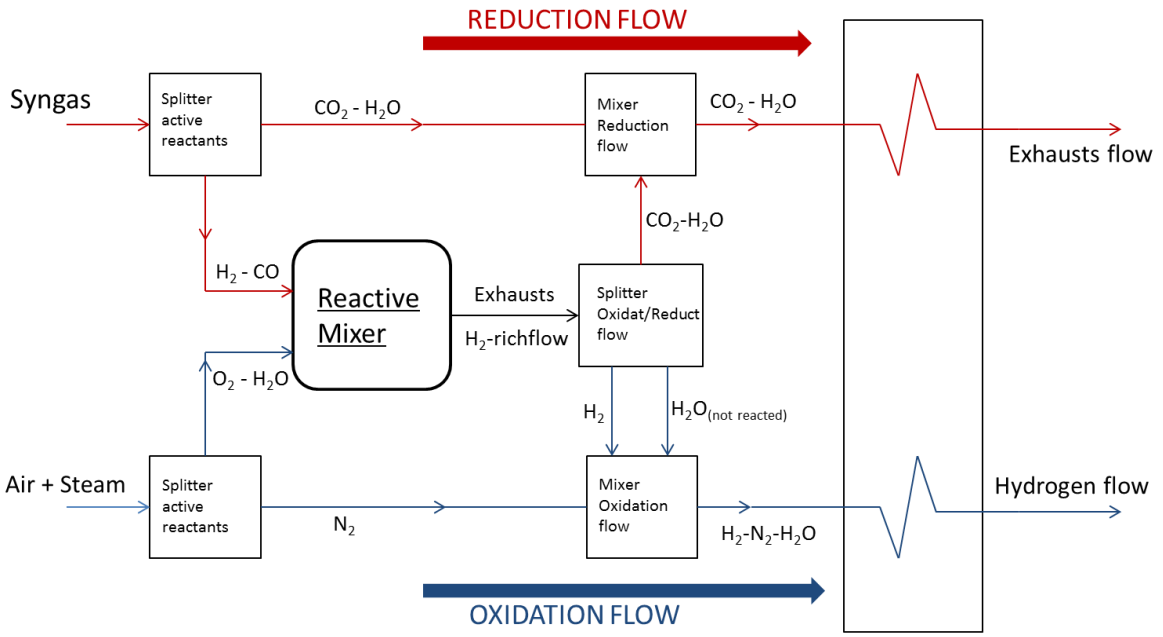

Figure 3.6: Conceptual simulation scheme of the CL island.

Assumptions and clarifications about the simulation of the PeCLET process are discussed here below:

1) Equivalent system of two reactions: based on the syngas oxidation and the WGS, as previously described.
2) Thermal balance: as said before, the two reactions system adopted for the simulation does not alter the overall energy balance of the process. Furthermore, the heat released in the CL unit, mostly created by the exothermic oxidation reaction, is totally allocated in the two outlet flows (hydrogen and exhausts flows). This results in an increase of the outlet temperature of the two streams, whose value is evaluated in accordance with the assumption explained in the following point 3).
3) Temperatures of the two outlet streams: the two temperatures are equalized at the outlet of the CL unit. This assumption has to be confirmed, but it is reasonable for the preliminary analysis of the reactors system required in this work.
   The kinetics of the reactions, the profile temperature of the PBR's and consequently the outlet flows temperatures should be subject to further investigation in future studies.
4) Total conversion: a complete conversion of CO and H_2 towards CO_2 and H_2O is assumed in the reduction reactor. In fact, except for some very limited fuel slip that always occurs, the conversion and the selectivity of a good OC can be very high, as the case of Ilmenite in the CLC [4]. Concerning the oxidation, the maximum H_2 production achievable is considered. Thermodynamically this is feasible by feeding the AR with a steam excess which assures a complete conversion of the Me to MeO (*Sec. 3.2.2* Air-to-Steam ratio in the feed).

5) Initial temperature and pressure: the simulations will be carried out at 20 bar and at the temperatures listed in the following Table 3.1: Operating temperatures in the simulation:

	T [°C]	Comment
Syngas inlet T	517	The syngas is pre-heated up to this T by cooling down the exhausts flow.
Air inlet T	450	The outlet temperature of a compression up to 20 bar.
Steam inlet T	450	The same temperature of the air were assumed.
Outlet streams T	Same T	Both the reduction and oxidation outlet

Table 3.1: Operating temperatures in the simulation

6) Initial Compositions: the syngas, as it will be shown in the next chapter (*Chapter 4*), before entering the fuel reactor is diluted with a certain quantity of recycled exhaust flow. The composition of the oxidation feed varies with the Air-to-steam ratio which will be discussed in depth in the following (*Sec. 3.2.3* Presentation of the results).

Molar fraction	Ar	CO	CO_2	H_2	H_2O	N_2
Syngas	0.01	0.3355	0.3408	0.1367	0.1640	0.013
Air + Steam	It varies as a function of the air-to-steam ratio					

Table 3.2: Inlet flows composition

3.2.2 Air-to-Steam ratio in the feed

The air-to-steam ratio in the feed to the oxidation stage is of particular importance, because it affects the design and the performance of the entire power plant. In this work a sensitivity analysis on this parameter is extensively carried out.
The air-to-steam ratio is studied in this case in relation to two different parameters:

a) **% of Oxygen from Air**: it is the percentage of equivalent oxygen[2], necessary for the entire bed oxidation, which is supplied by air. The remaining is provided by the H_2O-splitting reaction. The simulation will be carried out for values of this parameter ranging from 0% to 50%.

b) **Steam excess**: The oxidation reactor will be always fed with an excess of steam. As it is shown in 78 the thermodynamic equilibrium of the reactions involving the steam and the metal oxide is not fully towards the products. Hence, in order to reach a complete conversion of the OC in the H_2O-splitting reaction, an excess of

[2] Equivalent oxygen: When the FR is fed with a constant amount and composition of syngas, a fixed oxygen molar flow entering the CL unit is needed for the complete oxidation of the fuel. This fixed stoichiometric value is the "equivalent oxygen". In the PeCLET process, the oxidant is supplied by sub-stoichiometric air and steam. From the stoichiometry (3.1) and (3.2):

$$O_2, equivalent = \frac{1}{2} \times \dot{n}_{CO} + \frac{1}{2} \times \dot{n}_{H2}$$

steam has to be fed to the AR. The simulation will be carried out with an excess of steam ranging from 0% to 50%.

The air-to-steam ratio is strongly affected by the chosen oxygen carrier. In particular, a minimum value of the "% of Oxygen from air" is determined by the stoichiometry associated to the oxygen carrier, while the value of steam excess that is needed for achieving a complete conversion of the metal oxide is established by the thermodynamics. Two real cases with Fe and FeO as starting state of the oxidation step will be discussed in Chapter 5.

3.2.3 Presentation of the results

The air-to-steam ratio is a key parameter of the PeCLET process. As explained in (3.2.1 Simulation scheme, the process is studied by means of two reactions: the Oxidation Reaction and the WGS.

When the CL unit is operated at a high air-to-steam ratio, the weight of the oxidation reaction grows at the expense of the WGS and the exothermicity of the entire process is therefore increased. The LHV of the inlet syngas is then allocated more on sensible heat (temperature of the outlet streams) than on hydrogen production, as represented in the following (Figure 3.77).

The main characteristic of the air-to-steam ratio is therefore to establish the amount of energy entering the CL unit that is converted into hydrogen production rather than sensible heat.

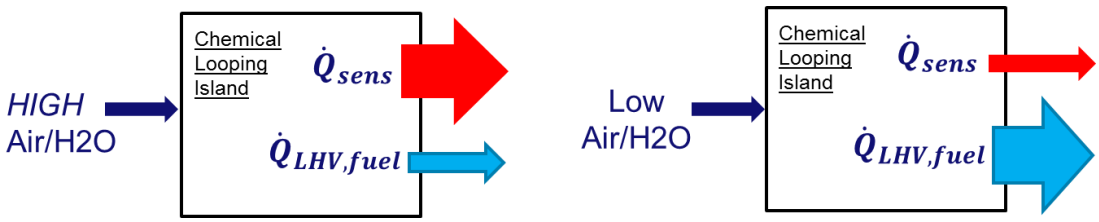

Figure 3.7: Air-to-steam ratio influence.

In other words, the air-to-steam ratio affects the allocation of the syngas LHV, since it sets the subdivision, between the two possible feeds (air and steam), in the supply of the equivalent oxygen required in the CL reactors.

For these reasons, the sensitivity analysis on the air-to-steam ratio carried out in the entire work are mostly made by means of the "% O_2 from air" parameter, which really defines the fraction of equivalent oxygen supplied by air (and, as a consequence, the fraction provided by the steam).

On the other hand, the steam excess quantifies in itself a surplus from the stoichiometric and doesn't affect the allocation of the syngas LHV, but only the steam dilution of the CL outlet flows.

Moreover, the study carried out in (58) shows that the Steam excess doesn't even affect the net electrical efficiency of the power plant.

In the following figure (Figure 3.88), the CGE[3] and the hydrogen production (expressed as $\dot{m}_{H2,\,out}/\dot{m}_{H2,eq,in}$) are shown as a function of the "% O_2 from air" (six values from 0% to 50%). As said, increasing the "% O_2 from air" means higher air-to-steam ratio in the AR feed.
From this figure, the hydrogen production decreases with the increase of the "% O_2 from air". This leads to a correspondent drop of the Cold Gas Efficiency (CGE) of this process.
This trend is not a direct expression of the global efficiency of the whole plant. In fact the syngas thermal power which is not converted in hydrogen, becomes sensible heat of the two outlet streams from the CL unit. Hence, the efficiency of the whole plant depends not only on the CGE, but also on how efficiently the sensible heat released in the CL unit is recovered in the thermodynamic cycle.
Nevertheless the CGE remains an important parameter because it can be seen as an expression of how simply the PeCLET process is integrated with the power plant. The net hydrogen production is indeed the easiest way for integrating this concept in the thermodynamic cycle, because the H_2-rich flow can be directly used as input of the gas turbine. Instead, an efficient sensible heat recovery needs the installation of additional steam generation facilities.

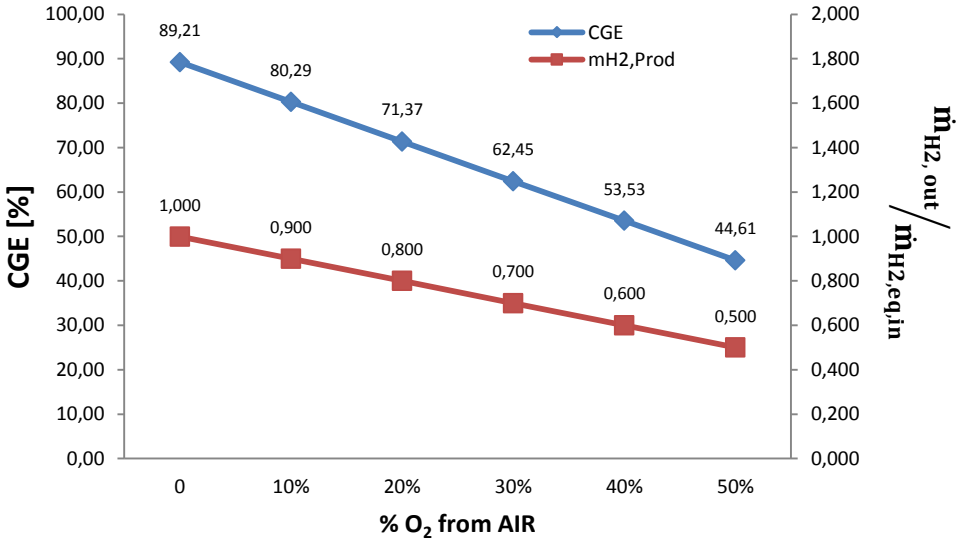

Figure 3.8: CGE and hydrogen production as a function of "% O_2 from air"

Other results of the work are shown in the following (Figure 3.99), representing the outlet temperature of the reactors vs. the "steam excess", at different "% O_2 from air" (from 0% to 50%).

[3] CGE: The cold gas efficiency of the PeCLET process is expressed as:

$$CGE = \frac{\dot{m}_{Hydrogen-flow,out} \times LHV_{hydrogen-flow,out}}{\dot{m}_{syngas,in} \times LHV_{syngas,in}}$$

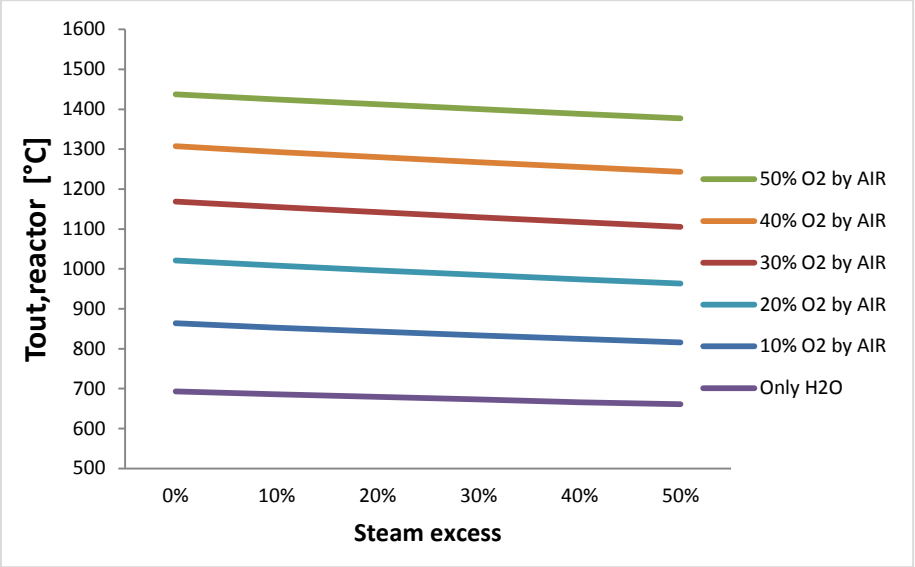

Figure 3.9: Outlet streams temperature as a function of "%O_2 from air" and "Steam excess".

From this figure, it is evident that the increase of the "% O_2 from air" leads to a strong increase of the reactor outlet temperature, due to the higher heat released associated to the oxidation reaction. The "Steam excess" has instead a lower influence on it.
For example, at 30% of steam excess, the reactor outlet temperature increases from 670°C to 1400°C when the oxygen from air is raised up from 0% to 50%.

To complete of the work results, also the trend of the hydrogen concentration in the fuel flow exiting the CL island is depicted in the following figure (Figure 3.1010), as a function of "steam excess" at different "% O_2 from air".
From this figure it can be seen that the increase of the "% O_2 from air" leads to a sensible decrease of the hydrogen molar fraction in the fuel produced in the CL reactors.
The influence of the steam excess on the hydrogen molar fraction depends on the considered "% O_2 from air": the "steam excess" has a little influence when the CL unit is operated with high air-to-steam ratio, because this excess, expressed in %, is calculated on a little quantity of steam present in the AR feed. On the other hand, when more steam is entering the CL unit (lower "% O_2 from air"), the influence of his excess on the outlet flows composition naturally increases.
The hydrogen molar fraction has to be in accordance with the gas turbine needs, in particular the LHV of the fuel flow should be enough high. On the other hand, the use of a diffusive combustor leads to a limitation of the adiabatic flame temperature in order to reduce the NO_x production. When the molar fraction of hydrogen is too high, additional nitrogen dilution should be provided.

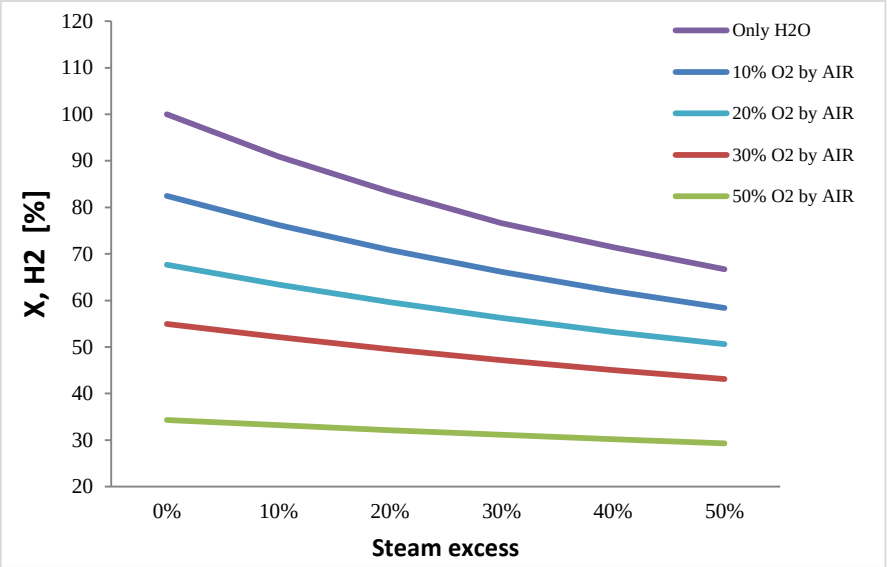

Figure 3.10: Hydrogen molar fraction in the outlet fuel flow

In conclusion, in order to work with an elevated hydrogen production and with relative low reactors exit temperature, the process should be operated with a low air-to-steam ratio. In this way the PeCLET process advantages could be completely exploited.

Though, when the OC forces to work with a higher ‘‘%O_2 from air”, it becomes fundamental to decrease the CL outlet temperature and to introduce an efficient heat recovery; otherwise the global efficiency would sensibly decrease.

As it will be widely discussed in the next chapter, a solution to this problem that can be worked out, is the addition of a Heat Removal phase in the reactor work cycle, accomplished by a pre-heating of the air exiting the gas turbine compressor.

Chapter 4

Integration of PeCLET process with IGCC plant

4.1 Integration guidelines and Description of the work

4.1.1 Integration guidelines

In the previous Chapter (*Chapter 1*) it has been explained that the energy outputs of the CL island based on PeCLET process are sensible heat, leading to an increase of the outlet flows temperature, and produced hydrogen. The allocation of the syngas LHV in these two components depends on the Air-to-steam ratio which the PeCLET process is fed with.
In the following Figure 4.1, a simplified integration scheme is presented. Two different ways of converting the fuel from the CL are shown: the combined cycle (gas turbine plus heat recovery steam cycle) and the steam cycle (much less efficient than the combined cycle). In order to reach the best performance, the combined cycle way should be walked through. In the combined cycle, the hydrogen flow is directly used as feed, while the sensible heat is not always easily converted.

In conclusion, the easiest way for achieving high efficiency is to allocate as much as possible the energy entering the CL island on the hydrogen production, by working with low "%O_2 from air". But with some OC this is not possible. In this case a new and efficient strategy for the sensible heat recovery needs to be developed.

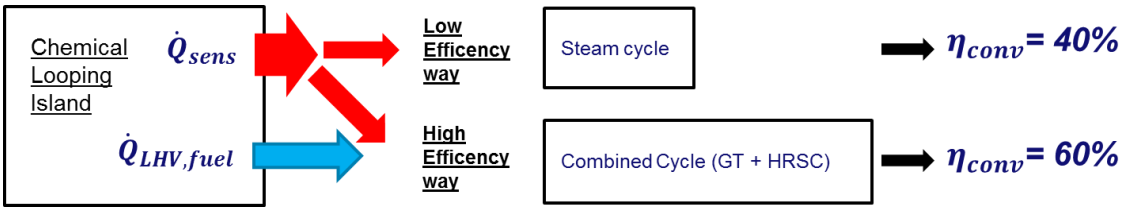

Figure 4.1: Integration guidelines

4.1.2 Description of the work

In this chapter different power plant designs are presented. Evaluation of the performance through plant simulation, as well as sensitivity analysis on the air-to-steam ratio and on the operating pressures carried out in this work, are also presented.

Two different plant configurations are proposed, depending on the Air-to-steam ratio. For low value of "%O from air" a simple integration of the PeCLET process as it was described in the Chapter 1 is considered ("Base case plant"). For higher value of this parameter a more integrated plant design is developed, with the addition of a heat removal phase in the reactor work cycle, accomplished by pre-heating of the compressed air of the gas turbine ("Heat removal plant").

The choice of Iron-based OC and his influence on the "% O_2 from air" and "Steam excess" parameters will be discussed in the next chapter (*Chapter 5*). However, the two possible reduced states of this metal oxide, Fe and FeO, fits perfectly the two kinds of power plant proposed so that they are used as real examples in this section. Pure iron, due to its "% O_2 from air" of 11.1%, is used in the Base case plant; on the other side, the Heat removal plant is suitable for the higher value of "%O_2 from air" needed when using the FeO as OC (33.3%). These two values of the "% O_2 from air" come out from the oxidation reaction stoichiometry of the correspondent iron-oxides, which are briefly presented here below:

a) FeO oxidation reaction:

$$3FeO + H_2O \leftrightarrow H_2 + Fe_3O_4 \tag{4.1}$$

$$Fe_3O_4 + \frac{1}{4}O_2 \leftrightarrow \frac{3}{2}Fe_2O_3 \tag{4.2}$$

From this stoichiometry, the %O_2 from air can be easily calculated as:

$$\%O_2\ from\ air = \frac{{}^1/_4\, mol, O_2\ from\ air}{{}^1/_2\, mol, O_2\ from\ steam + {}^1/_4\, mol, O_2\ from\ air} = 33.3\ \% \tag{4.3}$$

b) Fe oxidation reaction:

$$3Fe + 4H_2O \leftrightarrow 4H_2 + Fe_3O_4 \quad (4.4)$$

$$Fe_3O_4 + \frac{1}{4}O_2 \leftrightarrow \frac{3}{2}Fe_2O_3 \quad (4.5)$$

From the stoichiometry above the $\%O_2$ from air is easily calculated by:

$$\%O_2\ from\ air = \frac{^1/_4\ mol, O_2\ from\ air}{2\ mol, O_2\ from\ steam + {}^1/_4\ mol, O_2\ from\ air} = 11.1\ \% \quad (4.6)$$

For a broader discussion about the oxidation reaction of the iron-oxides, including the thermodynamics, see 73.

The direct competitor of the PeCLET process integrated with an IGCC is the IG-CLC plant presented in the [4]. A comparison between these two technologies is carried out in this work. To do that, some assumptions regarding the gasification and syngas cleaning process, the efficiency of the turbo-machines and the all process of the CO2 compressing unit, are taken from the IG-CLC case.
All the simulations carried out in this work consider the same coal thermal input (859 $MW_{th,(LHV)}$) and the same mass flow rate and composition of the syngas exiting the gasification and cleaning unit.

4.2 Base case plant

The Base case plant scheme is represented in the Figure 4.2. It originates from the integration of four main units:

- Syngas production and cleaning: the coal is gasified and the resulting syngas is cleaned from sulfur and other impurities. The output is a low temperature high-pressure purified syngas. This process is very similar to the one used in the IG-CLC case [4].
- CL island: in this unit the syngas is converted into CO_2-H_2O; H_2 rich flow is also generated and fed to the gas turbine combustor as described in the previous chapter (*0*).
- Power island: the power is in a combined cycle unit based on an advanced H_2-fuelled gas turbine. Additional steam at different pressure levels is firstly produced by cooling down hot streams from the CL island, and then it evolves in a highly integrated heat recovery steam cycle for extra electricity production.
  In addition to the main gas turbine compressor, an extra air compressor for the oxidation reactor feeding is provided.

- CO_2 treating unit: the CO_2-H_2O rich flow exiting the reduction reactor of the CL island, after a proper heat recovery process is cooled down to nearly ambient temperature and then dried and compressed in such a way to produce a high purity CO_2 stream ready for a long-term storage.

A detailed description of the Base case plant represented in Figure 4.2 is given in the following paragraphs 4.2.1 through 4.2.5.

The thermodynamic properties of the streams referred to this plant configurations are shown in Table 4.1: Thermodynamic properties of the streams reported in

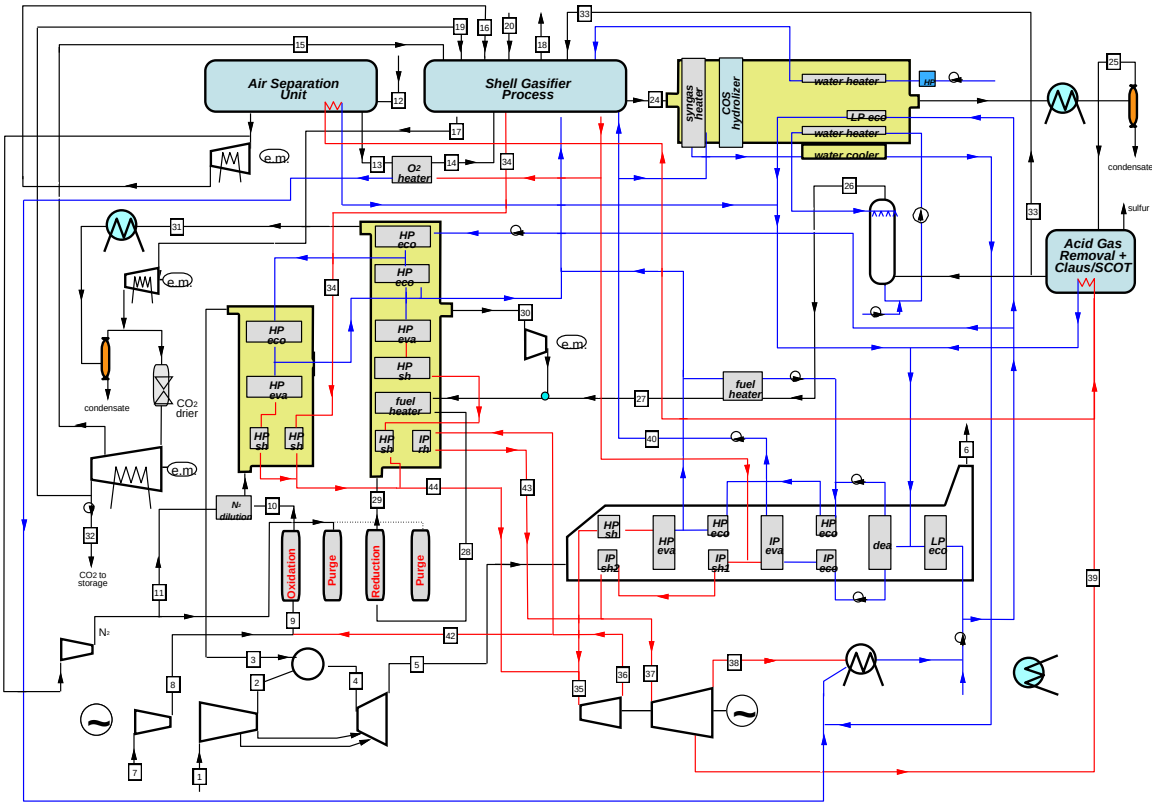

Figure 4.2: Detailed layout of the base case plant, ("Fe case")

and **Errore. L'origine riferimento non è stata trovata.**, "Fe case" (%O_2 from air = 11.1%; Steam,excess = 40%; $\beta_{gas\text{-}turbine}$= 18).Table 4.1.

The simulations of the plant scheme have been carried out by the proprietary computer code GS (Gecos, 2013) developed by the GECOS group at the Department of Energy of Politecnico di Milano. The calculation code is designed according to a modular structure allowing to calculate complex plant configurations [4]. Among the components available in the code (e.g. compressor, expander, splitter, mixer, heat exchanger, combustor, pump) the gas turbine model deserves particular attention, because it is able to simulate a cooled expansion on the basis of a one-dimensional design of the turbine stages for an accurate estimation of the cooling flows for each row, as described in [25]. The CO_2 compression unit is calculated by using Aspen Plus 7.3 (Aspen Technology, 2011), adopting the Peng–Robinson equation of state with default coefficient for the evaluation of the fluid mixture properties. AGR and ASU units are not simulated in this work, but specific electric and thermal consumptions are taken from [26] and [27] respectively.

The detailed plant layout (**Figure 4.2**) and the thermodynamic properties of the streams (**Table 4.1: Thermodynamic properties of the streams reported in**

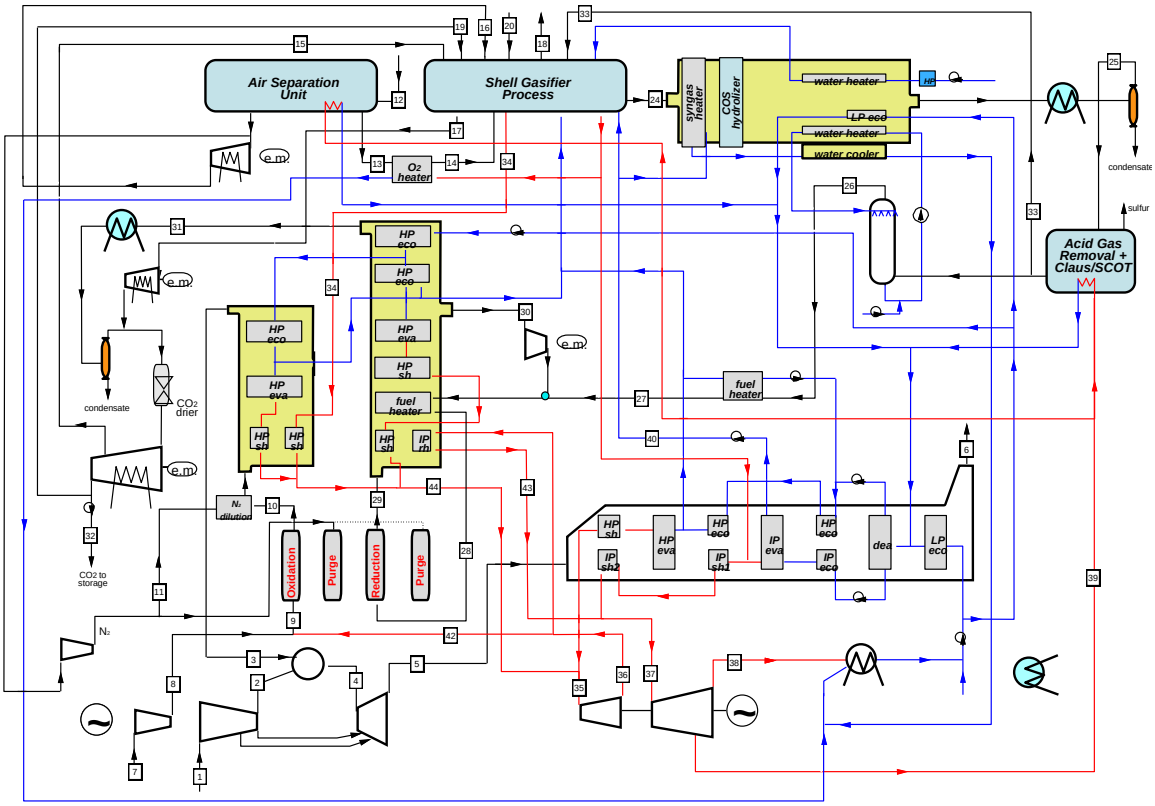

Figure 4.2: Detailed layout of the base case plant, ("Fe case")

and **Errore. L'origine riferimento non è stata trovata.**, "Fe case" (%O_2 from air = 11.1%; Steam,excess = 40%; $\beta_{gas\text{-}turbine}$= 18).Table 4.1) are referred to the "Base case plant" operated with "Fe" as most reductive state of the iron-based OC. In this case the CL unit works with: % O2 from air = 11.1%, Steam excess = 40% as calculated from the equilibrium composition.

The numbering of the streams shown in the Table 4.1.1 follows the numbering adopted in the detailed plant layout (Figure 4.2) and in the schematic drawing of the gasification unit (Figure 4.3).

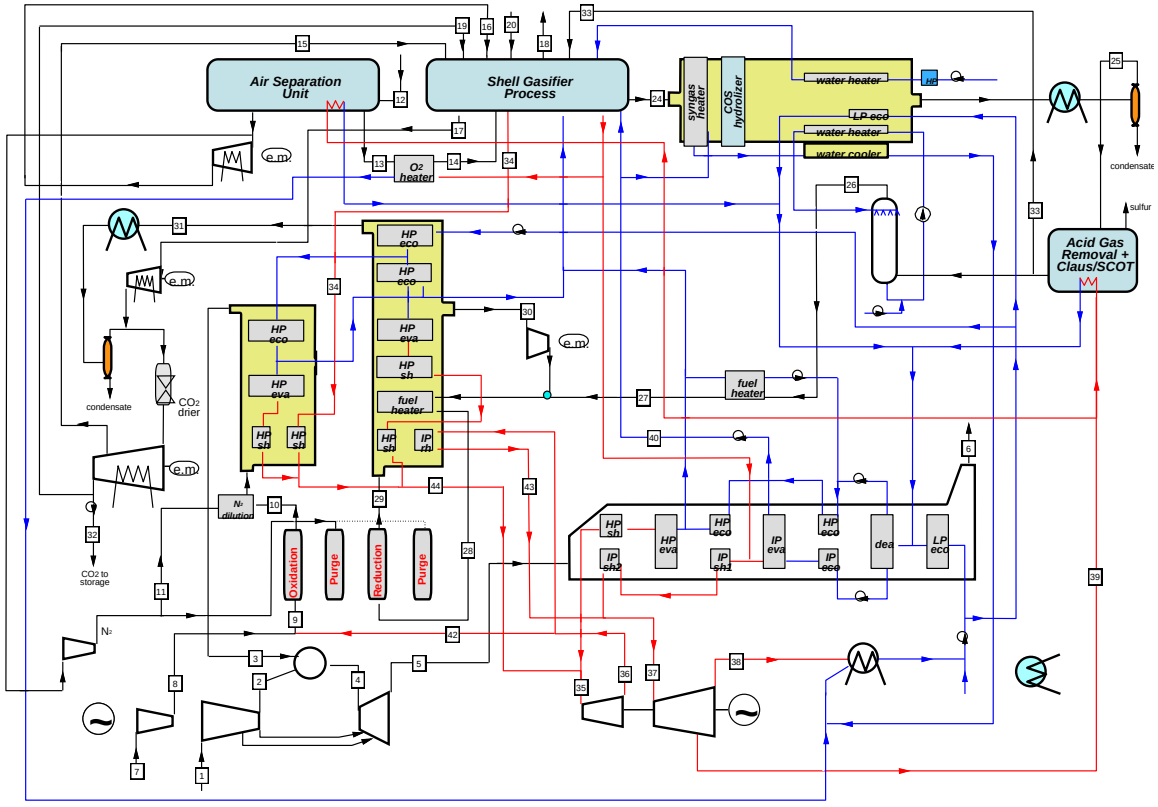

Figure 4.2: Detailed layout of the base case plant, ("Fe case")

	T	P	m	MW	Q	stream composition (vol. basis)									HHV	LHV
	°C	bar	kg/s	kg/kmol	kmol/s	*Ar*	*CO*	*CO_2*	*H_2*	*$H_2O(g)$*	*H_2S*	*N_2*	*O_2*	*$H_2O(l)$*	*MJ/kg*	*MJ/kg*
#1	15.0	1.0	430.9	28.9	14.9	0.9	-	0.03	-	1.0	-	77.3	20.7	-		
#2	416.8	18.0	367.77	28.9	12.7	0.9	-	0.03	-	1.0	-	77.3	20.7	-		
#3	200.0	18.0	46.6	11.4	4.1	0.2	-	0.01	55.3	22.3	-	22.3	-	-	14.7	11.7
#4	1460.9	17.3	365.1	26.1	14.0	0.8	-	0.03	-	23.4	-	67.5	8.3	-		
#5	602.4	1.1	477.5	26.7	17.9	0.8	-	0.03	-	18.5	-	69.6	11.0	-		
#6	80.0	1.0	477.5	26.7	17.9	0.8	-	0.03	-	18.5	-	69.6	11.0	-		

#7	15.0	1.0	19.6	28.9	0.7	0.9	-	0.03	-	1.0	-	77.3	20.7	-		
#8	602.8	36.1	19.6	28.9	0.7	0.9	-	0.03	-	1.0	-	77.3	20.7	-		
#9	510.0	36.1	76.5	20.3	3.9	-	-	-	-	84.5	-	13.8	3.7	-		
#10	816.5	35.74	35.9	9.7	3.7	0.2	-	0.01	61.0	24.6	-	14.2	-	-	19.1	15.2
#11	400	18.75	10.8	28.0	0.4	-	-	-	-	-	-	100	-	-		
#12	15.0	1.0	120.7	28.9	4.2	0.9	-	-	-	1.1	-	77.3	20.7	-		
#13	15.0	48.5	28.9	32.2	0.9	3.1	-	-	-	0.0	-	1.9	95.0	-		
#14	180.0	48.0	28.9	32.2	0.9	3.1	-	-	-	0.0	-	1.9	95.0	-		
#15	80.0	56.0	23.7	43.7	0.5	1.4	-	96.8	-	0.0	-	1.8	-	-		
#16	122.3	56.0	2.4	28.0	0.1	-	-	-	-	-	-	100	-	-		
#17	33.0	1.0	13.1	43.7	0.3	1.4	-	96.8	-	0.0	-	1.8	-	-		
#18	81.6	1.0	4.7	34.1	0.1	0.6	-	37.8	-	0.0	-	61.6	-	-		
#19	33.0	88.0	2.7	43.7	0.1	1.4	-	96.8	-	0.0	-	1.8	-	-		
#20	15.0	-	32.0	-	-	***Douglas Premium Coal***									27.7	26.8
#21	900.0	44.0	127.4	22.6	5.6	1.0	57.4	8.4	23.4	8.4	0.2	1.2	-	-	10.4	9.7
#22	300.0	41.7	127.4	22.6	5.6	1.0	57.4	8.4	23.4	8.4	0.2	1.2	-	-	10.4	9.7
#23	210.9	44.4	60.3	22.5	2.7	0.9	53.0	8.6	21.6	14.5	0.2	1.2	-	-	9.7	9.0
#24	165.0	41.7	79.0	22.3	3.5	0.9	51.5	8.5	21.0	16.8	0.2	1.1	-	-	9.6	8.8
#25	35.0	38.8	68.2	23.2	2.9	1.1	61.8	10.2	25.2	0.1	0.2	1.4	-	-	10.7	10.2
#26	126.8	38.42	71.7	22.9	3.1	1.0	58.1	9.6	23.7	6.4	-	1.3	-	-	10.3	9.7
#27	300.0	36.1	71.7	22.9	3.1	1.0	58.1	9.6	23.7	6.4	-	1.3	-	-	10.3	9.7
#28	517.0	36.1	152.6	28.4	5.4	1.0	33.6	34.1	13.7	16.4	-	1.3	-	-	5.0	4.5
#29	816.5	33.9	193.1	35.9	5.4	1.0	-	67.6	-	30.1	-	1.3	-	-	0.4	0.0
#30	348.9	32.2	81.5	35.9	2.3	1.0	-	67.6	-	30.1	-	1.3	-	-	0.4	0.0
#31	115.2	30.5	111.6	35.9	3.1	1.0	-	67.6	-	4.1	-	1.3	-	25.9		
#32	27.8	110.0	81.3	43.7	1.9	1.4	-	96.7	-	-	-	1.9	-	-		
#33	60.0	36.1	0.7	22.8	0.7	1.0	58.1	9.6	23.7	6.4	-	1.3	-	-	10.3	9.7
#34	400.0	144.0	71.3	18.0	4.0	-	-	-	-	100	-	-	-	-		
#35	563.2	133.9	162.0	18.0	9.0	-	-	-	-	100	-	-	-	-		
#36	359.8	36.1	162.0	18.0	9.0	-	-	-	-	100	-	-	-	-		
#37	563.8	33.1	110.3	18.0	6.1	-	-	-	-	100	-	-	-	-		
#38	32.2	0.05	105.9	18.0	5.9	-	-	-	-	100	-	-	-	-		
#39	267.4	4.1	2.3	18.0	0.1	-	-	-	-	100	-	-	-	-		
#40	244.2	36.1	7.7	18.0	0.4	-	-	-	-	-	-	-	-	100		
#41	300.0	54.0	2.9	18.0	0.2	-	-	-	-	100	-	-	-	-		
#42	359.8	36.1	56.9	18.0	3.2	-	-	-	-	100	-	-	-	-		
#43	565.0	36.1	105.2	18.0	5.8	-	-	-	-	100	-	-	-	-		
#44	565.0	133.9	95.3	18.0	5.3	-	-	-	-	100	-	-	-	-		

Table 4.1: Thermodynamic properties of the streams reported in

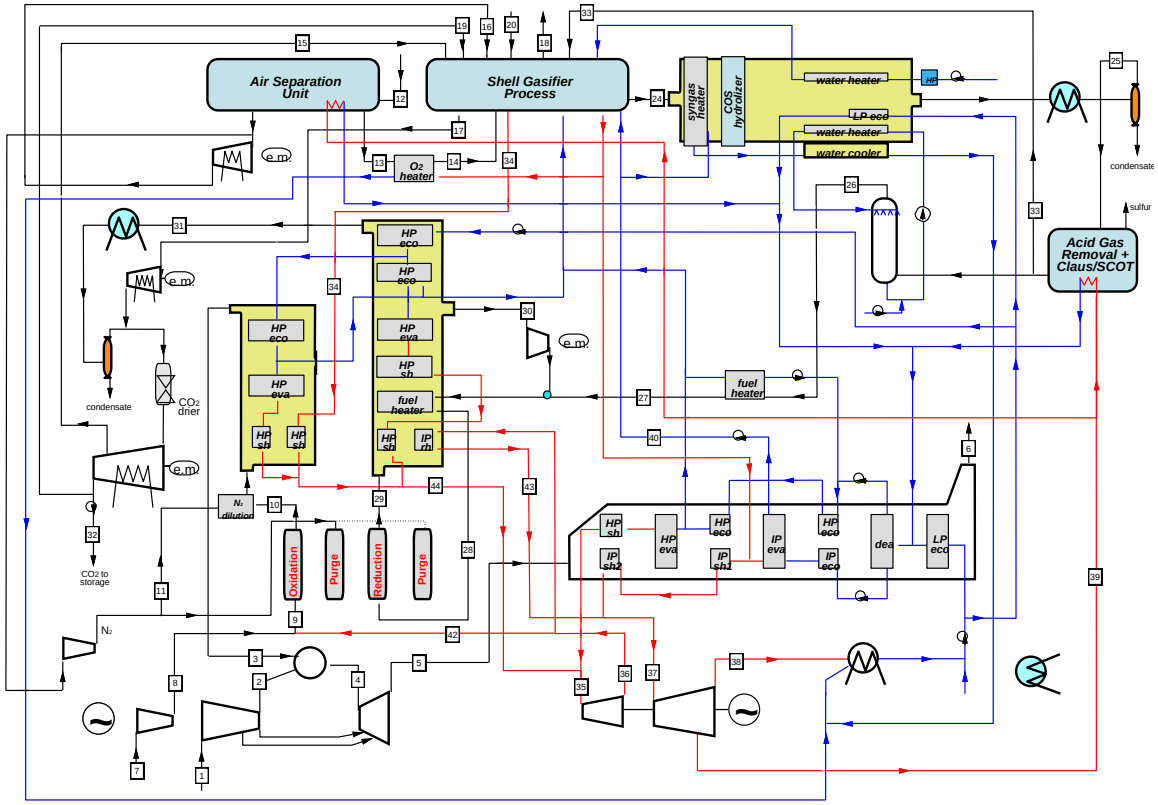

Figure 4.2: Detailed layout of the base case plant, (“Fe case”)

and Errore. L'origine riferimento non è stata trovata.**, “Fe case” (%O_2 from air = 11.1%; Steam,excess = 40%; $\beta_{gas\text{-}turbine}$= 18).**

4.2.1 Gasification and syngas cleaning

The streams numbering adopted in the schematic of the gasification unit (Figure 4.3) is the same as the power plant layout depicted in (Figure 4.2).

In this plant, the entrained flow, oxygen blown, dry feed Shell-type gasification process represented in **Errore. L'origine riferimento non è stata trovata.** is used. The coal is grinded and then dried by the combustion of free-sulfur syngas taken from the outlet of the AGR unit (#33). The dried coal is then fed to the gasifier, operating at 44 bar and 1560°C, by using pure CO_2 as carrier gas in the lock hoppers (#15) instead of N_2, as it is usual in dry feed gasifiers for IGCC plants. This choice was made in order to avoid excessive dilution of the final CO_2 stream. Part of the CO_2 released from lock-hoppers is recovered, re-compressed and fed to the CO_2 treating unit to reduce the CO2 emissions to the atmosphere (#17). Part of the N_2 from the Air Separation Unit (ASU) (#16) is also used in the lock hoppers (around 10% of the total amount of gas required) and then vented to the atmosphere with the remaining CO_2 (#18). The gasifier is a slagging reactor with membrane walls cooled with water boiling at 54 bar. It is characterized by high carbon conversion (>99%) and cold gas efficiency (around 80%). The high purity oxygen flow (95%) is provided by a stand-alone, dual-reboiler low-pressure cryogenic ASU, whose specific consumptions are taken from the [27]. In the ASU this O_2 stream is pumped in liquid phase to the required pressure, and then fed to the gasifier in gaseous phase after being heated up to 180°C (#18) by condensing IP steam.

The hot syngas exiting the gasifier is quenched to 900°C (#21) with low temperature recirculated syngas (#23) taken partially downstream the LT syngas cooler and partially downstream the scrubbing unit. Data on syngas composition at point #21 (after mixing with recycle quench stream (#23)) provided by the industrial partners of the Democlock project (FP7 Democlock, 2011-2015) were used to calibrate the gasifier model [4]. At the temperature of 900°C, the molten fly ashes entrained by the syngas solidify, and then the resulting flow is cooled down to 300°C in a convective heat exchanger by producing superheated steam at 400°C (#34). This temperature cannot be higher to limit the heating up of the heat exchanger tubes, thus avoiding the risk of the metal dusting caused by the CO present in the syngas. The syngas stream, after a first fly ashes removal in the cyclone, is washed in a wet scrubber unit which removes residual solids and soluble contaminants.

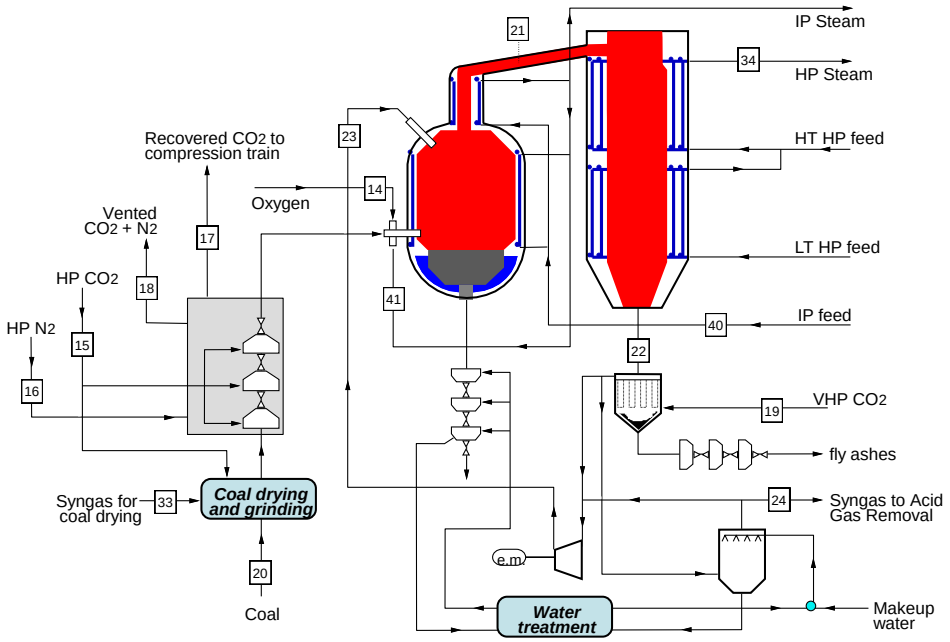

Figure 4.3: Schematic of the Shell gasification unit

SYNGAS UNIT CONVERSION MAIN ASSUMPTIONS	
Gasification and coal pre-treating unit	
Gasification pressure, bar	44
Oxygen to carbon ratio, kg_{O2}/kg_{coal}	0.903
Heat losses in gasifier, % of input LHV	0.7
H_2O in coal after drying, % wt.	2
Fixed carbon conversion, %	99.3
Moderator steam, kg_{H2O}/kg_{coal}	0.09
Moderator steam pressure, bar	54
Oxygen pressure, bar	48
Temperature of O_2 to gasifier, °C	180
Heat to membrane walls, % of input coal LHV	2
Slag handling, kJ_e/kg_{ash}	100
Syngas quench	
Quenched syngas temperature, °C	900
Cold recycled syngas temp, °C	300
Recycle compressor polytropic efficiency, %	75
Recycle compressor el./mech. efficiency, %	92
CO_2 operated lock hoppers	
VHP/HP CO_2 pressure, bar	88/56
CO_2 temperature, °C	80
CO_2 consumption, $kg_{CO2}/kg_{dry\text{-}coal}$	0.826
Electric consumption for coal milling and handling, kJ_e/kg_{coal}	50
CO_2 not recovered for CCS, % of CO_2 inlet flow rate	10

Bituminous Douglas Premium Coal composition (ult. analysis, %)	
C 66.52; N 1.56; H 3.78; S 0.52; O 5.46, Ash 14.15; Moisture 8;	
ASU	
Oxygen purity, % mol.	95
Pressure of delivered oxygen, bar	48
Pressure of delivered nitrogen, bar	1.2
Temperature of delivered O_2 and N_2, °C	22
Electric consumption, kWh_e/tO_2	325
LP steam heat rate for TSA beds regeneration, kWh_{th}/t_{O2}	58.3
Heat exchangers	
Minimum ΔT in liquid-liquid heat exchangers, °C	10
Minimum ΔT in gas-liquid heat exchangers, °C	10
Minimum ΔT in gas-gas , °C	25
Minimum ΔT in condensing fluid-liquid heat exchangers, °C	3
Heat losses, % of heat transferred	0.7
Gas side Pressure drop, %	2
Maximum steam T in the Syngas Coolers, °C	400
Sulfur removal unit (Selexol solvent)	
Syngas temperature at absorption tower inlet, °C	35
Syngas pressure loss, %	1
LP steam heat rate, MJ_{th}/kg_{H2S}	20.95
Electric consumption for auxiliaries, MJ_e/kg_{H2S}	1.93
Miscellaneous BOP, % of input coal LHV	0.15
Overall pressure losses before PBR, %	11

Table 4.2: Set of assumptions for the simulation of the syngas production and purification unit, [3].

Before removing sulfur from the syngas, the COS is hydrolyzed to H2S in a fixed bed catalytic reactor working at 180°C. The resulting syngas (#24) is then cooled down to nearly ambient temperature and sent to the Acid Gas Removal (AGR) unit. Here, H_2S is removed from syngas by washing it with selective solvents in an absorption tower operating at high pressure and low temperature. A Selexol physical absorption process, utilizing dimethyl ether of polyethylene glycol as solvent, has been assumed for evaluation of the plant mass and thermal balance: sulfur removal efficiency exceeds 99%. The heat for the reboiler of the solvent regenerator is provided by condensing LP steam (#42). The acid gas produced at the top of the regenerator is sent to a Claus Unit where the H_2S is converted to elemental sulfur. The Claus Unit tail gas, still rich in sulfur compounds, is afterwards treated in a SCOT unit, where the residual sulfur species are catalytically converted back to H_2S and recycled to the absorption column of the AGR unit [4].
The desulfurized syngas, after a first warm-up in the saturator (#26), is heated up to 300°C (#27) by cooling down HP saturated water.

4.2.2 CL unit

The PeCLET process characterizing the CL island has been already analyzed in the previous chapter (*0*). In this paragraph a description of the operating conditions is presented.
The operating pressure of this section is independent from the gas turbine and can be therefore kept higher in order to reduce the reaction volumes and the number of reactors, as well as the power consumption of the CO_2 compression unit. It was set at 36.1 bar, equal to the syngas pressure exiting the last process unit upstream of the CL island (#28).
The sulfur-free syngas, passed through the water saturator, needs some further treatment before being fed to the reactor: a proper dilution to avoid carbon deposition during the reduction and an additional warm-up to achieve the desired inlet temperature. The syngas is then mixed with recirculated exhaust gas (#30) with two scopes: obtain the required composition at reduction reactor inlet (CO_2+H_2O fraction higher than 50% molar basis) and accomplish the first heat up the syngas. The stream (#28) is further heated up to 517°C by cooling down the hot CO_2-rich stream exiting the Cl unit.
On the other side of the CL unit, the air feeding the oxidation reactor (#8) is compressed up to 36.1 bar by a dedicated compressor and then mixed with IP steam leaving the HP section of the steam turbine (#42). The resulting stream (#9) reacts with metal oxide producing a hydrogen flow (#10) which is then diluted with nitrogen and cooled down before entering the gas turbine combustor (#3).
The simulations will be carried out forcing the CL outlet temperatures to be at the same value (*0*).

4.2.3 CL Exhausts and hydrogen flow cooling

Both the reduction (#29) and oxidation (#10) flows exiting the CL reactors must be cooled down. In the CLC case the exhausts flow only was cooled down in the heat recovery process. Instead, in the PeCLET configuration, the hydrogen stream has to be cooled down because it is not allowed to enter the combustor at very high temperature.
In this paragraph the cooling schemes of the exhausts from the reduction reactor and of the hydrogen from the oxidation reactor are described.

- Reduction reactor outlet flow: the exhausts stream is mostly cooled down by the use of a typical heat exchanger train for the production of HP superheated steam, as it is conceptually depicted in the (**Errore. L'origine riferimento non è stata trovata.**): the stream is firstly used to heat up the saturated steam to 565°C and then to produce steam in the evaporation section. The reduction flow is then cooled down in an economizer which is divided in two parts at the dew point (185°C in this case). The low temperature part of the economizer (ECO A) exchanges a great quantity of heat associated to the steam condensation in the exhausts. Though this heat is available at low temperature (with a low thermodynamic value), it can be as well useful in the power plant to produce a great amount of hot water at 170°C. This hot water is used for feeding the following part of the economizer (ECO B) and also the economizer of the hydrogen flow cooling train (as depicted in the plant layout, Figure 4.2).

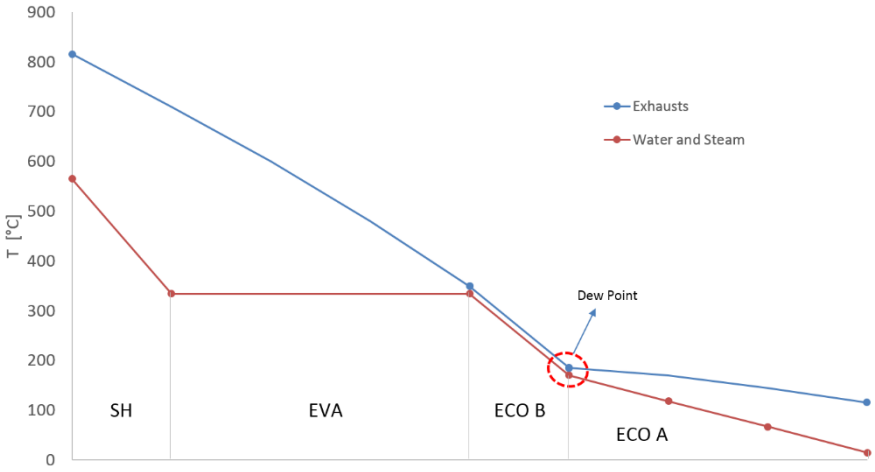

Figure 4.4: Conceptual representation of the exhausts and steam temperatures in the different sections of the cooling process.

As a result, a large amount of saturated water exits these economizers, more than what is needed in the associated evaporators and super-heaters; this occurs for both the cooling units (exhausts and hydrogen flow). The exceeding saturated water is thus used for feeding the syngas cooler in the gasification island. In this way the HRSG is lightened of the production of a large amount of saturated water, providing better performance. In fact, a limited production of saturated water in the

HRSG results in an increase of the pinch points and the consequent increase of the efficiency.

It is important to underline that this improvement of HRSG performance due to the limited production of saturated water, occurs only when the plant is operated with low air-to-steam ratio, as in the "Fe case". In fact, in the case the CL island was fed with an elevate air-to-steam ratio, more heat would be released in the reactors and the hotter reactors outlet flows (typical of high "% O_2 from air") would have more heat available for heating more saturated water. Hence, in the case of high air-to-steam ratio, the overall cooling unit, instead of producing an excess of saturated water available for the HRSG, on the contrary would need saturated water from the HRSG; this would cause the worsening of combined cycle efficiency.

As shown in the (Figure 4.2), in the hot part of this exhaust cooling train it is present also a fuel heater to increase the fuel temperature to 517°C (#28).

The HP superheating section work in parallel with the IP re-heating banks, which are fed with part of the steam exiting the HP section of the steam turbine at 360°C (#36) and heat the steam up to 565°C (#37). This highly interconnected configuration allows for high efficiency, but requires a broader use of HT pipes and headers to manage the superheated steam in different plant sections.

- Oxidation reactor outlet flow: as said above, the economizer is fed with hot water coming out from the economizer of the reduction reactor exhausts flow cooling train. Also in this case, an amount of saturated water higher than what it is needed in the following steam generation and superheating facilities is produced, making the excess of saturated water available for the syngas cooler of the gasification unit.

  After the economizer, a typical evaporator and super-heater section produces and heat up HP steam to 565°C; ready for being fed to the HP steam turbine.

  The oxidation flow is cooled down also by heating up to 565°C the HP steam coming out from the syngas cooler at 400°C (#34).

  The pressure of the hydrogen coming out from the CL island is 33.9 bar, much higher than the operating pressure of the gas turbine where will be fed to.

All the HP steam produced at 565°C in the cooling train of both the oxidation and the reduction flows is fed finally to the HP steam turbine (#44).

The main bases for the simulation of the heat exchangers of the CL island cooling trains are presented in the following Table 4.3.

Heat exchangers main bases			
Reduction flow		Oxidation flow	
Pinch point ΔT, °C	15	Pinch point ΔT, °C	15
Approach point ΔT, Economizer under dew point T, °C	15	Economizer inlet T, hot water, °C	170
Dew point temperature (CL island operating at 36bar), °C	185	Saturation steam pressure (HP)	Same of HRSG
Total exhaust Pressure drop (ΔP/P), %	10	Maximum steam temperature, °C	565

Saturation steam pressure (HP-IP)	Same of HRSG		
Maximum steam T	565 °C		

Table 4.3: Set of bases for the simulation of the cooling trains of the CL island outlet flows.

4.2.4 Power island

The integrated Gasification plant with Pre-Combustion Chemical Looping process (IG-PCCL) includes a Combined Cycle (CC) for power generation. Conventional large-scale combined cycle includes a heavy-duty gas turbine, whose outlet exhausts stream is cooled down in a Heat Recovery Steam Cycle (HRSC), recovering its sensible heat and producing further power in the steam turbine.

In the IG-PCCL, the combustor of the gas turbine is fed with hydrogen flow produced in the AR and cooled down to 200°C (#3). This inlet combustor temperature is reported in the EBTF document [26].

The use of hydrogen instead of natural gas as gas turbine fuel, leads to sensible changes in its design: first of all, "dry-low NO_x emission" pre-mixed combustor are not allowed, due to the much larger flammability limits and the lower ignition temperatures of hydrogen with respect to natural gas. Diffusion burners are thus used. In this type of burner, the Stoichiometric Flame Temperature (SFT) is representative of the actual flame temperature, strictly related to the nitrogen oxides formation rate. Hence, in order to control the SFT and the NO_x emission, massive steam and/or nitrogen dilution is used.

As it was described in Chiesa et al. [22], a reasonable value of 2300K for SFT can be set to get emissions comparable to power industry standards (about 25 ppmvd).

Making reference to Figure 4.2, the hydrogen flow (#10) exits the CL oxidation reactor already diluted with N_2 (present in the air) and H_2O (because the steam is always fed in excess to the reactor). Further nitrogen dilution is needed. The presence of the ASU offers "free" N_2, which is thus compressed (#11) and mixed with the hydrogen flow (#10), upstream of its cooling process.

An advanced heavy-duty gas turbine, re-engineered for the use of hydrogen, was considered in this work. Along with this basis, the TIT reduction which would be needed when H_2 is used as fuel in a gas turbine designed to run on natural gas, is no longer necessary. A value of 1350°C (common TIT in advanced state-of-art heavy-duty commercial unit) is therefore considered.

The air (#1) required for the combustion (in large excess compared to the stoichiometric ratio to limit the cycle peak temperature and to cool the blades of the expander) is compressed by the gas turbine compressor (#2) and the resulting reaction products (#4) are expanded in the turbine.

A supplementary compressor supplies the air (#8) required for the CL oxidation phase accomplished in the AR.

The gas turbine exhaust stream is cooled down in a double steam pressure level Heat Recovery Steam Generator (HRSG). Due to the large amount of saturated water which is

produced inside the HRSG, and then sent to other heat recovery sections (such as syngas coolers), a third low pressure level is not needed for a complete cooling of the exhausts.
Due to the amount of sensible heat available in the outlet streams of the CL unit, a large quantity of HP-SH steam is produced in both the CO_2-H_2O and hydrogen cooling sections, and then sent to the HP steam turbine (#44) together with the HP-SH steam generated in the HRSG.
The IP pressure level of the HRSG is always set as the same of the CL unit pressure (range: 18.6 to 36.1 bar depending on the case). As was described in [4] for the IG-CLC case, the second pressure level of the HRSG has a very little influence on the overall performance of the HRSC.
Part of the IP steam exiting the HP steam turbine is used for feeding the CL oxidation phase (#42); the remaining part is re-heated up to 565°C in the CL exhausts cooling section and then fed again to the steam turbine (#43).
Steam at 4.1bar is extracted from the steam turbine (#39), to supply the required amount of heat in the regeneration column of the H_2S removal unit.

The main design parameters assumed for the gas turbine and the HRSC are listed in Table 4.4. Some of these values (GT compressor pressure ratio and steam cycle pressure levels) are varied in the sensitivity analysis carried out in this work.

POWER ISLAND - Gas Turbine + HRSC			
Gas turbine		**Heat Recovery Steam Generator**	
Compressor pressure ratio	16-25.0	HRSG gas side pressure loss, kPa	3
Maximum compressor polytropic efficiency[a], %	92.5	Heat losses, % of heat transferred	0.7
Maximum efficiency of large turbine stages (cooled/uncooled)[a], %	92.1/93.1	HP Pressure level, bar	144
		IP pressure level, bar	18.6-36
Gas turbine auxiliaries consumption, %	0.35	Maximum steam temperature, °C	565
Mechanical efficiency of compressor/turbine, %	99.865	Minimum approach point ΔT, °C	25
Electric generator efficiency, %	98.7	Minimum pinch point ΔT in HRSG, °C	10
Air compressor		Sub-cooling ΔT, °C	5
Compressor pressure ratio	18.2-36.1	Pressure losses in HP/LP economizers, %	25
Maximum compressor polytropic efficiency[a], %	92.5	Pressure losses in superheaters, %	7
Steam Cycle			
Condensing pressure, bar	0.048		
Power for heat rejection, MJ_e/MJ_{th}	0.008	Turbine mechanical efficiency, %	99.6
Pumps hydraulic efficiency, %	70	Electric generator efficiency, %	98.5
HP/IP/LP steam turbine isentropic efficiency, %	92/94/88		

Table 4.4: Set of assumptions for the simulation of the power island.

[a] values in the table are referred to large machines: the actual efficiency is calculated by GS code as function of the machine/stage size.

4.2.5 CO2 compression

The exhaust flows originated in the reduction reactor exits the cooling section described in paragraph 4.2.3 at 115°C, 30.5 bar (#31). It is then cooled down to ambient temperature and, after water condensation, treated in a drier in order to decrease its water content below 50 ppm. A CO_2 purity of 96.5%, which is considered sufficient for CCS application, is

achieved. The impurities consist mostly of Ar and N_2, present in the O_2-rich flow produced in the ASU, and of the nitrogen contained in the primary feedstock.
The high purity CO_2 stream is compressed in a three-stage intercooled compressor up to 88 bar, liquefied at 23°C and finally pumped to 110 bar (#32).
The main parameters considered for the simulation of the CO_2 treating and compression unit are listed in the following Table 4.5.

CO_2 treating and compression unit	
IC compressor isentropic efficiency, %	82
IC compressor mechanical efficiency, %	94
Last stage IC compressor CO_2 discharge pressure, bar	88
Pressure drop in each intercooler, %	1
Pump mechanical efficiency, %	92
Pump hydraulic efficiency, %	75
CO_2 delivery pressure, bar	110
CO_2–rich stream condensation temperature , °C	23

Table 4.5: Set of assumptions for the simulation of the CO2 treating and compressor unit, taken from [4].

As it is shown in the **Errore. L'origine riferimento non è stata trovata.** and Figure 4.3, part of the CO_2-rich flow is taken at 56 bar from the compressor train and sent back to the gasifier for use as carrier gas in the lock-hoppers. This flow is then collected at ambient pressure and compressed to 30.5 bar in a dedicated intercooled compressor unit.
At this pressure it is mixed with the exhaust flow at the cooling section outlet.

4.2.6 Sensitivity analysis on air-to-steam ratio

A sensitivity analysis on the air-to-steam ratio in the feed to the Fuel Reactor, is presented in this section. The influence of this parameter on the global power plant performance and design is discussed. Particular attention is given to the behavior of the single islands of the power plant: the gas turbine, the Heat Recovery Steam Cycle (HRSC) and the plant auxiliaries (Aux).
The simulations were carried out by varying the "% O_2 from air" (resulting in a variation of the air-to-steam ratio) and by maintaining constant other simulation parameters, as shown in the following Table 4.6.

Air-to-steam ratio sensitivity analysis	
Turbine Inlet Temperature (TIT), °C	1350
GT compressor pressure ratio (β)	18.1
Inlet fuel temperature in the GT, °C	200
CL unit operating pressure, bar	36.1
"Steam excess", %	30
"% O_2 from air", variation range, %	**10-30**

Table 4.6: Parameters involved in the air-to-steam ratio sensitivity analysis

In the following (Figure 4.5), the Net Electrical Efficiency ($\eta_{,el,net}$) of the IG-PCCL plant is shown as a function of the "% O_2 from air".

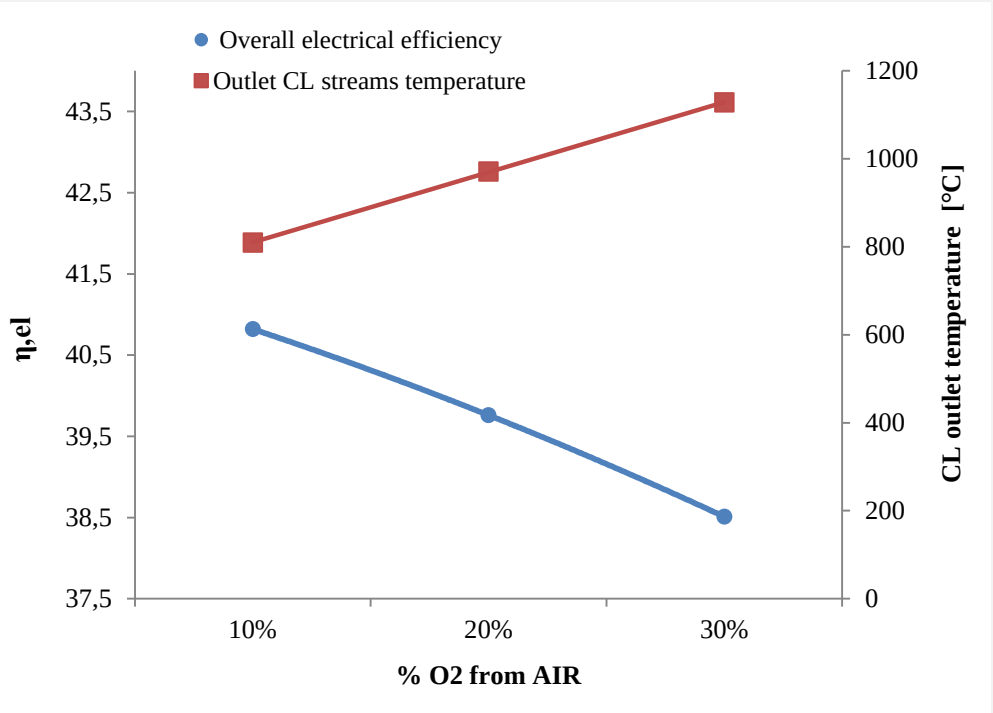

Figure 4.5: Net electrical efficiency and CL outlet streams temperature as a function of "% O_2 from air".

It can be clearly seen that an increase of the "% O_2 from air" leads to a significant decrease of the power plant performance: from 10% to 30% of "% O_2 from air", an efficiency drop of 2.3 percentage points occurs (from 40.82 to 38.51).
To explain this trend, a deeper analysis on the behavior of the single power plant islands is needed. Simulation results on the performance of the GT, the HRSC and the plant auxiliaries (Aux), as a function of the "% O_2 from air", are highlighted in (Table 4.7:), (Table 4.8:) and (Table 4.9:) and discussed here below:

a) Gas Turbine: as described in the 3.2.3 Presentation of the resultsthe increase of the "% O_2 from air" leads to an increase of the sensible heat released in the CL island and a decrease in the hydrogen production (from 4.6 kg/s, in the case of 10% O_2 from air to 3.56 kg/s in the 30% case).
   The drop in the fuel mass flow rate results directly in a strong decrease of the GT power: from 225.2 MW to 154.4 MW in the transition from 10% O_2 from air to 30%. Also the exhausts mass flow rate of the GT significantly decreases (from 486 kg/s to 386 kg/s).
   Regarding the fuel dilution, it is needed only in the 10% O_2 from air case. In the 20% case, the steam excess of 31% in the feed to the Fuel Reactor is enough for keeping the Stoichiometric Flame Temperature (SFT) at 2300°K without the necessity of any additional nitrogen dilution. In the 30% case, the low hydrogen production of the PeCLET process associated to the higher air mass flow rate that feeds the oxidation reactor, result in a fuel strongly diluted (without any further dilution, a SFT of 2180 K is achieved in this case).

Gas Turbine				
% O_2 from Air		10%	20%	30%
Pure hydrogen fed to the GT	*kg/s*	4.60	4.08	3.56
H_2 molar fraction in the fuel	*kg/s*	54.5	54.7	46.2
SFT	*K*	2300	2300	2180
Nitrogen dilution ($\dot{m}$)	*kg/s*	10.9	-	-
GT Exhausts mass flow rate	*kg/s*	486	433	378
GT electrical power	*MW*	225.2	186.9	154.4

Table 4.7: Air-to-steam ratio sensitivity analysis, simulation results on the GT.

b) Steam turbine: as described in the 3.2.3 Presentation of the results when the "%O_2 from air" increases, the higher sensible heat released in the CL leads to higher temperature of the CL outlet streams (the hydrogen flow and the CL exhausts). This sensible heat is recovered in two cooling sections described in (4.2.3 CL Exhausts and hydrogen flow cooling), producing steam. Hence, when the % O2 from air is raised up, a significant increase of the SH-HP steam generated outside the HRSG occurs (Table 4.8).
On the other hand, the steam produced inside the HRSG decreases with the increase of the "% O_2 from air", due to the lower GT exhausts mass flow rate and the sensible increase of the pinch points (later described).
Considering these two components (HRSG steam production and SH_HP steam generated outside the HRSG), on balance the steam flow rate fed to the ST grows with the increase of the % O2 from air.
A sensible enhancement of the ST power production therefore occurs when the plant is operated with high "% O_2 from air": a value of 226.4 MW is achieved at 30% O_2 from air vs. 187.6 MW in the 10% case.
Another important aspect is that this rise of the ST power is limited by the strong increase of the pinch point ΔTs in the HRSG from 35° (at 10% O2 from air) to 180°C (at 30%).
This is explained by the huge request of saturated water in the cooling sections outside the HRSG, when the plant is operated with high "% O_2 from air". This leads to an unbalance of the duties in the HRSG, since the economizers need much more heat for pre-heating the saturated water. This heat is "stolen" from the SH-EVA banks of the HRSG by increasing the pinch point ΔTs.

Steam Turbine				
% O_2 from Air		10%	20%	30%
ΔT Pinch point, HP	*°C*	35	110	180
ΔT Pinch point, IP	*°C*	22	56	87
Saturated water produced in the HRSG and sent to the heat recovery sections	*kg/s*	46	94	125

SH-HP steam generated in the HRSG	*kg/s*	67	39	17
SH-HP steam generated outside the HRSG	*kg/s*	93	128	160
SH-HP steam fed to the ST	*kg/s*	159	165	172
IP steam requested by the CL unit (air-to-steam ratio).	*kg/s*	54	49	42
ST electrical power	*MW*	187.6	204.6	226.4

Table 4.8: Air-to-steam ratio sensitivity analysis, simulation results on the ST.

c) Plant auxiliaries: The 10% case differs from the other two cases because it is the only one that needs the fuel dilution with nitrogen, accomplished by an additional compressor.

Plant Auxiliaries				
% O_2 from Air		10%	20%	30%
N2 dilution compressor	*MW*	12.0	-	-
Total consumptions	*kg/s*	62.2	49.9	49.3

Table 4.9: Air-to-steam ratio sensitivity analysis, simulation results on the auxiliaries

d) Overall power plant: the net electrical efficiency decreases with the increase of the "%O_2 from air" because the drop in the GT power is higher than the enhancement of the ST power. This can be explained by two reasons:
   - With the increase of the "%O_2 from air", the primary fuel (syngas) LHV is converted more in the steam cycle rather than in the combined cycle, resulting in a naturally drop of the net electrical efficiency.; in fact the energy (LHV or sensible heat) achieves higher conversion efficiency when it is used in the combined cycle rather than in the HRSC (ideally 60% efficiency vs. 40%)
   - The great increase of the pinch point ΔTs in the HRSG, occurring when the plant is operated at high "%O_2 from air", means lower efficiency in the heat recovery and less SH-HP steam produced in the HRSG.

In conclusion, the "base case plant" here described is a convenient choice only when the plant is operated with an OC that can guarantee low air-to-steam ratio (below 15% of O_2 from air). Otherwise the net electrical efficiency would be too low, making the plant not competitive with other similar CCS technologies (i.e. IG-CLC case).
If the plant is operated with an OC that requires higher air-to-steam ratio, another operating logic of the CL reactors and another integrated plant design is proposed in this work ("Heat Removal Plant", 4.3 Heat Removal Plant).

4.2.7 Sensitivity on the operating pressure

An advantages of the integrated PeCLET power plant (IG-PCCL) in comparison with the CLC plant (IG-CLC) is the possibility to disconnect the operating pressures of the CL unit and the GT, which can be therefore singularly optimized.

A sensitivity analysis for both the CL unit pressure and the GT compressor ratio has been developed in this work and is presented here below:

- GT compressor ratio ($\beta_{,GT}$): in this analysis the $\beta_{,GT}$ is varied maintaining constant the operating pressure of the CL unit (at 36.1 bar as will be described in the subsequent section).
  In the following (Figure 4.6) the net electrical efficiency of the plant is shown as a function of the GT compressor ratio. Although the net electrical efficiency presents a maximum for a $\beta_{,GT}$ equal to 22, his trend is relatively flat, without relevant variations, as normal for the combined cycle plant. For example, the difference in the net electrical efficiency is just 0.15 percentage points (40.83 Vs. 40.99) at 18 and 22 compressor ratio respectively.
  This trend can be explained by analyzing the GT and ST behaviors and the nitrogen consumption, as a function of the $\beta_{,GT.}$
  The net power of the GT rises up with the increase of the compressor ratio. The power increase is more remarkable in the low $\beta_{,GT}$ zone and it tends to decrease at higher GT compressor ratio.

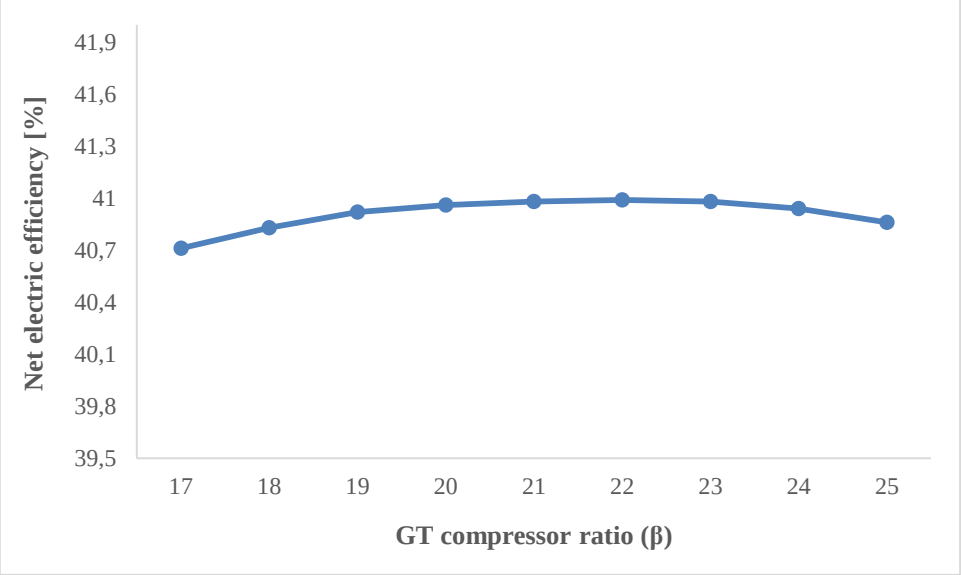

Figure 4.6: Net electrical efficiency as a function of the GT compressor ratio.

Instead, the Turbine Outlet Temperature (TOT) drops down when the $\beta_{,GT}$ is increased; consequently, the HRSC receives less heat available for the steam generation and the ST net power decreases.
The nitrogen compressor for the fuel dilution is responsible of the rise in the auxiliaries consumptions as a function of $\beta_{,GT}$. When the GT is operated with an elevated compressor ratio, the nitrogen for the fuel dilution has to be compressed to higher pressure. Moreover, with the increase of the $\beta_{,GT}$, the temperature of the compressed air entering the GT combustor increases and a correspondent higher nitrogen mass flow rate is needed to maintain the SFT at 2300 K.

The trends of GT net power, ST net power, nitrogen compressor consumption (which determines a variation of the overall auxiliary consumption as well tabulated) and power plant net electrical efficiency are shown in the following Table 4.10 as a function of the GT compressor ratio.

GT compressor ratio - sensitivity analysis										
GT β		17	18	19	20	21	22	23	24	25
Net electrical power (GT)	*MW*	217.1	220.2	222.9	225.3	227.4	229.2	230.7	231.9	232.7
Net electrical power (ST)	*MW*	188.1	186.8	185.7	184.4	183.3	182.2	181.4	180.6	179.9
Auxiliaries consumptions	*MW*	55.6	56.3	57.1	57.8	58.6	59.4	60.1	60.9	61.6
Nitrogen compressor consumption	*MW*	6.0	6.7	7.5	8.2	9.0	9.7	10.5	11.3	12.0
Net electrical efficiency	*%*	40.71	40.83	40.92	40.96	40.98	40.99	40.98	40.94	40.86

Table 4.10: Sensitivity analysis on the GT compressor ratio: results on the GT, ST, Auxiliaries.

In conclusion, at increasing GT compressor ratio the rise of the GT power roughly compensates the performance worsening of the ST and of the auxiliaries. The best efficiency is obtained at the compressor ratio value of 22.
However, the influence of the $\beta_{,GT}$ on the net electrical efficiency is very limited. For this reason the $\beta_{,GT}$ M chosen for the "base case plant" in this work is 18, corresponding to the average compressor ratio of the heavy-duty GT typical of large-scale power plant.

- CL unit operating pressure: the increase of this pressure results in the reduction in the consumption of the CO_2 compression (due to the higher pressure of the CO2-H2O stream exiting the CL island) and in the rise in the consumption of the air compressor that feeds the CL oxidation reactor. Also the ST power production is influenced by the rise of the CL operating a pressure: a slight decrease occurs, since the steam that is needed in the CL oxidation reactor is taken from the ST at gradually higher pressure and therefore less expanded in the ST.
  These effects are balanced, so that the net electrical efficiency remains constant in the large range of CL operating pressure considered (from 18 to 36.1 bar).
  The choice of this parameter is therefore affected by economic reasons. In particular, the maximum value of 36.1 bar is chosen because higher is the pressure, smaller is the plant volume, fewer the reactors and therefore lower the investment cost. More detailed explanation on this subject is reported in 88.

4.3 Heat Removal Plant

In this new configuration, a different operation logic of the CL reactors is adopted: a heat removal phase is added to the oxidation-reduction steps and an overall decrease in the CL outlet flow temperature occurs.
The plant layout is different compared to the base case: changes in the CL unit, GT, HRSC and cooling sections unit are described in the following paragraphs. The gasification and syngas cleaning unit and the CO_2 compression unit remain the same as the base plant and they were already described in the (**Errore. L'origine riferimento non è stata trovata.** and **Errore. L'origine riferimento non è stata trovata.**).

The detailed plant layout (Figure 4.7) and thermodynamic properties of the streams (Table 4.11Table 4.1: Thermodynamic properties of the streams reported in

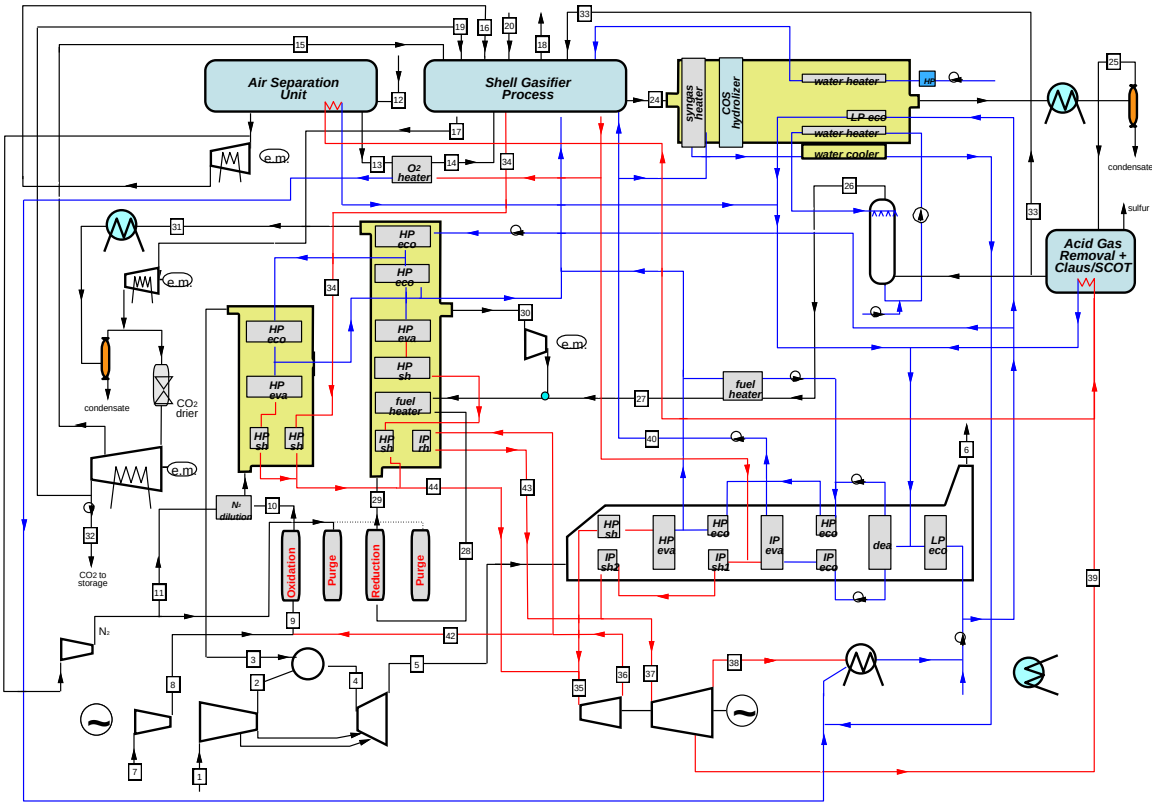

Figure 4.2: Detailed layout of the base case plant, ("Fe case")

and **Errore. L'origine riferimento non è stata trovata.**, "Fe case" (%O_2 from air = 11.1%; Steam,excess = 40%; $\beta_{gas\text{-}turbine}$= 18).) presented here below, are referred to the "HR plant" operated with "FeO" as most reductive state of the iron-based OC. In this case the CL unit works with: % O2 from air = 33.3%, Steam excess = 30% (an explanation on this values is provided in the 73).

The numbering of the thermodynamic properties of the streams shown in the following (Table 4.11Table 4.1: Thermodynamic properties of the streams reported in

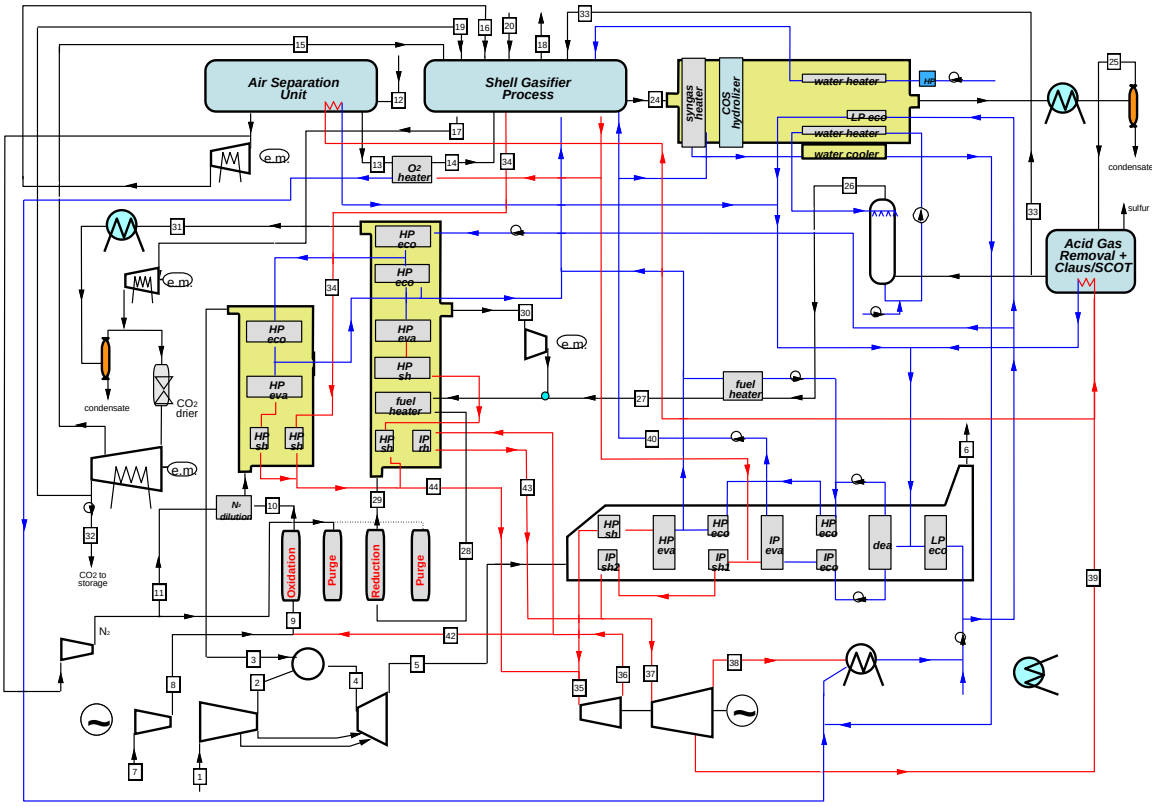

Figure 4.2: Detailed layout of the base case plant, ("Fe case")

and **Errore. L'origine riferimento non è stata trovata.**, "Fe case" (%O_2 from air = 11.1%; Steam,excess = 40%; $\beta_{gas\text{-}turbine}$= 18).) follows the numbering adopted in the detailed plant layout (Figure 4.7) and in the schematic of the gasification unit (Figure 4.3).

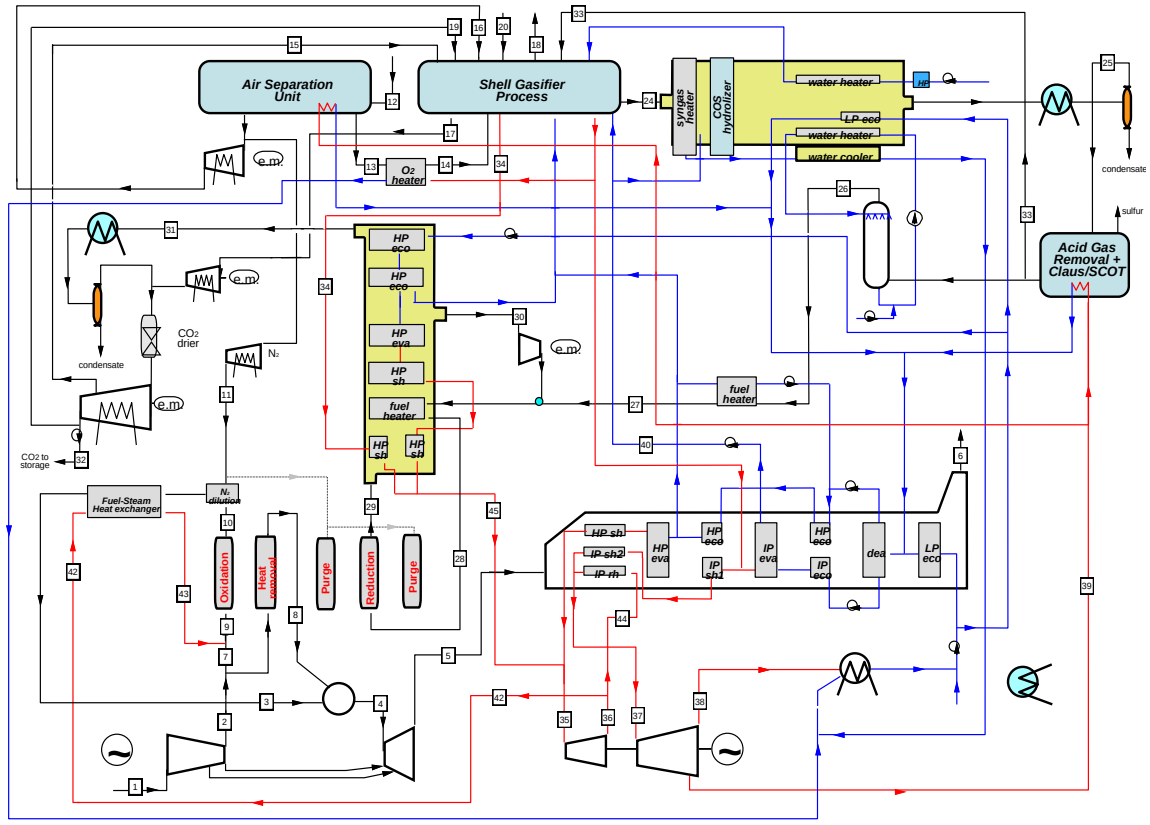

Figure 4.7: Detailed layout of the Heat Removal Plant, "FeO case".

	T	P	m	MW	Q	stream composition (vol. basis)									HHV	LHV
	°C	bar	kg/s	kg/kmol	kmol/s	*Ar*	*CO*	*CO_2*	*H_2*	*$H_2O(g)$*	*H_2S*	*N_2*	*O_2*	*$H_2O(l)$*	*MJ/kg*	*MJ/kg*
#1	15.0	1.0	619.2	28.9	21.5	0.9	-	0.03	-	1.0	-	77.3	20.7	-		
#2	442.7	20.5	574.2	28.9	19.9	0.9	-	0.03	-	1.0	-	77.3	20.7	-		
#3	364.7	19.3	70.9	16.6	4.3	0.4	-	0.01	39.5	12.3	-	47.7	-	-	7.2	5.8
#4	1305.3	18.5	549.0	27.4	20.0	0.9	-	0.03	-	12.0	-	74.2	13.0	-		
#5	538.7	1.1	631.3	27.6	22.9	0.9	-	0.03	-	10.6	-	74.6	13.9	-		
#6	80.0	1.0	631.3	27.6	22.9	0.9	-	0.03	-	10.6	-	74.6	13.9	-		
#7	442.7	20.5	58.8	28.9	2.0	0.9	-	0.03	-	1.0	-	77.3	20.7	-		
#8	800.0	19.7	478.1	28.9	16.6	0.9	-	0.03	-	1.0	-	77.3	20.7	-		
#9	453.0	20.5	98.4	23.2	4.2	0.4	-	-	-	52.4	-	37.2	10.0	-		
#10	500.0	19.7	57.8	15.2	3.8	0.5	-	0.02	44.4	13.8	-	41.3	-	-	8.8	7.1
#11	397.5	19.7	13.1	28.0	0.5	-	-	-	-	-	-	100	-	-		
#12	15.0	1.0	120.7	28.9	4.2	0.9	-	-	-	1.1	-	77.3	20.7	-		
#13	15.0	48.5	28.9	32.2	0.9	3.1	-	-	-	0.0	-	1.9	95.0	-		
#14	180.0	48.0	28.9	32.2	0.9	3.1	-	-	-	0.0	-	1.9	95.0	-		
#15	80.0	56.0	23.7	43.7	0.5	1.4	-	96.8	-	0.0	-	1.8	-	-		
#16	122.3	56.0	2.4	28.0	0.1	-	-	-	-	-	-	100	-	-		
#17	33.0	1.0	13.1	43.7	0.3	1.4	-	96.8	-	0.0	-	1.8	-	-		
#18	81.6	1.0	4.7	34.1	0.1	0.6	-	37.8	-	0.0	-	61.6	-	-		
#19	33.0	88.0	2.7	43.7	0.1	1.4	-	96.8	-	0.0	-	1.8	-	-		
#20	15.0	-	32.0	-	-	***Douglas Premium Coal***									27.7	26.8
#21	900.0	44.0	127.4	22.6	5.6	1.0	57.4	8.4	23.4	8.4	0.2	1.2	-	-	10.4	9.7

#22	300.0	41.7	127.4	22.6	5.6	1.0	57.4	8.4	23.4	8.4	0.2	1.2	-	-	10.4	9.7
#23	210.9	44.4	60.3	22.5	2.7	0.9	53.0	8.6	21.6	14.5	0.2	1.2	-	-	9.7	9.0
#24	165.0	41.7	79.0	22.3	3.5	0.9	51.5	8.5	21.0	16.8	0.2	1.1	-	-	9.6	8.8
#25	35.0	38.8	68.2	23.2	2.9	1.1	61.8	10.2	25.2	0.1	0.2	1.4	-	-	10.7	10.2
#26	126.8	38.4	71.7	22.9	3.1	1.0	58.1	9.6	23.7	6.4	-	1.3	-	-	10.3	9.7
#27	300.0	36.1	71.7	22.9	3.1	1.0	58.1	9.6	23.7	6.4	-	1.3	-	-	10.3	9.7
#28	517.0	20.5	152.6	28.4	5.4	1.0	33.6	34.1	13.7	16.4	-	1.3	-	-	5.0	4.5
#29	800.0	19.5	193.1	35.9	5.4	1.0	-	67.6	-	30.1	-	1.3	-	-	0.4	0.0
#30	348.9	18.5	81.5	35.9	2.3	1.0	-	67.6	-	30.1	-	1.3	-	-	0.4	0.0
#31	142.1	17.5	111.6	35.9	3.1	1.0	-	67.6	-	19.6	-	1.3	-	10.5	0.2	0.0
#32	27.8	110.0	81.3	43.7	1.9	1.4	-	96.7	-	-	-	1.9	-	-		
#33	60.0	36.1	0.7	22.8	0.7	1.0	58.1	9.6	23.7	6.4	-	1.3	-	-	10.3	9.7
#34	400.0	144.0	71.3	18.0	4.0	-	-	-	-	100	-	-	-	-		
#35	547.6	133.9	132.5	18.0	7.4	-	-	-	-	100	-	-	-	-		
#36	279.8	20.9	132.5	18.0	7.4	-	-	-	-	100	-	-	-	-		
#37	512.0	16.7	105.9	18.0	5.9	-	-	-	-	100	-	-	-	-		
#38	32.2	0.05	102.6	18.0	5.7	-	-	-	-	100	-	-	-	-		
#39	267.4	4.1	2.3	18.0	0.1	-	-	-	-	100	-	-	-	-		
#40	244.2	36.1	7.7	18.0	0.4	-	-	-	-	-	-	-	-	100		
#41	300.0	54.0	2.9	18.0	0.2	-	-	-	-	100	-	-	-	-		
#42	279.7	20.9	39.6	18.0	2.2	-	-	-	-	100	-	-	-	-		
#43	464.0	20.5	39.6	18.0	2.2	-	-	-	-	100	-	-	-	-		
#44	279.7	20.9	92.8	18.0	5.2	-	-	-	-	100	-	-	-	-		
#45	564.1	133.9	93.3	18.0	5.2	-	-	-	-	100	-	-	-	-		

Table 4.11: Thermodynamic properties of the streams reported in Figure 4.7 and Figure 4.3, "FeO case" (%O_2 from air = 33.3%; Steam excess = 30%; βgas-turbine = 20).

4.3.1 CL unit

In the "Base case plant" (4.2 Base case plant), the work strategy for the CL reactor was the following: "Oxidation-purge-Reduction-purge", where all the heat released in the oxidation reaction was allocated on the two outlet streams (hydrogen and exhausts), which exited the CL unit at high temperature.

In the "HR plant", a heat removal phase is added to the reactor work strategy, leading to a natural decrease of the CL outlet temperatures (in comparison with the "Base case plant" and at the same "%O_2 from air"). The strategy changes to "Oxidation-Heat removal-purge-Reduction-purge" and the main outputs of the CL unit become three: the outlet flows of the oxidation, the heat removal (HR) and the reduction steps.

The HR phase is carried out with air and has to be run out when the bed is still oxidized. Hence, before the reduction can be accomplished, a decrease in the bed temperature will occur, resulting in potential problems for the kinetics. This issue should be more deeply investigated in future studies (regarding the kinetics and the reactor model).

The air used for the HR phase is compressed by the main GT compressor (#7) and pre-heated in the reactors before entering the combustor (#8). Hence, in the HR plant the CL reactor pressure is strictly connected to the operating conditions of the GT and vice versa. In fact, since the HR air has to be compressed to the same pressure as the reactor, when the CL operating pressure is raised up also the GT compressor ratio has to be increased. The two sections (CL and GT) cannot be optimized singularly as it was possible in the Base case plant.

As a result, a significant difference between this plant configuration and the "Base case plant" emerges: the CL unit operating pressure was set at a lower value (20.49 bar) resulting in a higher number of reactors required in the HR plant case (due to the higher total volumes).
The pressure drops in the CL unit are here reported: 4.1% for the oxidation reactors, 5.5% for the reduction reactors and 4.2% for the heat removal reactors. These values derives from the reactors analysis carried out in the (88).

As concerns the CL reduction phase, the syngas stream is diluted and pre-heated before entering the FR, in the same way as it was described for the Base case plant (**Errore. L'origine riferimento non è stata trovata.**). The output is an exhausts flow (CO_2-H_2O rich) at relative high temperature (#29).
On the other hand, the feed air to the oxidation reactor (#7) is compressed in the GT compressor together with the air used for the heat removal phase (#8).
The IP steam needed at the oxidation reactor, is taken at the outlet of the HP section of the steam turbine (#42), pre-heated (#43) and then mixed with the compressed air (#7). The resulting stream (Air + Steam) (#9) reacts with metal oxide producing a hydrogen flow (#10) which is diluted and cooled down before entering the gas turbine combustor (#3), like in the Base case plant.

In the simulation of the HR plant, the value of the CL outlet temperatures was fixed at: $T_{out,reduction} = T_{out,HR} = 800°C$ and $T_{out,oxidation} = 500°C$. The reason of these temperatures will be explained in the (Chapter 1), where the ΔT of the beds after the reduction and the oxidation reaction and the temperature profiles of the reactors will be discussed.

4.3.2 CL Exhausts and hydrogen flow cooling unit

The temperatures decrease that occurs in the HR plant configuration, results in less heat available in the cooling section of CL exhausts and hydrogen streams. This leads to changes in these heat recovery units, which are described here below:

- Reduction reactor outlet flow: the exhausts outlet temperature from the CL unit is 800 °C (#29). They are cooled down to 142°C (#31), mostly with the SH-HP steam production train already adopted in the Base case plant (ECOa-ECOb-EVA-SH).
  Opposed to the Base case plant, the RH banks are not placed in this cooling section but inside the HRSG. In substitution of the RH banks, the steam coming from the syngas cooler at 400°C (#34) is heated up to 565°C. This steam is added to the other SH-HP steam produced in this section and sent to the steam turbine (#45).
- Oxidation reactor outlet flow: in the HR plant, in order to achieve a higher efficiency, the cooling logic of this flow is completely changed. The steam production train of the Base case plant is substituted with the "fuel-steam heat exchanger". This unit cools down the hydrogen flow exiting the CL unit from

489°C to 365°C (#3), pre-heating the IP steam fed to the oxidation reactor from 280°C (#42) to 464°C (#43). For this Heat Exchanger (HE) a pressure drop (Δp/p) of 2% for both sides is assumed.
The use of this HE leads to two advantages. Firstly, the steam feeding the CL unit is at higher temperature and the correspondent kinetics of the oxidation reactor are enhanced. Furthermore, the sensible heat present in the hydrogen flow is transferred to the IP steam entering the CL unit and finally allocated in the HR stream that feds the GT. As a result, the sensible heat present in the hydrogen flow is not transferred to the steam cycle but it evolves in the CC (first the GT and then the HRSC).

The main assumptions on the heat exchangers train of the reduction flow cooling section are the same reported in Table 4.3 for the Base case plant, while the assumptions regarding the oxidation flow cooling section have been entirely described in this paragraph.

4.3.3 Power Island

In the HR plant, the addition of the heat removal phase in the CL reactor work strategy affects strongly the GT operation. The influence on the HRSC is instead less important.

In this plant configuration, the compressed air required for the CL oxidation reaction and for the heat removal phase is completely supplied by the GT compressor (#2). The GT compressor handles these two streams only. The hot air, exiting the reactors that work in the HR step, is entirely fed to the GT combustor (#8).
It's important to underline how this HR mass flow rate is calculated in the simulation. As was said before, the three outlet temperatures of the CL unit are fixed ($T_{out,reduction} = T_{out,HR} = 800°C$ and $T_{out,oxidation} = 500°C$). The outlet mass flow rate of the hydrogen stream and the CL exhausts are respectively set by the "$\%O_2$ from air" plus the "steam excess" and by the syngas stream, which is maintained constant in all the cases.
In conclusion, once the amount of heat released in the CL is fixed by the "$\%O_2$ from air", the HR mass flow rate can be calculated by the overall energy balance of the CL island, since it is the only unknown variable.
The influence of the "$\%O_2$ from air" on the HR mass flow rate will be widely described in the sensitivity analysis carried out in (58). However, it is reasonable to anticipate that with the increase of this parameter, the rise of the sensible heat released in the CL unit leads to a correspondent increase of the HR mass flow rate. In fact, since the outlet streams temperature of the CL unit are kept constant, more air is needed for removing the higher amount of sensible heat released in the reactors when the CL unit is operated with high "$\%O_2$ from air".
In the HR plant considered in this section (FeO case, 33% O_2 from air), the mass flow rate of the air used for the heat removal phase is very high (478 kg/s), compared to the hydrogen produced in the CL island. With this amount of air entering the GT combustor, the TIT of 1350°C that was used in the "Base case plant" cannot be reached. The operating logic of the GT is then completely changed. The HR air stream becomes the element that

controls the GT operation: the TIT that is achieved depends on the mass flow rate of this stream.
Regarding the fuel, it is diluted (for the SFT) and cooled down, before entering the combustor at 360°C (#3). The exhausts flow, with GT compressor ratio equal to 20, exits the GT at 539°C; a lower value than the 600°C obtained in the "Base case plant".
In comparison with the Base case plant, the GT combustor and its control valves are more complex; since the fuel enters at higher temperature (360°C vs. 200°C) and the air is pre-heated by the HR up to 800°C.
The assumptions for the simulation of the GT, not discussed in this paragraph, are the same as those presented in Table 4.4 for the "Base case plant".

The HRSG considered in the HR plant is double-pressure level. In this case also a three-pressure level would be feasible, but the performance of the HRSC would remain substantially the same. The first level is at 144 bar, the second level at 20.45 bar (since it follows the CL unit pressure).
A change, in comparison with the Base case plant, regards the hot banks of the HRSG: the section of the SH-HP and the SH-IP works in parallel with the RH banks (in the Base case plant this section was located outside the HRSG).
The maximum steam temperature achieved in the output of the SH banks is 513°C, lower than the 565°C of the Base case plant, in relation to the lower gas turbine outlet temperature of the exhausts (540°C vs. 600°C).
This steam at 513°C is then mixed with the steam produced outside the HRSG at 565°C (#45) and fed to the HP steam turbine (#35).
The assumptions for the simulation of the HRSC, not discussed in this paragraph, are the same as those presented in Table 4.4 for the "Base case plant".

The nitrogen compressor for the fuel dilution comes out as an important component in the overall energy balance of the power plant. When the CL unit is operated at 20.49 bar, it works with an outlet pressure of 19.7 bar, due to the pressure drop of the hydrogen flow in the oxidation reactor. In the case of using a traditional compressor, the high temperature of the nitrogen outlet (555°C) would lead to non-acceptable cost for this kind of plant component. An Inter-Cooled Compressor (ICC) has to be adopted.
A three stage ICC, with constant $\beta_{,stage}$, is a possibility, with an outlet temperature of around 180°C. From the analysis is emerged that the adoption of this kind of ICC, leads to a decrease of the net electrical efficiency in comparison with the use of a compressor without the Inter-Cooler (IC). This worsening in the performance is correlated to the fact that the dilution nitrogen stream evolves directly in the GT and, as a result, his energy (in the form of sensible heat) is converted with a high efficiency in the entire combined cycle. The adoption of the ICC leads indeed to a decrease in the compressor consumptions, but, on the other hand, it removes part of the sensible heat that would be converted in the GT; the balance between this effects lead to a decrease of the net electrical efficiency.

The final choice is the adoption of a two stages ICC with different $\beta_{,stage}$. The first stage compresses the nitrogen up to 2.5 bar. The stream is then cooled down to 35°C before being fed to the second stage, in which the compression is completed, reaching 19.67 bar and 400°C in the outlet. This temperature is more acceptable in relation to the costs, and leads to a less invasive heat removal.
A pressure drop ($\Delta p/p$) of 1% was adopted in the intercooler.

4.3.4 Sensitivity analysis on the air-to-steam ratio

In this paragraph, the sensitivity analysis on the air-to-steam ratio for the HR plant case is carried out by means of the correspondent parameter "% O_2 from air" (30). A study on the "Steam excess" is also presented, but its effect on the power plant performance and operation is much smaller.
The simulation are carried out keeping fixed the outlet temperatures of the CL unit: $T_{out,reduction} = T_{out,HR} = 800°C$ and $T_{out,oxidation} = 500°C$. These temperatures have been adopted so far for the HR plant and they will be explained more deeply in the (Chapter 5).

In order to explain the influence of the $\%O_2$ from air, a deep analysis on the behavior of the single power plant islands is needed. Simulation results on the performance of the GT, the HRSC and the plant auxiliaries (Aux), as a function of the "% O_2 from air", are highlighted in Table 4.12, Table 4.13, Table 4.14, Table 4.15, and discussed here below:

a) Gas Turbine: the (Table 4.12) shows the trend of GT parameters as a function of the "$\%O_2$ from air".
   From this table, it can be clearly seen how the mass flow rate of the heat removal air rises strongly when the "% O_2 from air" is increased (from 10% to 40% of O_2 from air: 114 kg/s vs. 583 kg/s). In fact, more air is required to remove the higher sensible heat released in the CL unit when the reactors are operated with high $\%O_2$ from air.
   This trend leads to important consequences on the GT behavior. Two different cases with two different GT operation logics are identified:

   - Low $\%O_2$ from air (10%-20%): in these cases the mass flow rate elaborated by the compressor is calculated in order to reach the desired TIT of 1350°C. Moreover, since the heat removal mass flow rate is not high, only part of the stream exiting the compressor is sent to the CL unit. This heat removal stream, after being heated in the reactors, is fed to the combustor.
     The remaining compressed air, which is not used for removing the heat in the reactors, is fed directly to the combustor.
     In these two cases (10% and 20% of oxygen from air), the TIT of 1350°C is achieved.
   - High $\%O_2$ from air (30%-40%): in these cases, the heat removal mass flow rate is high: in particular it is higher than that required for achieving the TIT of 1350°C. Hence, with the increase of the $\%O_2$ from air, the GT is operated

with higher mass flow rate, but with lower TIT. In the 30% case the TIT is still quite high (1308°C), instead in the 40% case it decreases strongly (1165°C).

Summarizing the discussion about the GT behavior, when the $\%O_2$ from air is increased these effects are obtained: higher mass flow rate evolved in the turbine, drop in the TIT and, over all, decrease in the hydrogen mass flow rate fed to the combustor (due to the lower H_2 production in the CL oxidation reactors).
The sum of these three effects leads to an overall drop of the GT power production with the increase of the $\%O_2$ from air.
Moreover, with the TIT drop a proportional decrease of the Turbine Outlet Temperature (TOT) occurs: from 600°C of the 10-20% case to 492°C of the 40% case). Hence, when the plant is operated with high $\%O_2$ from air, the HRSG receives less sensible heat and at lower temperature.

Gas Turbine					
% O_2 from Air		10%	20%	30%	40%
HR mass flow rate	*kg/s*	114	269	426	583
TIT	*°C*	1350	1350	1308	1165
TOT	*°C*	600	598	563	492
GT electrical power	*MW*	260.3	252.6	250.6	236.6

Table 4.12: "$\%O_2$ from air" sensitivity analysis, simulation results on the GT.

b) Steam turbine: The Table 4.13 shows the trend of HRSC parameters as a function of the "$\%O_2$ from air".
From this table, the steam mass flow rate required by the CL oxidation reactors decreases with the increase of the $\%O_2$ from air: from 54 kg/s in the 10% case to 36 kg/s in the 40% case. This effect would lead to an enhancement of the HRSC performance, because more steam would be expanded in the intermediate-low pressure sections of the steam turbine. This performance improvement is limited by the TOT drop described above.
Hence, in order to explain better the behavior of the HRSC as a function of the $\%O_2$ from air, two cases are identified:

- Low $\%O_2$ from air (10%-20%): in this case, since the TIT remains constant at 1350°C, the value of the TOT is maintained at 600°C.
  Hence, in both cases, the same amount of HP-SH steam is produced inside the HRSG.
  With the increase of the $\%O_2$ from air the overall performance of the HRSC are enhanced because less steam is extracted from the steam turbine, while the sensible heat available in the HRSG remains constant.

- High $\%O_2$ from air (30%-40%): in this case, when the $\%O_2$ from air is increased, a drop of the TOT occurs. As a result, the mass flow rate and the maximum temperature of the SH-HP steam produced in the HRSG decrease with the rise of the $\%O_2$ from air. The effect of this worsening prevails on the enhancement of extracting less steam (for the reactors) from the turbine.
  As a result, the trend of the HRSC power production is decreasing with increase of the %O2 from air.
  This occurs even more for the $40\%O_2$ from air case, where the significant drop in the TOT leads to a considerable decrease in the power production: 7.5 MW less than the 30% case.

In conclusion, the HRSC power production as a function of the $\%O_2$ from air is shown in the diagram below (Figure 4.8). The trend presents a maximum for a value around 25%.

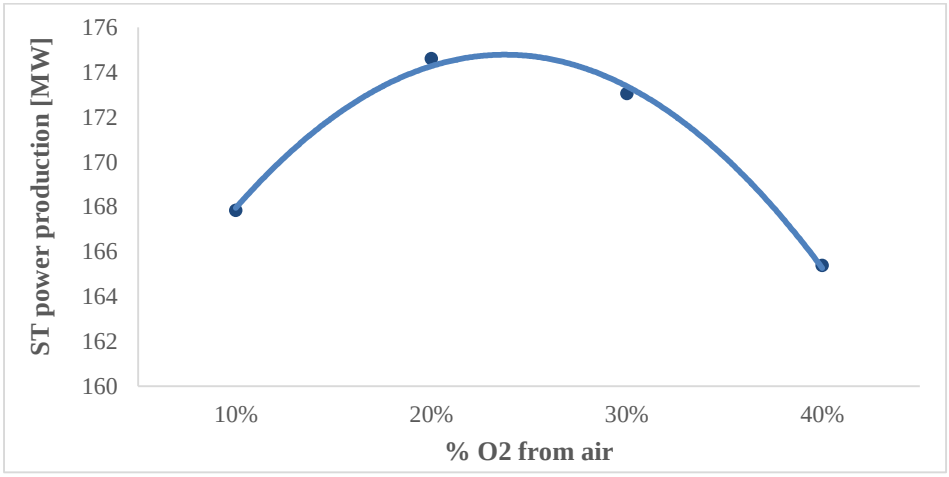

Figure 4.8: ST power production as a function of the $\%O_2$ from air.

Steam Turbine					
% O_2 from Air		10%	20%	30%	40%
Steam requested by the CL oxidation reactor	*kg/s*	54	49	42	36
Maximum steam T (produced in the HRSG)	*°C*	565	565	538	462
ST electrical power	*MW*	167.8	174.6	173.0	165.4

Table 4.13: "$\%O_2$ from air" sensitivity analysis, simulation results on the ST.

c) Plant auxiliaries: The change in the auxiliaries consumption is related only to the nitrogen compressor for the fuel dilution.
   This nitrogen mass flow rate decreases with the increase of the $\%O_2$ from air, since the CL oxidation reactor is fed with a higher amount of air and more diluted

hydrogen is produced. The fuel stream that feeds the combustor is therefore more nitrogen diluted when the plant is operated with high $\%O_2$ from air.
The Table 4.14 shows the drop of the compressor power consumption with the increase of the $\%O_2$ from air, due to the decrease of the nitrogen mass flow rate required. In the "40%O_2 from air" case, the dilution is even no more necessary.

Auxiliaries					
% O_2 from Air		10%	20%	30%	40%
N_2 dilution mass flow rate	*kg/s*	38.6	30.2	20.6	-
N_2 compressor electrical consumption	*MW*	19.6	15.5	10.7	-

Table 4.14: "%O_2 from air" sensitivity analysis, simulation results on the plant auxiliaries.

d) Overall power plant: the net electrical efficiency of the plant as a function of the $\%O_2$ from air is depicted in the following Figure 4.9.

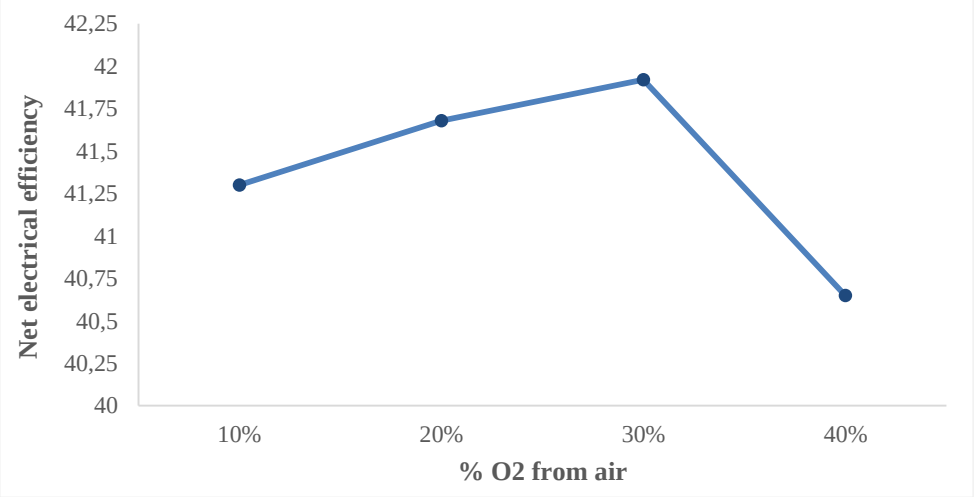

Figure 4.9: "%O_2 from air" sensitivity analysis, trend of the net electrical efficiency.

From the figure above, at increasing of $\%O_2$ from air an enhancement of the global performance occurs until the TIT remains high (10-20-30% of oxygen from air). The improvement of the HRSC and the auxiliaries is higher than the slight power production decrease of the GT. Above 30% of oxygen from air, a significant drop in the net electrical efficiency occurs: the TIT and the TOT decrease is progressively more significant, resulting in a worsening of both the GT and the HRSC performance.

HR power plant					
% O_2 from Air		10%	20%	30%	40%
Net electrical efficiency	%	41.30	41.68	41.92	40.65

Table 4.15: "%O_2 from air" sensitivity analysis, trend of the net electrical efficiency.

The sensitivity analysis above discussed is carried out at fixed outlet CL reactor temperatures.
In order to complete the study on the %O_2 from air, other two cases are presented, in which the outlet temperatures of the HR and the reduction streams are changed: a 30% case in which the TIT of 1350°C is achieved and a 40% case with $T_{out,reduction} = T_{out,HR} = 850°C$.
The reason of considering higher outlet temperature of the HR and reduction flow is that, with the increase of the %O_2 from air a significant rise of the HR mass flow rate occurs. This leads to the TIT drop and the consequent performance worsening.
So a possible solution, when the plant is operated with high %O_2 from air, is to increase the outlet temperature of the HR and reduction flow, in order to decrease the mass flow rate required for the HR phase and avoid or limit the TIT drop.
The two new cases are described here below:

- 30%O_2 from air, TIT=1350°C: with the outlet temperature of the HR and reduction streams equal to 830°C, the TIT of 1350°C adopted so far is achieved. The results of the simulation regarding the GT and the ST are shown in the following (Table 4.16). It can be clearly seen that this rise in the CL outlet temperature leads to a better performance of the power plant: a net electrical efficiency of 42.00% is reached. The lower mass flow rate of the GT is partly compensated by the increase of its TIT. The rise of the TOT results in a sensible increase of the ST power production.

HR plant - 30% O_2 from air – TIT=1350 °C		
% O_2 from Air		30%
$T_{out,reduction}$ & $T_{out,HR}$	*°C*	830
HR mass flow rate	*kg/s*	373
TIT	*°C*	1350
TOT	*°C*	584
GT electrical power	*MW*	247.3
Maximum steam T (produced in the HRSG)	*°C*	559
ST electrical power	*MW*	178.3
Ney electrical efficiency	*%*	42.00

Table 4.16: Simulation results on the power plant performance, 30% O_2 from air case with TIT=1350°C.

- 40%O_2 from air, TIT=1254°C: in this case, in order to reduce the HR mass flow rate and achieve the max TIT of 1350°C, a very high outlet temperatures from the CL unit would be necessary. It is has been however chosen to limit this increase in the temperature at 850°C, resulting in a TIT equal to 1254°C.
  In comparison with the 40% case described before, a significant increase in the net electrical efficiency is achieved: from 40.65% to 41.37%. This means that, with a proper choice of the outlet CL unit temperatures, very good performance of the power plant can be achieved for a large range of %O_2 from air (i.e. for different OC).
  The results of the simulation regarding this case are presented here below (Table 4.17):

HR plant - 40% O_2 from air – TIT=1250°C		
% O_2 from Air		40%
$T_{out,reduction}$ & $T_{out,HR}$	*°C*	850
HR mass flow rate	*kg/s*	480
TIT	*°C*	1254
TOT	*°C*	536
GT electrical power	*MW*	233.0
Maximum steam T (produced in the HRSG)	*°C*	511
ST electrical power	*MW*	174.2
Net electrical efficiency	*%*	41.37

Table 4.17: Simulation results on the power plant performance, 40% O_2 from air case with TIT=1250°C.

In conclusion, when the OC used in the CL reactors forces to work with %O_2 from air higher than 30-35%, an increase in the outlet temperature of the HR and reduction flow shall be provided to improve the power plant efficiency. In the range of %O_2 from air lower than 30-35%, temperatures around 800°C are suggested.

As concern the "Steam excess" parameter, its influence on the net electrical efficiency of the plant is much less significant than the % O_2 from air, as it is shown in the following diagram (Figure 4.10).

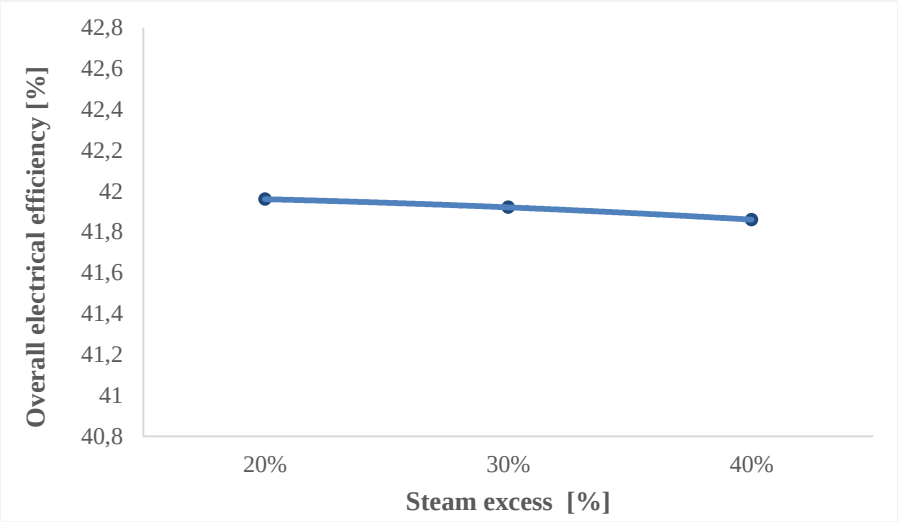

Figure 4.10: Net electrical efficiency as a function of the "Steam Excess".

This analysis was carried out with a fixed value of 30% of O_2 from air, and showed how the performance of the power plant is very slightly affected by the steam excess.

4.3.5 Sensitivity on the operating pressure of the CL unit

In the Base case plant, the operating pressures of the CL unit and of the GT were optimized singularly, because they are not strictly connected. In the Heat Removal (HR) plant configuration, the addition of the heat removal stream, compressed by the GT and fed to the reactors, creates a strict link between these two operating pressures. In particular, the GT compressor ratio has to be chosen in order to reach an outlet pressure equal to the operating pressure of the CL unit.
In the following sensitivity analysis, the reactors pressure and the $\beta_{,GT}$ have the same absolute value (because the suction pressure of the GT compressor is around 1 bar) and they are varied concurrently.
The simulation of the HR plant has been carried out with "FeO" as OC (%O_2 from air =30%, Steam excess =40%) and constant CL outlet temperatures ($T_{out,reduction}$ = $T_{out,HR}$ = 800°C and $T_{out,oxidation}$ = 500°C).

The results of the sensitivity analysis are reported in the following (Table 4.18).

HR plant - Operating pressure sensitivity analysis					
CL unit operating pressure (bar) & GT turbine compressor ratio		16	18	20	22
TIT	*°C*	1581	1557	1535	1515
GT power production	*MWel*	231.3	239.1	244.8	249.7
ST power production	*MWel*	185.9	179.3	172.5	165.3

Total Aux consumptions	*MWel*	-60.3	-60.0	-59.7	-59.5
N_2 compression	*MWel*	-5.6	-6.2	-6.7	-7.2
CO_2 compression	*MWel*	-11.9	-11.0	-10.2	-9.5
Net electrical efficiency	*%*	41.54	41.72	41.62	41.38

Table 4.18: Results of the sensitivity analysis on the CL operating pressure.

When the CL operating pressure and therefore the GT compressor ratio ($\beta_{,GT}$) are increased, the typical performance trend of the combined cycle is observed: the GT power production rises up, while the generation of the ST decreases. This is due to the drop of the TOT which results in a higher extracted work from the GT, but less sensible heat available in the HRSG.

As shown in the table above (Table 4.18), the TIT is significantly influenced by the rise of the CL unit pressure. In fact, with increasing of the GT compressor outlet pressure, the starting temperature of the heat removal stream rises up (the more the $\beta_{,GT}$ the higher the compressor outlet T); resulting in a higher heat removal air mass flow rate needed to remove the same amount of sensible heat released in the CL reactors. This rise in the mass flow rate leads finally to a drop of the TIT with the increase of the $\beta_{,GT}$.

As a consequence, the maximum of the electrical efficiency is not obtained at the highest $\beta_{,GT}$, but at the value equal to 18 (Figure 4.11), since the increase of the GT power production as a function of the $\beta_{,GT}$ is limited by the drop of the TIT.

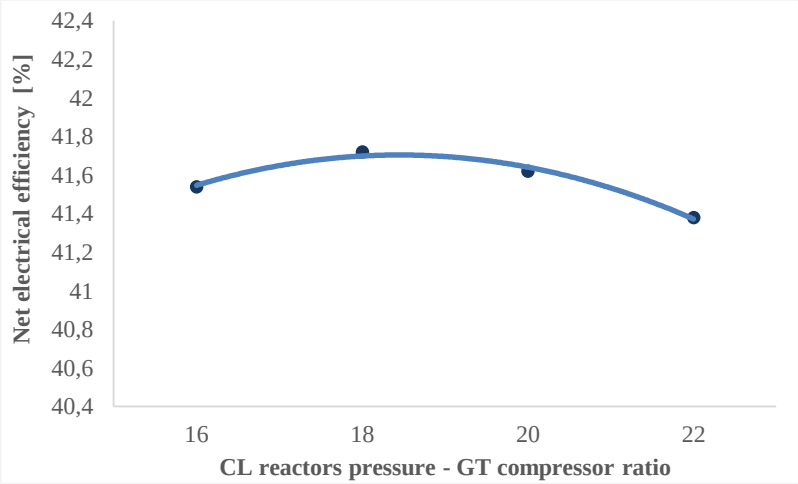

Figure 4.11: Sensitivity analysis on the CL operating pressure, results of the net electrical efficiency.

Regarding the auxiliary power consumptions, with the increase of the reactor pressure the decrease in the CO_2 compression unit (the compressor suction is higher) and the rise in the N_2 compressor (the discharge pressure is higher) occur.

In conclusion, the influence of the CL operating pressure on the net electrical efficiency is little: moving from the maximum (18 bar) to 16 or to 22 bar, a difference of just 0.18 or 0.34 percentage points respectively occur.

4.4 Comparison between the Base case plant and the HR plant

The performance summary of the IG-PCCL in both the proposed configurations, "Base case plant" and "HR plant", is reported in Table 4.19.
The Base case plant is operated with Fe (11.1% O_2 from air, 40% steam excess), while for the HR plant FeO is used (33.3% - 40% respectively).
For the Base case plant a significant part of the power is produced by the steam-turbine of the HRSC, which generates 46% of the gross power, vs. 54% of the gas turbine. In the HR plant this share is more similar to the benchmark of the IGCCs: 59% produced by the gas turbine and 41% by the HRSC.
This difference is related to several reasons; the main ones are here below presented.
In the HR plant, although the mass flow rate of the hydrogen produced in the CL unit is less than the Base case plant (because of the higher $\%O_2$ from air, 33.3% vs. 11.1%), the heat removal mass flow rate that is fed to the GT expander is so huge that the GT power production is significantly higher than in the Base case plant (246 MWe vs. 220 MWe).
Concerning the HRSC, the Base case plant produces more power in this section than the HR plant. In fact, in the Base case plant much more steam is produced inside and outside the HRSG which more than compensates the higher steam extraction from the ST for feeding the oxidation reactor. The steam generation in the HR plant is instead limited by the lower TOT and does not receive any contribute from by the cooling section of the hydrogen flow (56) As a result the HP steam turbine is fed with a less steam and at lower temperature.
Moreover, in Table 4.19 shows that the difference in the auxiliaries power consumption between the two plant configurations, is mostly due to the CO_2 compression unit. In the Base case plant the consumption of this unit is lower because of the lower suction pressure (the CL unit is operated 36.1 bar vs. 20.49 of the HR plant).
In conclusion, although the HR plant shows higher auxiliaries consumption and lower ST power production, the much higher production of the GT assures a better net electrical efficiency compared to the base case plant: 41.59% vs. 40.83%.

Investigating in detail the auxiliaries consumption, most of them are associated to the O_2 production in the ASU, causing a plant efficiency decay of almost 4 percentage points. The second most important contribution is related to the CO_2 compression unit; this is true in particular for the HR plant, in which the pressure of the CO_2-H_2O rich stream exiting the reduction reactor is lower than the Base case plant (19.47 bar vs. 33.93 bar).
Another relevant efficiency penalty is associated to the N_2 compression for the fuel dilution. As emerged from the sensitivity analyses presented in this work, it always plays an important role in the overall energy balance of the plant.

Plant configurations		Base case (Fe)	HR case (FeO)
GT power production	*MWel*	220.2	246.0

HP-SH steam fed to the ST ($\dot{m}$ & T)	*kg/s - °C*	162 - 565	133 - 548
ST power production	*MWel*	186.8	170.9
Auxiliaries consumptions	*MWel*	-56.3	-59.6
Net electrical efficiency	*%*	40.83	41.59
ASU	*MWel*	-33.85	-33.85
CO_2 compressor (lock hoppers)	*MWel*	-4.03	-4.03
Gasification and syngas cleaning unit AUX	*MWel*	-3.45	-3.45
CO_2 compressor (CO_2 capture unit)	*MWel*	-5.94	-9.98
Nitrogen compressor (fuel dilution)	*MWel*	-6.71	-6.78

Table 4.19: Performance of the "Base case plant" operated with Fe and the "HR plant" operated with FeO.

4.4.1 Influence of the Air-to-steam ratio on the two plant configurations

In the air-to-steam ratio sensitivity analysis carried out for the Base case plant and the HR plant, different responses to the "%O_2 from air" have emerged.

In the Base case plant, the net electrical efficiency diminishes significantly with the increase of the % O_2 from air, since the higher amount of sensible heat released in the CL unit is recovered at low thermodynamic quality in the HRSC.

In the HR plant, the drop in the hydrogen production related to the increase of the %O_2 from air, is more than compensated by a very efficient recovery of the heat available from the CL unit, released to the air feeding the GT and converted into electric power with the efficiency of the combined cycle. On balance, the HR plant efficiency rises with the increase of the %O_2 from air. This trend occurs up to 30% of oxygen from air; for higher values other effects prevails and the efficiency starts to decrease, as described in (58).

The different behaviors of the two plant configurations are depicted in the following figure (Figure 4.122), showing the trend of the net electrical efficiency as a function of the %O_2 from air.

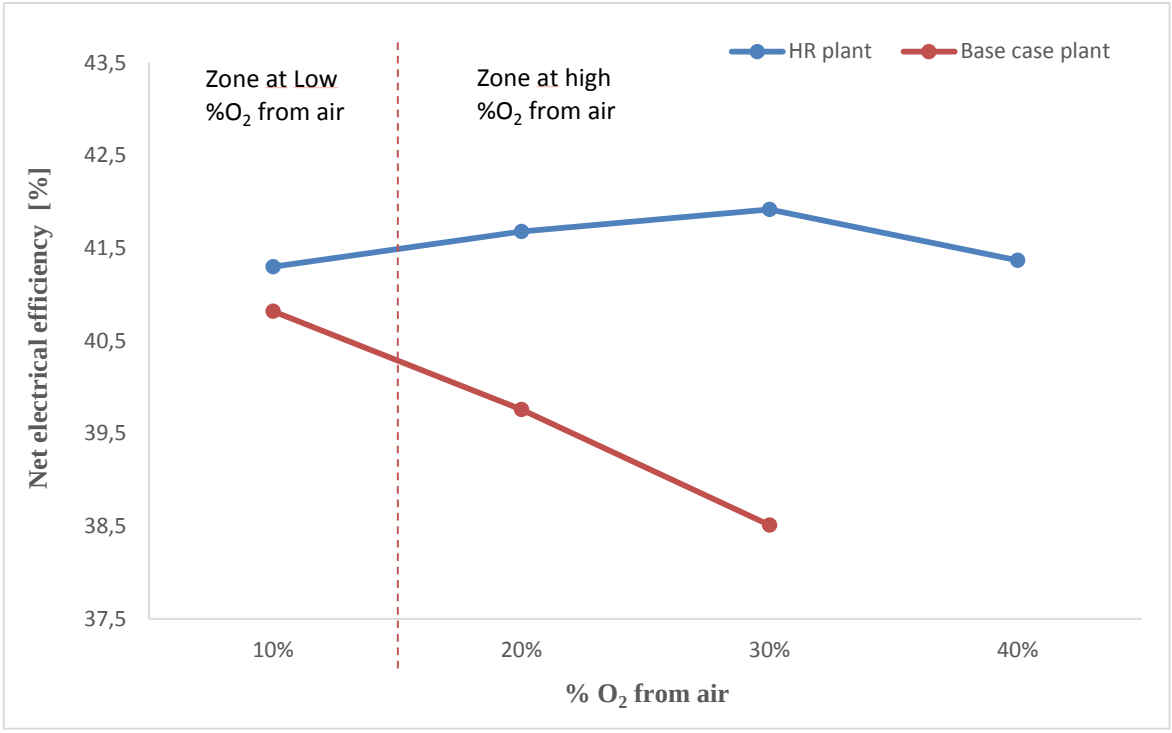

Figure 4.12: Comparison on the $\%O_2$ from air response, between the base case plant and the HR plant.

Different considerations apply to the two zones of the diagram.
When the plant is operated with low $\%O_2$ from air (less than 15%), the efficiency of the HR plant is higher than the Base case plant, but the difference is limited (0.5% at 11% of oxygen from air). On the other hand the Base case plant offers significant advantages in terms of integration simplicity (no heat removal phase), number of reactors (since it requires lower reaction volumes) and, as a consequence, potentially lower costs.
Instead, for $\%O_2$ from air exceeding 15% the advantage of the HR plant in terms of efficiency becomes so remarkable to suggest the use of this configuration independently from other considerations.

In conclusion, the selection of the OC, which set the minimum value of the "$\%O_2$ from air", drives the choice between the two possible plant configurations.
In fact, if an OC requiring a high air-to-steam ratio is used, the adoption of the HR configuration is recommended; while the use of the Base case plant is an attractive option when the OC can work with a $\%O_2$ from air lower than 15%. In fact, in this condition both the configurations are feasible, the HR plant has a limited advantage in efficiency but the Base case plant offers a significant potential reduction of the investment cost.

4.5 Comparison between the IG-PCCL and reference IGCC plants with and without CO_2 capture

The reference plant without CO_2 capture is an IGCC based on the same gasification island as the IG-PCCL plants. The only difference is that a conventional N_2 coal loading system is used, instead of a CO_2-based one. The clean syngas is saturated, pre-heated and diluted with N_2 from ASU, before being sent to the combustor of the combined cycle gas turbine. Regarding the gas turbine, an advanced machine fuelled by a H_2-rich stream is considered in this analysis. The properties of the GT are derived from the EBTF assumptions [26]; a TIT of 1350°C is achieved, in line with the state-of-the-art, natural gas-fired commercial machines available on the market. This scenario assumes that the current technological development is fully incorporated in gas turbines specifically designed to run on H_2-rich fuel [4].

The reference IGCC with pre-combustion CO_2 capture derives from the IGCC plant described above, but it includes the Water Gas Shift (WGS) reactors and the CO_2 removal unit based on physical absorption by Selexol® process (IGCC-Sel). The WGS reaction is carried out after scrubbing and IP steam addition, with two reactors operating at different temperatures, to combine a high H_2 yield in the cold stage with fast kinetics and efficient high temperature heat recovery in the hot one. After the acid gas removal by the Selexol® process, featuring two absorption columns for sequential separation of H_2S and CO_2, H_2-rich gas is humidified, pre-heated and mixed with N_2 from ASU before combustion in the GT combustor.
The main efficiency penalty of the IGCC with CO_2 capture is associated to CO_2 separation and compression, responsible for a net electric efficiency loss of 3.7 percentage points. Another important efficiency decay is associated to the steam addition to the syngas before the WGS reactors. IP steam extraction brings about a reduction of the steam turbine power output accounting for efficiency loss of 2.8 percentage points on the overall balance. The remaining efficiency loss is due to the lower CGE caused by the exothermic WGS reaction that correspondingly reduces the gas turbine power output at a given coal input [4].

The IG-PCCL is compared also with the IG-CLC, which is, so far, the most studied way of exploiting the CL technology for power production. The CLC was described in the (6) and the full discussion about the integrated plant is presented in [4]. The comparison between the IG-CLC and the IG-PCCL is very interesting due to the use of the same CL technology, but operated in a different way, the CLC vs. PeCLET process.

The (Table 4.20) shows the performance of the IG-PCCL cases, in comparison with the benchmark IGCC plants both with and without CO_2 capture (data taken from [4]).
The power plants with O_2 capture are compared by means of the typical performance indexes usually defined for CCS power plants. In addition to the electric efficiency and the specific CO_2 emission, the specific primary energy consumptions for CO_2 avoided (SPECCA) is used for performance assessment:

$$\text{SPECCA} = \frac{\left(\frac{1}{\eta_{el,CCS}} - \frac{1}{\eta_{el,ref}}\right)}{E_{CO2,ref} - E_{CO2,CCS}} \times 3600 \quad (4.1)$$

As it is shown in the (Table 4.20), the IG-PCCL configuration achieves a very interesting net electrical efficiency, higher than 41% in the HR plant case, operated with FeO as OC.
In addition, an extremely high CO_2 capture rate of about 96% is reached. In the assessed process (HR plant), most of the CO_2 is emitted from the lock hopper system (66%), while the remaining fraction is caused by the syngas combustion for coal drying. A small quantity of CO_2 is emitted also from the exhausts flow exiting the HRSG. Even lower emissions would hence be possible if CO_2 recovery from lock hoppers could be further optimized and if the purity of the oxygen produced in the ASU could be increased.
As a result of the high efficiency and the high carbon capture, specific emission of around 35 g/kWh are obtained (about one third of the reference IGCCs with CO2 capture), resulting in a lower SPECCA index (1.53-1.70 vs. 3.07 of the Selexol® absorption process). This value is very similar to the IG-CLC case.

The IG-PCCL case presents another advantage: the net efficiency decay related to the CO_2 compression is relatively low (0.67 and 1.2 % points, for the Base case plant and the HR plant respectively). Such a penalty is significantly lower than the decay for the CO_2 separation in the AGR and compression unit for the reference IGCCs (3.8 percentage points) and highlights an intrinsic advantage of the PCCL system, which produces a concentrated CO_2 stream at high pressure requiring relatively low energy consumption to be compressed. These values (0.67% and 1.2 %) are also slightly lower than the ones reached by the competing CL technology, the IG-CLC.

Looking at performance, the net electrical efficiencies of the IG-PCCL are very promising and comparable with the IG-CLC plant.
In particular, in the HR plant operated with “FeO” a value of 41.59% was achieved, slightly better than the IG-CLC case. This improvement in the efficiency is related to the higher TIT which can be reached in IG-PCCL plant, where the use of an advanced H_2-fuelled gas-turbine can assure a significant maximum temperature of the thermodynamic cycle. Instead, in the CLC case, the TIT is limited by the thermal stability of the OC and a maximum value of 1200°C is possible.
In conclusion, for the choice of the CL technology between the CLC and PeCLET schemes, the efficiency is not the most significant parameter. Instead, the choice should be rather based on the technological feasibility, availability and cost of the CL reaction system and the associated power plant.

Configuration Name	*units*	*IGCC*	*IGCC*	*IG - CLC*	*IG-PCCL Base case plant*	*IG – PCCL Heat removal plant*
CO_2 capture technology		*N/A*	*Selexol®*	*CLC 20 bar*	*PeCLET 36.1 bar*	*PeCLET 20.49 bar*
Gas Turbine						
GT net power production	MWe	309.62	322.41	255.82	220.16	245.96
Air compressor (for CL oxidation reactor)	MWe	-	-	-80.66	-12.21	-
N_2 compressor (only fuel dilution)	MWe	-	-	-	-6.71	-6.78
Steam Cycle						
ST net power production		191.14	179.1	234.92	186.84	170.9
Gasification island						
ASU + fan + coal milling and ash handling	MWe	-35.54	-41.25	-36.93	-36.93	-36.93
Acid gas removal	MW_e	-0.37	-16.80	-0.37	-0.37	-0.37
N_2 compressors*	MW_e	-43.66	-31.30	-1.36	-1.36	-1.36
CO_2 treating system						
CO_2 compression	MW_e	-	-22.50	-11.01	-5.94	-9.98
CO_2 LHs recovery	MW_e	-	-	-3.10	-4.03	-4.03
Overall Net Power	MW_e	417.3	386.3	350.5	350.7	357.3
Coal thermal input, MW_{LHV}	MW_{th}	882.4	1027.0	853.9	859.0	859.0
Net electric efficiency	%	47.34	37.62	41.05	40.83	41.59
Cold Gas Efficiency	%	81.71	73.31	80.65	80.65	80.65
Carbon Capture Rate	%	-	93.0	96.1	95.8	95.8
CO_2 avoided (ref to IGCC)	%	-	87.0	95.5	95.1	95.2
CO_2 specific emissions	kg_{CO2}/MWh_e	736.0	96.0	33.4	35.7	35.0
$SPECCA_{ADV}$	MJ_{LHV}/kg_{CO2}	-	3.07	1.66	1.73	1.50

Table 4.20: Power balances and CCS indexes of the IG-PCCL plant, the IG-CLC plant and the benchmark IGCC with and without CO2 capture. Data of the IGCCs and IG-CLC taken from [4].

*The consumption of these N_2 compressors for IGCC cases includes the consumptions for the N_2 used for coal loading in the lock hoppers and N_2 that is used for the syngas dilution before the combustor. In the IG-CLC and IG-PCCL it includes only the N_2 used for coal loading, which is mostly accomplished by the CO_2.

Chapter 5

Iron-based OC and CL reactions system

5.1 Description of the work

The choice of the OC, as was discussed in the Chapter 1, is of fundamental importance because it affects the all feasibility of the CL process and the power plant. Furthermore, in the specific PeCLET case, the OC affects both the performance and the design of the power plant, since it establishes the "%O_2 from air" which the process is operated with.
The parameters which the decision can be made through, were described in the Chapter 1.
In this work, for the PeCLET technology, iron-based oxygen carriers are chosen. The reasons are here below explained:

1) The iron-based OCs are cheap, common in nature, and with low environmental impact.
2) They have high melting point (1565°C), which make them suitable for the use in the CL integrated in the power plant.
3) They can reach a high oxygen capacity, when FeO or Fe are reached as most reductive state.
4) A full conversion of fuel could be achieved by adding Alumina or Titanium to the metal oxide: using Al_2O_3, $MgAl_2O_4$ or TiO_2 as inert matter, the porosity of the particles increases and therefore gas-solid reactions are enhanced.
5) The use of Ilmenite ($FeTiO_3$) is a very interesting possibility. It is a natural material that can be extracted from pits and used directly as OC in the reactor because it contains already the inert matter (TiO_2) and the reacting metal oxide (FeO). Ilmenite has been demonstrated as a very good oxygen carrier for converting syngas (high conversion and selectivity towards CO_2 and H_2O).
6) The iron-based OC was chosen also in the study regarding the competitor CL technology power plant, the IG-CLC presented in [4].
7) Due to the similaraties of the PeCLET concept to the steam-iron process, iron-based OCs are considered as promising material for this technology.

Two possible minimum states of iron oxidation are considered: FeO (wustite) and Fe (pure iron). In this Chapter, for both pure iron and wustite, the following features are discussed:

1) CL oxidation reaction: the stoichiometry and the thermodynamics of this reaction are described. Furthermore, the active solid fraction of the OC and the ΔT that occurs in the bed, due to the heat released during the OC oxidation, are studied by means of the Zero Dimensional (0D) reactor model described in (74).
2) CL reduction reaction: the same discussion about the stoichiometry, the thermodynamics and the ΔT in the bed are presented as for the oxidation reaction.

The chapter is introduced by the description of the 0D model adopted for the reactor and by a presentation of the assumptions regarding the initial and the maximum temperatures achieved in the CL reactor.

5.1.1 Zero Dimensional Model

As it was already described, the mass flow rate of the air and the steam fed to the CL unit are such that they ensure the complete oxidation of the OC present in the reactor. Inside the bed, when the oxidation exothermic reaction occurs, the gas-phase and solid temperature rise up. Since these CL reactors are PBRs, it is not possible to control the temperature with an excess of air (as it could be accomplished in the IFBR). The way to reach the proper maximum temperature in the bed, is to vary the weight content of the active material in the OC (ω_{act}) and, as a consequence, the inert content.

The Zero Dimensional (0D) model proposed by S. Noorman in [15], for investigating the maximum temperature achieved in PBRs, is used in this work.
Initially, the solid material is assumed to be fully reduced, the gas present in the bed is non-reactive (purge) and the entire system is at uniform initial temperature T_0. The system is fed with a reactive flow that is also at temperature T_0. As a consequence of the gas-solid reaction, which may continue until the complete particle is oxidized, a reaction front propagates through the bed at velocity (w_{rf}). As a result of the reaction heat, the temperature of the bed changes, so that the same reaction front can be observed in the temperature profile [29]. Along with the reaction front, as a result of the temperature difference between the bed and the incoming gas flow, a heat front propagates through the bed. The rate at which this front moves is referred to as heat front velocity (w_{hf}).
As explained in [29], it is possible to represent the concentration profiles of the gaseous reactant and the temperature evolution, (Figure 5.1).

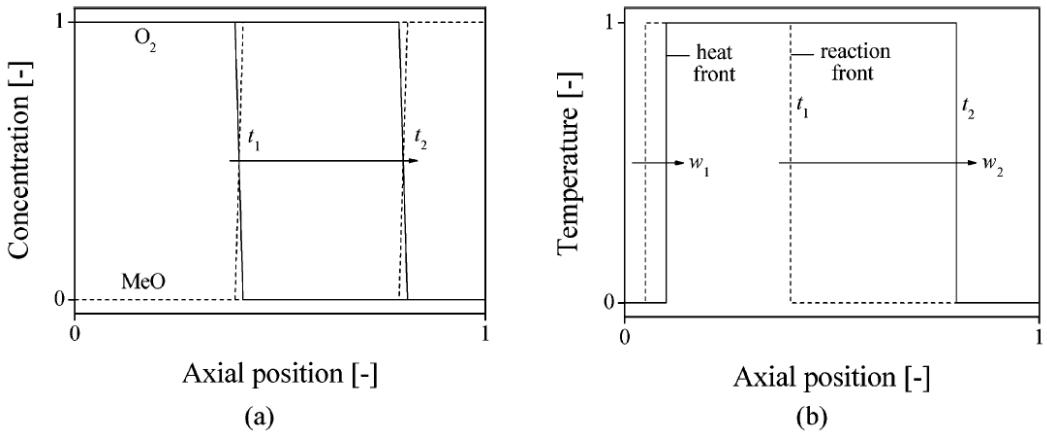

Figure 5.1: Schematic representation of the evolution of dimensionless axial concentration (a) and temperature (b) profiles in PBRs.

The assumptions of this model are here reported:

- An ideal system is considered, where the rate at which the non-catalytic gas-solid reaction proceeds is infinitely high.
- No heat and mass transfer limitations between the gas and solid phase is considered.
- Axial conduction and dispersion effects can be neglected.

With these assumptions, considering constant the heat capacity of the solid and negligible the heat capacity of the gas, and considering that the reaction front propagates more rapidly than the heat front, an overall energy balance can be formulated for the system:

$$\frac{\rho_g v_g \omega_{g,O2,in}}{M_{O2}} (-\Delta H_r) = \epsilon_s \rho_s C_{p,s} (w_{rf} - w_{hf})(T_1 - T_2) \tag{5.1}$$

Expressions for the front velocities are obtained considering that at the heat front, the heat present in the solid material is transferred to the gas phase and at the reaction front all the gaseous reactant reacts with a stoichiometric amount of the solid material, so that:

$$w_{rf} = \frac{\rho_g v_g \omega_{g,O2,in} M_{act}}{\epsilon_s \rho_s \omega_{act,0} M_{O2} \zeta} \tag{5.2}$$

$$w_{hf} = \frac{\rho_g v_g C_{p,g}}{\epsilon_s \rho_s C_{p,s}} \tag{5.3}$$

where ζ denotes the stoichiometric ratio of number of moles of gas and solid material needed in the reaction, $\omega_{act,0}$ denotes the weight content of the active solid material in the oxygen carrier at the initial state and M_{act} is the molecular weight of the initially present active material. The other symbols are explained in the nomenclature. By combination of equation (5.1-5.2-5.3), the expected maximum temperature change in the PBR can be rewritten by:

$$\Delta T = \frac{(-\Delta H_R)}{\frac{C_{p,s} M_{act}}{\omega_{act} \zeta} - \frac{C_{p,g} M_{O2}}{\omega_{g,O2,in}}} \tag{5.4}$$

It is interesting that the maximum temperature increase due to the oxidation of the OC in the PBR is independent of the gas flow rate.
The properties of the gas phase and, especially, the solid material are the parameters that affect this change in the temperature (as long as the reaction front velocity w_{rf} is higher than the heat front velocity w_{hf}).
In particular, once the inlet composition and temperature of the gas flow is set, the maximum change in the temperature is affected only by the weight content of the active solid material in the OC (ω_{act}).

Furthermore, it is noted that, if the heat front velocity was similar to the actual reaction front velocity, lower amount of solid would be heated up, but at higher temperature.
Finally, the same derivation and conclusions are valid for the reduction cycle.

5.1.2. Assumptions on the initial and maximum temperatures of the CL reactors

In this paragraph the assumptions related to the initial and maximum temperatures achieved in the reactor are presented. It is important to underline that this assumptions has to be further verified in future studies which shall include a 1D reactor model and the kinetics of the reaction involved.
The amount of heat released during the oxygen carrier oxidation (due to the $\Delta H_{R,oxi}$) is large and results in a significant increase in the reactor temperature. Instead, as regards the oxygen carrier reduction with syngas, the heat of reaction ($\Delta H_{R,red}$) is almost neutral. As a consequence, in all the work the change in the bed temperature associated to the reduction reaction is neglected.
Furthermore, in the PBRs the solid temperature profile at the beginning of each phase depends on the operation of the previous one. When a gaseous stream is fed to the reactor, the temperature of the initial part of the bed tends to be close to the inlet gas temperature because the solid is continuously in contact with a stream at constant (moderate) temperature.
On the other hand, the gas outlet temperature in each phase depends mostly on the temperature profile of the final part of bed that was created in the previous step.
The assumptions on the reactor temperatures are reported for both the plant configurations proposed in Chapter 4, the HR plant and the Base case plant:

- HR plant operated with FeO: the maximum temperature achieved in the reactors is assumed at 800°C. As explained in the Chapter 4, this value keeps the HR flow rate at a level which allows the GT to achieve a good TIT, at least when the $\%O_2$ from air is lower than 30-35%. This maximum temperature leads to exploit at the best the main advantage of the PeCLET process compared to the CLC: the CL unit can be operated at max 800°C instead of 1200°C, resulting in a much lower cost of the reactors, including valves and piping (14).
  The only feasible choice for the operation of the CL reactors in the HR plant is the "Strategy B" (Oxidation-HR-purge-Reduction-purge) reported in (14), since the heat removal step, accomplished by compressed air, can be carried out only when the bed is still oxidized (before the reduction step).
  Once the operation strategy is set, knowing the inlet temperature of the streams fed to the CL (Table 5.1), the outlet temperature of the reactors will be as follows: initially the oxidation bed is supposed to be entirely at T_0=500°C (the inlet temperature of the syngas in the previous reduction phase). The exothermicity of the oxygen carrier oxidation leads to the increase in the reactor temperature. The

bed, except that in the first part where the temperature is close to the inlet temperature of the gas reactant (450°C), will be at 800°C.
With this temperature profiles the HR step begins: the compressed air removes the heat released in the previous stage, leading larger part of the bed at its inlet temperature (450°C). The remaining part is still at the maximum temperature of 800°C. In fact, this HR step is a partial heat removal so that also the reduction outlet flow can exit the reactor at 800°C.
After the reduction, the heat released in the oxidation step is completely extracted from the reactors and the temperature of the entire bed will be close to the inlet temperature of the syngas (500°C). Now the cycle can start over from the oxidation step.

Temperature Assumptions - HR plant operated with FeO			
Reactor side		INLET	OUTLET
Oxidation step Air – Steam Hydrogen flow	 °C °C	 450 – 450 -	 - 500
HR step (compressed air)	°C	450	800
Reduction step Syngas Exhausts	 °C °C	 500 -	 - 800

Table 5.1: Temperature assumptions of the reactor for the HR plant configurations.

- Base case plant operated with Fe: in this configuration the strategy adopted for the work cycle of the reactors does not foresee the heat removal phase and consists in: Oxidation-purge-Reduction-purge. The absence of the heat removal step, which in the HR plant removes most of the heat released in the oxidation step, makes it more difficult to assume the profile temperature without knowing the real internal mechanism of the reactors.
  The assumption made in Chapter 1 and Chapter 4, was to equalize the two outlet temperatures, exhausts and hydrogen stream. This could be accomplished by properly tuning the heat management with a counter-current feeding of the reactor so that both the reduction and oxidation outlet flows would be at high temperature.

Temperature Assumptions – Base case plant operated with Fe			
Reactor side		INLET	OUTLET
Oxidation step Air – Steam Hydrogen flow	 °C °C	 600 – 360 -	 - 800
Reduction step Syngas Exhausts	 °C °C	 500 -	 - 800

Table 5.2: Temperature assumptions of the reactor for the Base case plant configurations.

Initially, the oxidation step starts with most of the bed at 500°C (the inlet temperature of the syngas). The heat released in this phase leads to a bed temperature increase up to 800°C. The subsequent reduction stream, removing part of the heat caused by the oxygen carrier oxidation, exits the CL reactor at 800°C. As a result, at the end of the reduction step the bed will be most at 500°C, while the remaining part at higher temperature. This heat still present after the reduction step can be used for making the oxidation outlet stream exit the reactor at high temperature.

5.2 Oxidation reaction

The OC oxidation is the key reaction of the PeCLET concept, since it makes this process different from the other CL technology. The presence of the double feed, air and steam, results in an outlet stream which is an hydrogen already diluted with H_2O and N_2 ready to bed used as fuel in the GT.
As it was deeply described in the previous Chapter 1 and Chapter 4, a very important parameter of the PeCLET process is the air-to-steam ratio in the feed of the oxidation reactor, whose value is set by the $\%O_2$ from air and the H_2O excess.
In this paragraph, the calculation of these two parameters by the study of the stoichiometry and the thermodynamic equilibrium of the oxidation reactions is described for both the cases Fe and FeO.
Moreover, the evaluation of the weight content of the active solid material in order to obtain the desired maximum temperature of 800°C is presented.

5.2.1 FeO case - stoichiometry and thermodynamics of the oxidation reaction

In the PeCLET "FeO" case, the complete oxidation considered is from FeO to Fe_2O_3 and it is accomplished in two steps: firstly the steam-iron process (5.5), where the Wustite is transformed in Fe_3O_4 by reacting with steam producing hydrogen and, lastly, the oxidation is completed to Fe_2O_3 by the reaction between the metal oxide and the air (5.6). The stoichiometry of these two main reactions is shown here below:

$$3FeO + H_2O \leftrightarrow H_2 + Fe_3O_4 \tag{5.5}$$

$$Fe_3O_4 + \frac{1}{4}O_2 \leftrightarrow \frac{3}{2}Fe_2O_3 \tag{5.6}$$

From this stoichiometry, assuming that the FeO and Fe_3O_4 considered are entirely converted, the $\%O_2$ from air can be easily calculated as:

$$\%O_2\ from\ air = \frac{{}^1/_4\, mol, O_2\ from\ air}{{}^1/_2\, mol, O_2\ from\ steam + {}^1/_4\, mol, O_2\ from\ air} = 33.3\ \% \tag{5.7}$$

It is correct to assume that all the oxygen present in the feeding air reacts with the metal oxide, because the thermodynamics of this reaction is very moved towards the products.

Different is the behavior of the steam-iron process, in which, at the thermodynamic equilibrium, all the species involved are present. As a consequence, in order to achieve a complete conversion of the oxygen carrier for a maximum hydrogen production, the steam is needed to bed fed in excess.
The goal of the brief analysis that follows is to quantify this steam excess by means of simulations carried out with the GS software.
The results, referred to the steam-iron process, are presented in the following Figure 5.2, where the steam excess needed for the complete metal oxide conversion at the thermodynamic equilibrium is shown as a function of the temperature.
It is noted the typical trend of the exothermic reaction, which is not favored at high temperature. As a result, the steam excess needed in the oxidation feed rises up when the reaction temperature increases.

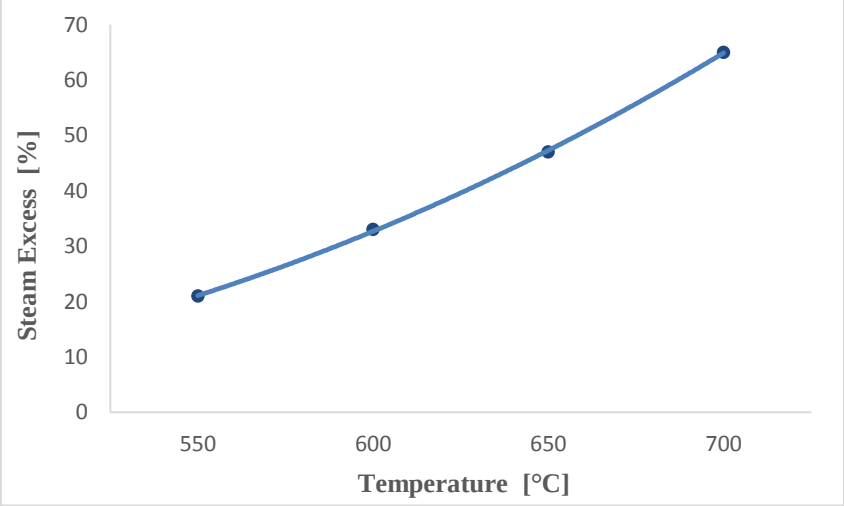

Figure 5.2: Steam excess needed for the complete conversion of the metal oxide at the thermodynamic equilibrium as a function of the temperature (FeO case).

As explained in the following 81, the simulations carried out for the evaluation of the active solid material fraction, has shown that, with the inlet and outlet temperature set for the HR plant, the steam-iron process is accomplished at around 600°C. For this temperature, a steam excess of around 30% is needed, the same value used in the HR power plant simulation described in Chapter 4.
The eventual need to raise the Steam excess, due to a high temperature which the reaction is accomplished at, would not lead to significant difference in the net electrical efficiency, as shown in 4.3.4 Sensitivity analysis on the air-to-steam ratio.

It is important to note that this discussion on the calculation of the $\%O_2$ from air and the steam excess, is carried out with the assumption of feeding the reactor in a sequential way: the air enters the reactor only after the steam has converted all the FeO present in the bed to Fe_3O_4. In this way, the maximum hydrogen production potential is exploited.
On the other hand, if a sort contemporary-feed is considered, the faster kinetics of the O_2 compared to the steam results in a part of the FeO that is converted directly by air into

Fe_2O_3. In this case, more sensible heat would be released and less hydrogen would be produced in the CL unit, like the process was fed with a higher $\%O_2$ from air.
As example, two simplified cases in which 5% and 10% of the FeO present in the bed is converted directly by air are presented.
By means of the stoichiometry (5.5 and 5.6) and considering as calculation bases the same syngas flow rate and composition of the HR plant case, 5.075 kmol/s of FeO are converted in the CL unit.
In the sequential feed, all this amount reacts entirely with the steam, but, in the contemporary feed example, part of the oxygen fed to the reactor oxidizes directly the FeO into Fe_2O_3. This means that a less amount of FeO is available for the reaction with the steam and less hydrogen is therefore produced. As a result, the entire CL process has to be operated with higher $\%O_2$ from air for completing the metal oxide oxidation.
The discussion above is summarized in Table 5.3, where the amount of FeO which is converted into Fe_3O_4 by steam and the amount of FeO which is directly oxidized by air into Fe_2O_3, are reported at different value of "% of FeO directly oxidized by air" (0%-5%-10%)
From a stoichiometric balance the correspondent molar flow of air and the $\%O_2$ from air can be calculated.

% O_2 from air for two contemporary-feed cases				
% FeO directly oxidized by air		**0%**	**5%**	**10%**
FeO converted directly into Fe_2O_3 by air	*kmol/s*	0.0	0.084	0.168
FeO converted into Fe_3O_4 by steam	*kmol/s*	1.682	1.598	1.513
O_2 that oxidizes directly FeO	*kmol/s*	0.0	0.063	0.126
O_2 that oxidizes Fe_3O_4	*kmol/s*	0.140	0.133	0.126
O_2 total fed to the reactor	*kmol/s*	0.140	0.196	0.252
% O_2 from air	**%**	**0.111**	**0.156**	**0.200**
Calculation basis: 152.56 kg/s of syngas which leads to 5.075 kmol/s of FeO converted in the oxidation reactor.				

Table 5.3: FeO case, $\%O_2$ from air and stoichiometric amount of steam in the oxidation reactor feed as a function of the $\%O_2$ that directly oxidizes the FeO into Fe_2O_3.

Although further study on the kinetics and the reactor model are needed to achieve more precise concluding remarks, from this analysis it has emerged that a non-sequential feed should be avoided, since the results would be higher $\%O_2$ from air with consequent lower hydrogen production, in comparison with the sequential-feed.

5.2.2 FeO case - calculation of the active solid material

The 0D model proposed by Noorman was developed specifically for the CLC technology, with the use of only air as reactant of the oxidation reactor. In the PeCLET process instead, a double-feed (steam and sub-stoichiometric air) is used.
For the scope of this work it was decided not to modify the Noorman's model and, using its same assumptions and logical steps, to simulate the process by means of the GS software. In this new GS model of the CL unit, all the possible iron states of oxidation (Fe-FeO-Fe_3O_4-Fe_2O_3) and two different inert matters are included.

Regarding the temperatures, the same values presented in 76 for the oxidation phase are used: initial temperature of FeO and inert matter 500°C, inlet temperature of air and steam 450°C.
In the simulation model the oxidation reaction is divided in two phases: firstly the FeO is entirely converted into Fe_3O_4 by steam (since it is fed with the proper steam excess) and finally the air completes the metal oxide oxidation to Fe_2O_3. All the calculations are carried out by the GS software at the thermodynamic equilibrium.
The maximum temperature chosen for the PeCLET process was 800°C; the weight content of the active material in the OC needed to bring the entire amount of solid present in the bed to this maximum temperature, is calculated by the GS software, with the gas-phase outlet temperature set at 500°C, as explained in 76.
Moreover, this calculations was carried out with two possible inert matters (the TiO_2 and the $MgAl_2O_4$ described in the 9) and considering also a non-sequential feed in which 10% of the FeO present in the bed is directly oxidized into Fe_2O_3 by air.
The results are here below presented, Table 5.4 for the sequential-feed and Table 5.5 for not-sequential feed:

Sequential-feed – Maximum temperature 800°C		
Inert Matter	TiO_2	$MgAl_2O_4$
Weight content of the active solid material in the OC (ω_{act})	0.370	0.435

Table 5.4: Weight content of the active solid material for two different inert matters (sequential-feed).

Not-sequential feed – 10% O_2 to FeO		
Inert Matter	TiO_2	$MgAl_2O_4$
Weight content of the active solid material in the OC (ω_{act})	0.322	0.382

Table 5.5: Weight content of the active solid material for two different inert matters, not-sequential feed with 10% of O_2 that oxidizes directly the FeO.

From these tables, the difference between the sequential and not-sequential feed in the fraction of active material has emerged: as soon as part of the oxygen fed to the reactor oxidizes directly the FeO, the overall oxidation reaction becomes more exothermic and therefore less active solid material is needed to keep the temperature at 800°C. As example, with TiO2 as inert the value of ω_{act} changes from 37.0% to 32.2%, due to the more heat released by the reaction.
The two inert materials lead to different value of ω_{act} for the same type of feed: the heat capacity of the $MgAl_2O_4$ is higher than the TiO_2 (1258 vs 939 J/kgK) and therefore less inert matter is needed to keep the maximum temperature at 800°. As a result, when $MgAl_2O_4$ is used as inert, more active solid material fraction is present in the OC (43.5% vs 37.0% of the TiO_2 case, with the sequential feed).

5.2.3 Fe case - stoichiometry and thermodynamic equilibrium of the oxidation reaction

The discussion and the main concepts about the stoichiometry and the thermodynamics of the oxidation reaction regarding the Fe case are very similar to those described for the FeO case in the 78.
Hence, only the results of the Fe case are presented, while the comparison between these two cases is carried out in the next 84.

The stoichiometric of the oxidation reaction regarding the Fe case, with the same division in steam-iron process and air oxidation as the FeO case, is presented here below:

$$3Fe + 4H_2O \leftrightarrow 4H_2 + Fe_3O_4 \tag{5.8}$$

$$Fe_3O_4 + \frac{1}{4}O_2 \leftrightarrow \frac{3}{2}Fe_2O_3 \tag{5.9}$$

From the stoichiometry above the $\%O_2$ from air is easily calculated by:

$$\%O_2\ from\ air = \frac{{}^1/_4\, mol, O_2\ from\ air}{2\ mol, O_2\ from\ steam + {}^1/_4\, mol, O_2\ from\ air} = 11.1\ \% \tag{5.10}$$

As it was described before for the FeO case, the reaction between the iron oxide and the steam for the production of hydrogen (Eq. 5.8) is not totally moved towards the products. The following Figure 5.3 shows the steam excess, at the thermodynamic equilibrium, needed for the complete conversion of the Fe (in order to reach the maximum hydrogen production), as a function of the temperature.
As occur in the FeO case, the simulations show that the temperature which the steam-iron reaction is accomplished at, is around 600°C. For this temperature, from the diagram below, the 40% of steam excess, chosen for the Base case plant described in 35, appears as a correct value.

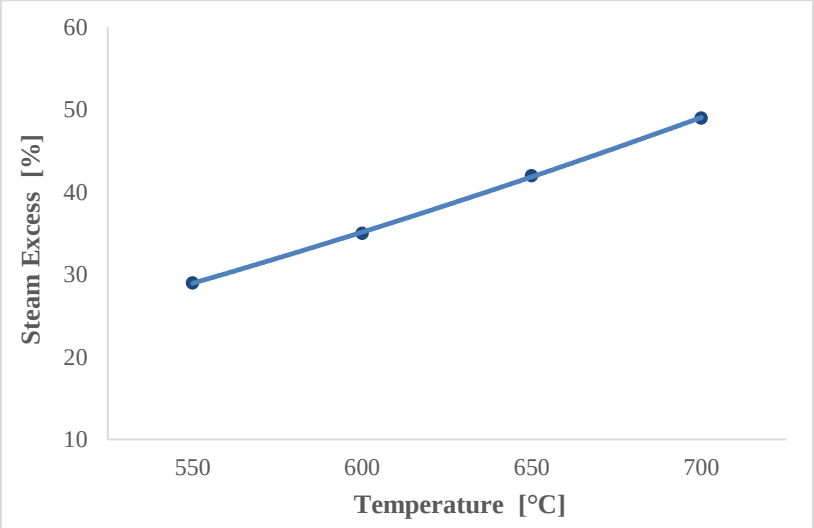

Figure 5.3: Steam excess needed for the complete conversion of the metal oxide at the thermodynamic equilibrium as a function of the temperature (Fe case).

5.2.4 Fe case - calculation of the active solid material

The same model and assumptions described in 81for the FeO case, are used for the study of the CL unit operated with Fe.

The Table 5.2 reports the temperatures for the Fe case: inlet temperature of air and steam 600°C and 450°C respectively, outlet streams (hydrogen and exhausts) at 800°C, bed at the beginning of the oxidation entirely at 500°C.

The simulation results on the weight content of the active solid material needed for achieving the maximum temperature of 800°C, are presented in the following Table 5.6 and Table 5.7, for the two inert matters and two possible types of feed already described for FeO case (Sec. 5.2.2).

Sequential-feed – Maximum temperature 800°C		
Inert Matter	TiO_2	$MgAl_2O_4$
Weight content of the active solid material in the OC (ω_{act})	0.420	0.474

Table 5.6: Weight content of the active solid material for two different inert matters (sequential-feed).

Not-Sequential feed – Maximum temperature 800°C		
Inert Matter	TiO_2	$MgAl_2O_4$
Weight content of the active solid material in the OC (ω_{act})	0.298	0.276

Table 5.7: Weight content of the active solid material for two different inert matters, not-sequential feed with 10% of O_2 that oxidizes directly the Fe.

5.2.5 Comparison between the Fe and FeO case

In this paragraph, a comparison between the Fe and FeO cases presented before, is carried out.

As regards the stoichiometry, it is soon noted the higher hydrogen production for the steam-iron process operated with Fe. From 1 kmol of Fe, 4 kmol of H_2 are formed and 0.25 kmol of O_2 are needed for the oxidation completion, resulting in a much lower $\%O_2$ from air compared to the FeO case (11.1% vs. 33.3%). As example, feeding the CL unit with always the same flow rate and composition of syngas (152.56 kg/s), 2.256 kmol/s of hydrogen are produced in the Fe case compared to the 1.692 kmol/s of the FeO case.

This leads to very important consequence: when Fe is chosen as most reductive state both the configurations of the power plant are allowed, since, as it is shown in Figure 4.12, for a low $\%O_2$ from air the difference between the HR plant and the Base case plant is not very significant.

On the other hand, the 33.3% of oxygen from air needed when the CL unit is operated with FeO forces the HR plant to be the only feasible choice.

As far as the thermodynamics is concerned, the trend of the steam excess as function of the temperature is the same of exothermic reaction for both the cases. From a comparison between Wustite(FeO) and pure-iron (Fe), it is noted that, for the FeO case, the necessary steam excess starts from lower value, but then it rises faster when the equilibrium temperature is increased.

As example, at 550°C the steam excess is 22% for FeO and 29% for Fe, while at 650°C is 47% for FeO and 42% for Fe.

Regarding the calculation of the ω_{act}, when the reactors are fed with the sequential feed, the weight content of active solid material for the Fe and the FeO case is comparable.

What emerged mostly from this study is the large difference between the two possible feeds in the CL unit operated with Fe: using TiO_2 as inert, a change from 42% (sequential feed) to 29.8% (not-sequential feed) occur. This is due to the very high exothermicity of the Fe direct oxidation by air. As soon as part of the oxygen reacts directly with the Fe, a significant increase in the temperature occur and therefore much lower active solid content is needed for achieving the 800°C.

On the other hand, the FeO direct oxidation by air is very exothermic but not as the Fe oxidation, resulting in a lower difference between the two possible feeds when FeO is chosen as most reductive state in the CL unit.

5.3 Iron oxides reduction reaction

The metal oxide reduction presents more issues in comparison with the oxidation reaction described in the previous paragraph.
As regards the thermodynamics, all the three possible reductive states of iron (Fe, FeO and Fe_3O_4) can be formed at the equilibrium during the reduction, depending on several factors, above all the temperature and the composition of the syngas fed to the reactor.
Hence, for a complete study on this reaction, additional deeper studies on the thermodynamics, kinetics and internal mechanism of the reactor are needed. In this work the discussion is focused only on the Baur-Glaessner diagram, which shows the equilibrium of the gas-solid system composed of CO-CO_2, H_2-H_2O and the possible iron-oxide reductive states Fe, FeO and Fe_3O_4.
Other issues that are outside the scope of this investigation, but required for a complete feasibility study of the reduction, are here below reported:

- Slow kinetics of the reaction between the CO and the iron-oxides, when the reduction is carried out at relative low temperature, as described in [16].
- Influence of the WGS reaction in the iron-oxide reduction.
- Carbon deposition: according to the chemical equilibrium with the syngas composition considered in this study, graphite could be formed in the range of 400-800°C. Additional studies related to the carbon formation kinetics over the iron-oxide would be required.

5.3.1 Reduction with FeO as most reductive state

In the plant operated with FeO, the addition of the heat removal phase in the reactor work cycle strategy is mandatory. This step is done by air and has to be carried out when the beds are still oxidized. As a result, before the reduction can be accomplished, a decrease in the reactor temperature occurs, resulting in possible slow kinetics especially for the CO reactions. The slow kinetics causes fuel slip during the reduction cycle.
The low temperature could be a problem also from the thermodynamic point of view, since, as it is shown in the Baur-Glaessner diagram below (Figure 5.4), the FeO is the predominant phase only when the reduction is carried out at more than 570°C.

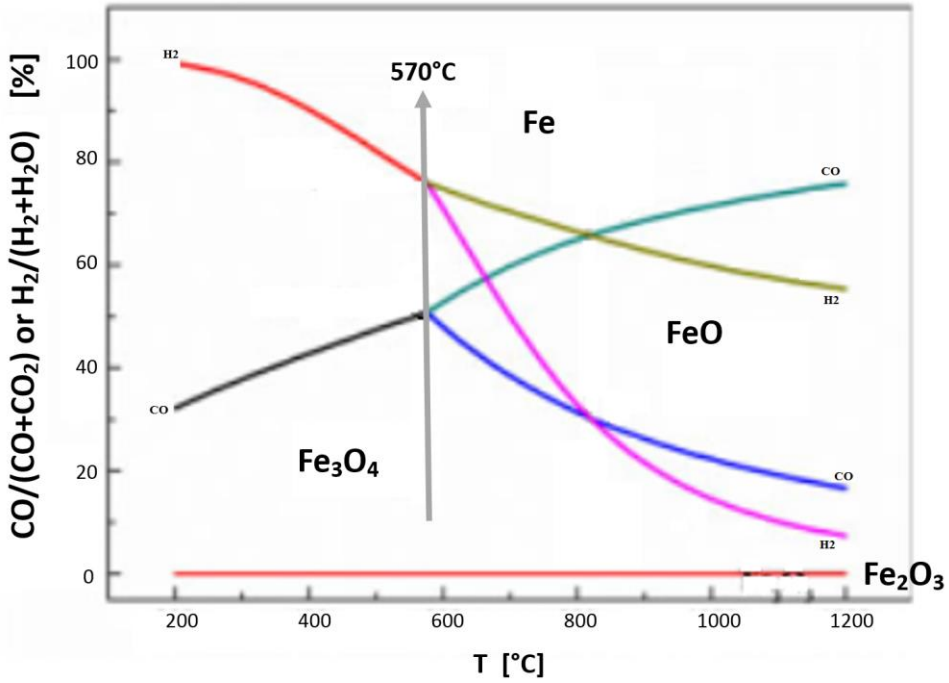

Figure 5.4: Baur-Glaessner diagram, predominance area diagram for iron oxides reduction reaction.

This issue is deeply described in [30], where only two possible iron-oxides reduction mechanisms are identified: Fe_2O_3 → Fe_3O_4 → Fe for process below 570°C and Fe_2O_3 → Fe_3O_4 → FeO → Fe for temperature higher than 570°C. In other studies, the dividing temperature between the two mechanisms (eutectoid temperature) has been evaluated to be lower, but never below 536°C.

As a consequence, for a total formation of FeO during the reduction, the process should be accomplished at temperature higher than 540-570°C.

In the IG-CLC plant described in [4], the power plant was operated with a semi-closed thermodynamic cycle with nitrogen used as work fluid. The heat removal phase could be therefore carried out with the beds reduced. As a result, the reduction was accomplished before the HR step at very high temperature, avoiding any kinetic and thermodynamic problem.

In IG-PCCL plant investigated in this work, the solution applied to the IG_CLC is obviously not viable and other solutions have to be worked out:

a) Partial HR: a possible solution is to proceed with a partial HR, leaving part of the bed at high temperature after this step. This was the assumption s that was made for the HR plant configuration, where in fact the reduction flow exits the reactor at 800°C.

   In order to guarantee this integration between the HR cycle and, as much as possible, a relative high temperature reduction, a very careful heat management strategy has to be elaborated.

   However, the partial HR solution brings along some related consequences: as shown in the Baur-Glaessner diagram (Figure 5.4), the formation of Fe_3O_4

(magnetite) in the low temperature part of the bed has to be accepted. This will cause a decrease of the hydrogen productivity and an increase of the $\%O_2$ from air in the subsequent oxidation step. To overcome these problems, a possible solution could be to obtain a mixing of the phases Fe_3O_4 and Fe, so that the negative effects of the magnetite are mitigated by the advantages of the pure-iron during the steam-iron process (high hydrogen production and low $\%O_2$ from air).

b) Partial HR with mixed oxygen carriers: this solution is equal to the previous one, but a mixture of FeO and Cu/Cu_2O is used as active part of the solid material. In this way, the exothermicity of the copper oxide reduction reaction can be exploited in the low temperature part of the bed for increasing the temperature up to the eutectoid value of 570°C and form all the possible FeO in the reduction reactions.
The copper oxide would not react with the steam in the following oxidation step, but with the air only, leading again to a lower hydrogen productivity and higher $\%O_2$ from air.

c) New OC: another possibility is to look for a complete different oxygen carrier that can accomplish the hydrogen production in the oxidation step and achieve the proper reductive state at relative low temperature in the reduction (about 450°C).

5.3.2 Reduction with Fe as most reductive state

In the plant operated with Fe as most reductive state of the iron oxide, the heat removal phase in the reactor work cycle strategy is not mandatory, and both the power plant configurations proposed in Chapter 4 are feasible. Nevertheless, as already anticipated in the 66, the base case plant would be preferable due to its potential lower costs and more integration simplicity.
The thermodynamics of the iron oxide reduction up to Fe derives from the same equilibrium described in the previous paragraph (85) with the use of the Baur-Glaessner diagram (Figure 5.4).
The Fe state, opposed to FeO, can be reached at any temperature and therefore the process is feasible for both the cases with or without the heat removal phase.
The reduction reaction is here below described for both the possible reactor work cycle strategies:

a) Fe case without HR: the reduction can be easily carried out at relative high temperature, since the bed is almost entirely at the maximum temperature of 800°C. As a result, the kinetics are improved and no particular thermodynamic issues exist.
b) Fe case with HR: Fe appears in the iron oxides reduction also at low T, as depicted in the Baur-Glaessner diagram (Figure 5.4). The formation of Fe by iron oxide reduction with CO does not present any particular thermodynamic issue (only the slow kinetics could become an issue).
The behavior of the iron oxide reduction by H_2 is different. This reaction is in fact a sort of reverse of the steam-iron process, and therefore is not really favored, especially if the process is operated at relative low temperature. As it is shown in

the Baur-Glaessner diagram, in this condition the equilibrium is characterized by a very high H_2/H_2O ratio in the Fe predominance area. Probably, in this case the reduction of Fe_2O_3 by reacting with H_2 will stop at the Fe_3O_4 state of oxidation, and then could be completed by reacting with CO.
However, for a full understanding of the reaction mechanism, additional studies on the kinetics are required.

When the Fe state is reached during the reduction, the design of the CL process must take into account the possible occurrence of the "sintering" phenomenon: the particles tend to agglomerate even though the melting point is not reached. This leads to a progressive decrease of the reactivity with the work cycle steps.
Recent studies of the Professor Fan, from Ohio State University, seem to demonstrate that with the proper support material this phenomenon can be avoided, and the Fe state can be reached fully exploiting its advantages.

5.3.3 Comparison between the Fe and FeO case

The choice of the oxygen carrier affects, as well as the plant layout, the performance and the reactor work cycle strategy, also the feasibility of the PeCLET process reactions, in particular the reduction.
In fact, when the OC forces to work with high air-to-steam ratio, the energy analysis performed in this work suggests that the reactor work cycle should include an HR phase that has to be carried out when the bed is still oxidized. Hence, before the reduction can be accomplished, a decrease in the bed temperature will occur, leading to thermodynamic and kinetic issues in the reduction. New strategies, as the ones proposed in the previous paragraph (5.3.1 Reduction with FeO as most reductive state) have to be worked out.
On the other hand, it would be easier to work with an oxygen carrier that can guarantee very low air-to-steam ratio, with which the HR phase addition can be avoided and hence the reduction can be more easily accomplished at high temperature.
In conclusions, the preliminary analysis on the iron oxides reduction reactions suggests that the Fe state, due to the possibility to accomplish a high temperature reduction, would be the preferable choice.

Chapter 6

Sizing of the CL reactors

6.1 Scope of the work

One of the scopes of this work is to size the packed bed reactors needed for the accomplishment of the PeCLET process reactions. More precisely, the optimal numbers and geometry of the reactors are investigated in order to reach the following goals:

- Reasonable pressure drop in the reactors, to limit the penalization of the downstream power island.
- Ensure the required stability to the operating cycle of the reactors.

6.2 CL unit and plant description

The sizing of the CL reactors system is carried out for both the plant configurations proposed in the previous chapter: the Base case plant operated with Fe (as most iron reductive state) and the HR plant operated with FeO.
In the Base case plant the reactor work cycle starts firstly with an oxidation of the active solid (Fe) by means of steam and compressed air; then, after a short reactor purge cycle to remove any traces of oxygen (with a stream of inert gas, typically nitrogen), the syngas enters the reactor and the reduction step can be accomplished. Both the outlet stream temperatures of the oxidation and reduction steps are relatively high, around 800°C.
One of the significant feature of this configuration is the high operating pressure of the CL unit (36.1 bar), which, as will be shown in this Chapter, affects considerably the necessary number of reactors and the investment cost of the plant.
As regards the HR plant, the addition of a heat removal phase before the reduction step is needed. In this configuration the outlet temperatures of the exhausts flow from reduction reactor and the heat removal air are equal to 800°C, while the hydrogen flow exits the oxidation reactor at 500°C.
The flow rates, compositions and thermodynamic properties of these streams shown in the following tables are the results of the power plant simulations described in Chapter 4.

				Molar composition [%]					
	T [°C]	**P [bar]**	$\dot{m}$ **[kg/s]**	**CO**	**CO_2**	**H_2**	**H_2O**	**O_2**	**N_2**
Air + Steam (Oxid)	510	36.1	76.5	-	-	-	84.5	3.7	13.8
Syngas (Reduct)	517	36.1	152.6	33.6	34.1	13.7	16.4	-	2.3

Table 6.1: Base case plant: flow rates, temperatures and compositions of the CL reactors inlet streams. The nitrogen molar fraction includes possible traces of Ar in the streams.

				Molar composition [%]					
	T [°C]	**P [bar]**	***ṁ* [kg/s]**	**CO**	**CO_2**	**H_2**	**H_2O**	**O_2**	**N_2**
H_2 stream (Oxid)	800	33.0	35.9	-	-	61.0	24.6	-	14.4
Exhausts (Reduct)	800	33.0	193.1	-	67.6	-	30.1	-	2.3

Table 6.2: Base case plant: flow rates, temperatures and compositions of the CL reactors outlet streams. The nitrogen molar fraction includes possible traces of Ar in the streams.

				Molar composition [%]					
	T [°C]	**P [bar]**	***ṁ* [kg/s]**	**CO**	**CO_2**	**H_2**	**H_2O**	**O_2**	**N_2**
Air + Steam (Oxid)	453	20.5	98.4	-	-	-	52.4	10.0	37.6
Syngas (Reduct)	517	20.5	152.6	33.6	34.1	13.7	16.4	-	2.3
HR air (HR)	443	20.5	478.1	-	0.03	-	1.0	20.7	78.2

Table 6.3: HR plant flow rates, temperatures and compositions of the CL reactors inlet streams. The nitrogen molar fraction includes possible traces of Ar in the streams.

				Molar composition [%]					
	T [°C]	**P [bar]**	***ṁ* [kg/s]**	**CO**	**CO_2**	**H_2**	**H_2O**	**O_2**	**N_2**
H2 stream (Oxid)	500	19.5	57.8	-	0.02	44.4	13.8	-	41.8
Exhausts (Reduct)	800	19.5	193.1	-	67.6	-	30.1	-	2.3
HR air (HR)	800	19.5	478.1	-	0.03	-	1.0	20.7	78.2

Table 6.4: HR plant: flow rates, temperatures and compositions of the CL reactors outlet streams. The nitrogen molar fraction includes possible traces of Ar in the streams.

6.2.1 Operating parameters

In order to properly size the reactors of the considered plants, the definition of the operational parameters of the fixed beds technology is needed. A typical parameter that characterizes the fluid dynamics of the reactor is the void fraction of the bed. Table 6.5 shows the main values of this parameter for different disposals of the solid [31].

Packing arrangement	**Bed voidage (ε)**
Spheres - rhombohedral	0.2595
Spheres – tetragonal	0.3019
Spheres - random	0.36 – 0.43
Spheres – orthorombic	0.3954
Spheres - cubic	0.4764

Table 6.5: Void fraction of the bed for different solid disposal.

For this work it has been decided to set this parameter at a value of 40%, typical of a random packing arrangement of the solid in the reactor. These particles can be considered to be spherical with a diameter of 5 mm and with a porosity of about 60%. The first parameter is of great importance for the sizing of the reactor because, as it will be described in 91, it strongly affects the pressure drop inside the bed.

Typically, increasing the size of the particles, a strong reduction in the pressure drop is observed. Hence, it would be convenient to operate with spheres of large dimension.
However, a too high diameter value would lead to diffusion problems of the reactant gas within the particles, leading to a slowdown of the reactions kinetics. In this study, a sensitivity analysis of the chemical diffusion of the gas has not been carried out and it is considered that a particle diameter of 5 mm can be a reasonable value in order to avoid problems of diffusion.

To calculate the properties of the solid material inside the reactor, it is needed to know the weight content of active material in the solid. In the previous chapter (73), the weight content of active material necessary at the beginning of the oxidation process for achieving the maximum temperature (T_{max}) of 800°C was calculated. From this value the correspondent quantity at the beginning of the reduction process has been calculated. These two values are presented in Table 6.6.

Base case plant	ω_{act} [%wt]	ω_{inert} [%wt]
Beginning of the oxidation	42.0	58.0
Beginning of the reduction	50.9	49.1
HR plant	ω_{act} [%wt]	ω_{inert} [%wt]
Beginning of the oxidation	37.0	63.0
Beginning of the reduction	39.5	60.5

Table 6.6: Active and inert material content at the beginning of the oxidation and reduction steps, for both the plant configurations.

6.3 Pressure drop

After determining the main reactor operational parameters, it is possible to calculate the pressure drop that occurs as a result of the flow of the gas through the bed. This is a fundamental parameter for the entire operation of the system, since it affects:

- Downstream power island, in a way depending on the configuration:
  - in the HR plant the operating pressure of the GT and CL units are strictly correlated, due to the significant flow rate of the heat removal air that is pre-heated in the reactor before entering the GT combustor. Hence, a high pressure drop in the packed beds would result in an efficiency penalty of the entire downstream power island.
  - As regards the Base case plant, the pressure drop inside the reactors does not substantially affect the efficiency of the power island, at least as long as it is not very high. In fact, since the heat removal step is not present in the reactor work cycle, the operating pressure of the GT and CL units are not strictly connected and very different (18 bar vs. 36.1 bar respectively). The only flow that connects the reactors to the power island is the hydrogen

flow, whose pressure is much higher than the GT operating pressure even in case of significant pressure drop in the reactor.
This discussion is valid only if the use of an expander is not considered, as in the plant configuration proposed in this work.

- CO_2 capture section: the CL exhaust gases exiting the reduction step, mainly composed of CO_2 and H_2O, after various treatments of dehydration, is compressed. High pressure drop in the reactor would lead to a rise in the energy consumption for the downstream compressor, affecting negatively the efficiency of the entire plant.

In conclusion a pressure drop inside the reactors is inevitable, but it is important that its value is not excessively high. A maximum pressure drop of 8% (Δp/p) is considered in this work.

The pressure drop inside the reactor can be estimated by means of the Ergun equation:

$$\frac{\Delta P}{L} = 150\frac{(1-\varepsilon)^2}{\varepsilon^3}\frac{\mu U}{\varphi^2 d_p^2} + 1.75\frac{(1-\varepsilon)}{\varepsilon^3}\frac{\rho U^2}{\varphi d_p} \tag{6.1}$$

Where L is the height of the bed, ε is the void fraction of the bed, μ the viscosity of the gas, φ is the sphericity (defined as the ratio between the surface area per unit volume of a sphere and of the particle considered), d_p is the diameter of the particle, ρ is the density of the gas and U is the superficial gas velocity (calculated considering the reactor as if it were empty), all in their proper units of measure.

The gas viscosity was calculated according to the method of Chung et al. reported in [32].
To be more conservative, it was decided to calculate the thermodynamic properties (viscosity and density) and the reactor inlet velocity, at the maximum reactor temperature. At this temperature the combined effects of these parameters determines the maximum pressure drop.
Hence, assuming that the reactors operate always at T_{max}, the real pressure drop inside the beds will always be less than or equal to the value calculated.

Also the void fraction of the reactor and the size of the particles affect the pressure drop. Increasing the first parameter, the amount of solid present in the reactor and consequently the resistance to the flow of the gas decrease, determining lower pressure difference between the inlet and the outlet of the reactor.
Similarly, the rise in the diameter of the solid particles within the reactor leads to a significant decrease of the pressure drop.

The geometry of the reactor (diameter D and height L) has a considerable impact on the reactor pressure drop. The two main effects are here explained:

- With the increase of the diameter the velocity decreases and as well as the pressure drop.
- With the rise of the reactor height, the gas path becomes longer. As a result, keeping constant the other factors, the pressure drop will increase.

In conclusion, to limit the pressure drop inside the reactors, it is necessary to use beds with large diameter and limited L/D ratio. But, on the other hand, by operating at low L/D ratio significant critical issues can emerge: difficulty in assuring a uniform distribution of the gas inside the bed, high probability of incurring in the bed fluidization phenomenon and operation of the reactors with too short duration of the single phases, as it will be explained in the following paragraph.

6.4 Optimization of the geometry

Due to the consistent mass flow rates present in the plant, as shown in Table 6.3 and Table 6.1, it will not be always possible to use a single reactor, but the flows of air, steam and syngas may have to be divided in multiple reactors working in parallel. If the feeds of the various reactors are suitably shifted in time, the system can be managed as in steady state. It is then necessary to choose an appropriate geometry (diameter and height of the bed). For this reason a sensitivity analysis has been carried out, showing how the number of reactors needed in the process varies when their diameter and height are changed.
It is important to underline that in this analysis the variation of the pressure drop with the change of the bed geometry is not examined, but rather it is analyzed how the number of reactors required to maintain the pressure drop around a value of 8% ($\Delta p/p$) varies as a function of the geometry.

6.4.1 Oxidation and reduction

Once the geometry is fixed, the pressure drop can be reduced (or raised) by increasing (or decreasing) the number of reactors, since the change in the reactors number affects directly the flow rate operated by each reactor and, consequently, the gas velocity.
The logic process to determine the reactors number and sizing, applied to the oxidation and reduction phases, is shown in Figure 6.1.

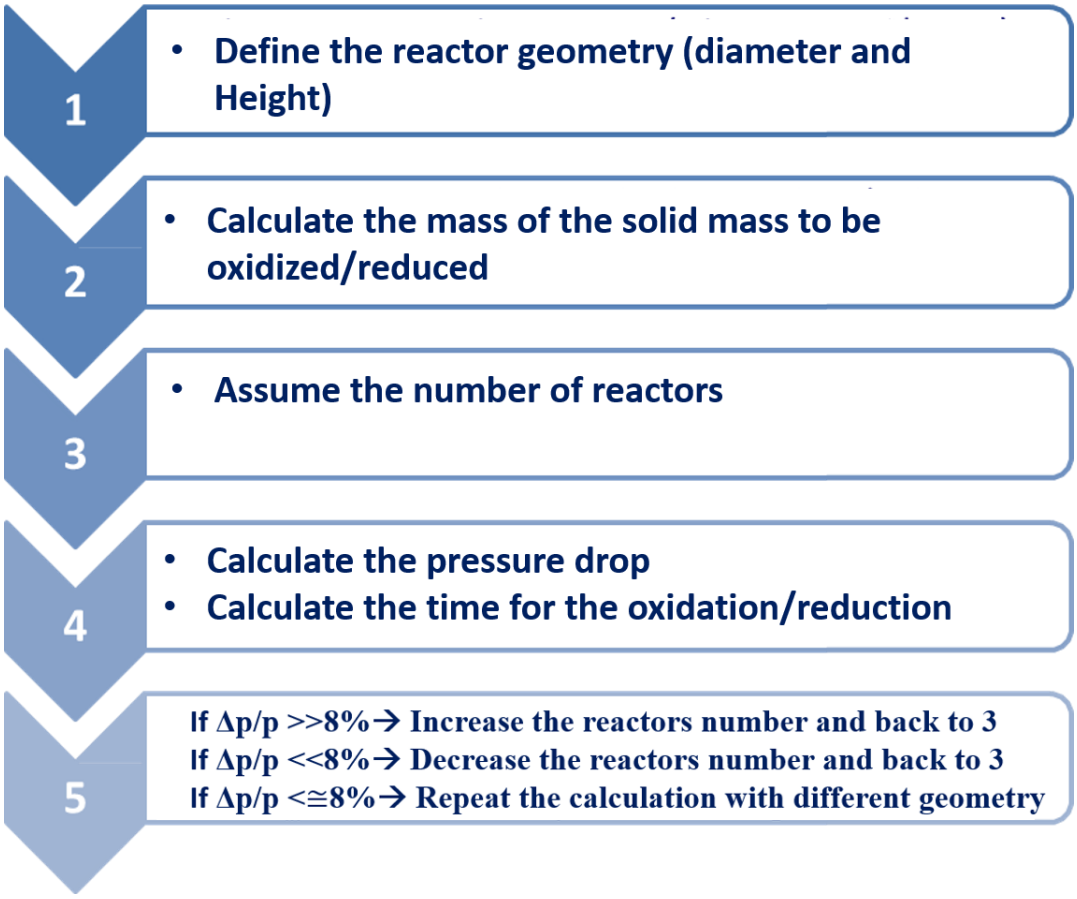

Figure 6.1: Logic process used in the sizing of the oxidation and reduction reactors.

The total volume of the solid material present in the reactors can be estimated knowing the geometry and the number of the beds.
Through the material density and the weight content of the active phase, the time required for the oxidation step can be calculated as:

$$\tau_{oxi} = \frac{(V_{tot}\,\rho_{bed}\omega_{act})/MM_{act}}{\dot{N}_{O2,air\&steam}/N_{beds}\cdot\zeta} \tag{6.2}$$

The calculation of the bed density used in the equation (6.2) is explained hereinafter. Defining the particle porosity (here assumed equal to 60%) as in the following equation (6.3),

$$\alpha = \frac{V_{solid}}{V_{total}} \tag{6.3}$$

and considering the mass fractions, the molecular weights and the densities of the solid species involved during the reaction as reported in the following Table 6.7 for Base case plant and HR plant,

BASE CASE PLANT	**FeO**	**Fe_2O_3**	**TiO_2**
ρ *[kg/m³]*	5745	5240	4230
MM *[kg/kmol]*	71.85	159.70	79.87
ω_{act} Oxid *[% wt]*	42.0	-	58.0
ω_{act} Reduct *[% wt]*	-	50.9	49.1
HR PLANT	**FeO**	**Fe_2O_3**	**TiO_2**
ω_{act} Oxid *[% wt]*	37.0	-	63.0
ω_{act} Reduct *[% wt]*	-	39.5	60.5

Table 6.7: Properties of the solid material involved in the reactions.

it is possible to calculate the bed density with the following equations:

$$\rho_{solid} = \frac{1}{\left(\frac{\omega_{act}}{\rho_{act}} + \frac{\omega_{inert}}{\rho_{inert}}\right)} \tag{6.4}$$

$$\rho_{bulk} = \rho_{solid} \cdot \alpha \tag{6.5}$$

$$\rho_{bed} = \rho_{bulk} \cdot (1 - \varepsilon) \tag{6.6}$$

Actually the value of porosity for the oxidation phase is different from that of the reduction phase. Considering a particle of unitary and constant volume, the metal, passing from its oxidized form to the reduced form, presents different densities (Table 6.7) and different masses. During the reduction phase, the metal releases oxygen to the reducing gas diminishing its mass, while, during the oxidation, the metal mass is increased for the reverse process. During these reactions, the amount of inert material present in the particles, which does not take part to the chemical reaction, remains constant. By imposing the mass conservation of such material, it is possible to observe, in Table 6.8, how the porosity of the particles changes.

Base Case Plant	**Beginning Oxidation**	**Beginning Reduction**
α $[m^3_{solido}/m^3_{tot}]$	0.60	0.45
ρ bulk $[kg/m^3]$	2384	2814
ρ solid $[kg/m^3]$	5251	4691
M inert *[kg]*	1383	1383
M total *[kg]*	2384	2814
HR plant	**Beginning Oxidation**	**Beginning Reduction**
α $[m^3_{solido}/m^3_{tot}]$	0.56	0.60
ρ bulk $[kg/m^3]$	2639	2747
ρ solid $[kg/m^3]$	4687	4579
M inert *[kg]*	1662	1662
M total *[kg]*	2639	2747

Table 6.8: Porosity calculation, mass balance for the reactive particle with unitary and constant volume, for both the plant configurations.

The calculations were carried out by varying the diameter from 3 m up to a maximum of 7 m. Instead of directly changing the bed height it was decided to modify the L/D ratio, whose values are between 0.25 and 5. The results obtained are presented in Table 6.9 and Table 6.10 for the Base case plant and the HR plant respectively).
It is noted that, when the reactors number are the same for the two phases, the time needed for the reduction step is equal to that of the oxidation step.
Similarly, when the number of reactors is different, the reduction time is the oxidation time multiplied for a factor which is the ratio between the respective reactor (bed) numbers: $N_{beds,reduction}/N_{beds,oxidation}$.

As regards the oxidation phase, the pressure drop in the Base case plant is lower than in the HR plant, for the following two reasons:

- The Base case plant CL reactors are operated at 36.1 bar (vs. 20.5 bar in the HR plant). Higher pressure means, at constant fluid cross section (constant geometry and number of reactors), higher gas density and lower gas velocity.
- The oxidation feed of the Base case plant is lower than in the HR configuration, 76.5 kg/s vs. 98.5 kg/s.

On the other hand, the pressure drop of the reduction reactor is significantly higher than that of the oxidation reactor of the respective plant configuration, due to its higher feed flow rate.
Once again, the pressure drop in the Base case plant is lower compared to the HR plant, due to the higher operating pressure of this configuration.

BASE CASE PLANT - OXIDATION										
		L/D								
	D *[m]*	0,25	0,5	0,75	1	1,5	2	3	4	5
N Letti		1	1	1	1	1	1	1	2	2
τ	**3**	34	68	102	136	203	271	407	1085	1356
Δp/p		0,006	0,012	0,018	0,025	0,037	0,049	0,074	0,025	0,032
N Letti		1	1	1	1	1	1	1	1	1
τ	**4**	80	161	241	321	482	643	964	1285	1607
Δp/p		0,003	0,005	0,008	0,011	0,016	0,021	0,032	0,042	0,053
N Letti		1	1	1	1	1	1	1	1	1
τ	**5**	157	314	471	628	941	1255	1883	2510	3138
Δp/p		0,001	0,003	0,004	0,006	0,008	0,011	0,017	0,022	0,028
N Letti		1	1	1	1	1	1	1	1	1
τ	**6**	271	542	813	1085	1627	2169	3254	4338	5423
Δp/p		0,001	0,002	0,003	0,003	0,005	0,007	0,010	0,014	0,017
N Letti		1	1	1	1	1	1	1	1	1
τ	**7**	431	861	1292	1722	2583	3444	5167	6889	8611
Δp/p		0,001	0,001	0,002	0,002	0,003	0,004	0,007	0,009	0,011
HR PLANT - OXIDATION										
		L/D								
	D *[m]*	0,25	0,5	0,75	1	1,5	2	3	4	5
N Letti		1	1	2	2	2	2	3	3	3
τ	**3**	9	17	51	68	102	136	307	409	511
Δp/p		0,029	0,059	0,023	0,030	0,045	0,060	0,041	0,055	0,069
N Letti		1	1	1	1	1	2	2	2	2
τ	**4**	20	40	61	81	121	323	485	646	808
Δp/p		0,013	0,025	0,038	0,050	0,076	0,027	0,040	0,053	0,066
N Letti		1	1	1	1	1	1	2	2	2
τ	**5**	52	105	157	210	315	420	1260	1679	2099
Δp/p		0,007	0,013	0,020	0,027	0,040	0,053	0,021	0,029	0,036
N Letti		1	1	1	1	1	1	1	1	1
τ	**6**	68	136	204	273	409	545	818	1090	1363
Δp/p		0,004	0,008	0,012	0,016	0,024	0,032	0,048	0,064	0,079
N Letti		1	1	1	1	1	1	1	1	1
τ	**7**	108	216	325	433	649	866	1298	1731	2164
Δp/p		0,003	0,005	0,008	0,010	0,016	0,021	0,031	0,042	0,052

Table 6.9: Reactors number, pressure drop and duration of the oxidation phase for both the power plant configurations (Base case and HR plant).

HR PANT - REDUCTION										
		L/D								
	D *[m]*	0,25	0,5	0,75	1	1,5	2	3	4	5
N Letti		1	1	2	2	2	2	3	3	3
τ	**3**	34	68	203	271	407	542	1220	1627	2033
Δp/p		0,036	0,071	0,027	0,036	0,054	0,072	0,049	0,065	0,081
N Letti		1	1	1	1	2	2	2	2	2
τ	**4**	80	161	241	321	964	1285	1928	2571	3213
Δp/p		0,015	0,030	0,046	0,061	0,023	0,031	0,047	0,062	0,078
N Letti		1	1	1	1	1	1	2	2	2
τ	**5**	157	314	471	628	941	1255	3766	5021	6276
Δp/p		0,008	0,016	0,024	0,032	0,047	0,0631	0,025	0,033	0,041
N Letti		1	1	1	1	1	1	1	1	2
τ	**6**	271	542	813	1085	1627	2169	3254	4338	10845
Δp/p		0,005	0,009	0,014	0,019	0,028	0,037	0,056	0,074	0,025
N Letti		1	1	1	1	1	1	1	1	1
τ	**7**	431	861	1292	1722	2583	3444	5167	6889	8611
Δp/p		0,003	0,006	0,009	0,012	0,018	0,024	0,036	0,048	0,060
HR PLANT - REDUCTION										
		L/D								
	D *[m]*	0,25	0,5	0,75	1	1,5	2	3	4	5
N Letti		2	2	3	3	4	4	5	6	6
τ	**3**	17	34	77	102	205	273	512	818	1023
Δp/p		0,030	0,061	0,041	0,055	0,047	0,063	0,061	0,057	0,072
N Letti		1	2	2	2	3	3	3	4	4
τ	**4**	20	81	121	162	364	485	728	1293	1617
Δp/p		0,051	0,026	0,039	0,053	0,036	0,048	0,072	0,055	0,069
N Letti		1	1	2	2	2	2	3	3	3
τ	**5**	53	105	315	420	630	841	1891	2522	3152
Δp/p		0,027	0,053	0,021	0,028	0,042	0,055	0,038	0,051	0,064
N Letti		1	1	1	1	2	2	2	2	3
τ	**6**	68	136	205	273	818	1091	1637	2183	4092
Δp/p		0,016	0,031	0,047	0,063	0,025	0,033	0,050	0,066	0,039
N Letti		1	1	1	1	1	2	2	2	2
τ	**7**	108	217	325	433	650	1733	2599	3466	4332
Δp/p		0,010	0,020	0,030	0,040	0,060	0,022	0,033	0,043	0,054

Table 6.10: Reactors number, pressure drops and duration of the oxidation phase for both the power plant configurations (Base case and HR plant).

6.4.2 Heat removal

The discussion carried out in this paragraph concerns the HR plant configuration only.

For the heat removal phase, the steps reported in Figure 6.1 can be followed with the exception of point 2, required for reactive phases only. The duration of this step depends on the number of reactors chosen and will be determined so as to ensure a correct operation

of the plant. Once set the duration and the number of reactors for the oxidation and reduction processes, the time relevant to the heat removal phase is a direct consequence of the number of beds chosen for this step. In particular, to be able to operate the plant in stationary state, the time phase results to be:

$$\tau_{heat\ removal} = \tau_{oxi} \frac{N_{beds,heat\ removal}}{N_{beds,oxid}} \tag{6.7}$$

The number of reactors of this phase, the corresponding pressure drop and the duration are shown in the following Table 6.11:

HR PLANT - HEAT REMOVAL										
		L/D								
	D [m]	0,25	0,5	0,75	1	1,5	2	3	4	5
N Letti		4	5	7	8	10	11	14	16	18
τ	**3**	34	85	179	273	511	749	1431	2180	3066
Δp/p		0,061	0,079	0,061	0,063	0,061	0,068	0,064	0,066	0,066
N Letti		3	4	5	5	7	7	9	11	12
τ	**4**	61	162	303	404	848	1131	2180	3553	4845
Δp/p		0,046	0,053	0,051	0,068	0,054	0,071	0,066	0,060	0,064
N Letti		2	3	4	4	5	5	7	8	9
τ	**5**	105	315	630	840	1574	2099	4408	6718	9447
Δp/p		0,054	0,049	0,042	0,056	0,054	0,072	0,057	0,059	0,060
N Letti		2	2	3	3	4	4	5	6	7
τ	**6**	136	273	613	818	1635	2180	4088	6541	9539
Δp/p		0,032	0,063	0,043	0,057	0,050	0,066	0,065	0,062	0,058
N Letti		2	2	2	3	3	4	4	5	5
τ	**7**	216	433	649	1298	1948	3462	5193	8656	10819
Δp/p		0,020	0,040	0,061	0,037	0,056	0,043	0,065	0,057	0,071

Table 6.11: Reactors number, pressure drop and duration of the heat removal step.

From all the previous tables, it is noted that, for all phases, the pressure drops are often far from the maximum design value of 8%. This is especially true in the oxidation phases due to the lower flow rate. Another reason is that the number of reactors must be obviously discrete and, by increasing it by one unit, the pressure drops can decrease significantly.

In Figure 6.2, it is possible to observe, for different analyzed geometries, the minimum number of beds needed to fulfill the conditions previously set. The number of beds presented in this diagram takes into account the reactors required by the oxidation, reduction and heat removal steps, excluding, for now, the beds needed by the purge phase. Two main considerations can be made:

- At constant diameter, the rise of the L/D ratio leads to an increase of the bed height and, consequently, the pressure drop.

It will be necessary to operate with a greater number of reactors in order to maintain the pressure drop below the value of 8%.

- At constant L/D ratio, rising the diameter, the height of the reactor and the cross section increase; the first factor would lead to a rise of the pressure drop while the second to a reduction. It is observed that the cross section effect is predominant; in fact, as shown in Figure 6.2, it is possible to work with a lower number of beds by increasing the diameter.

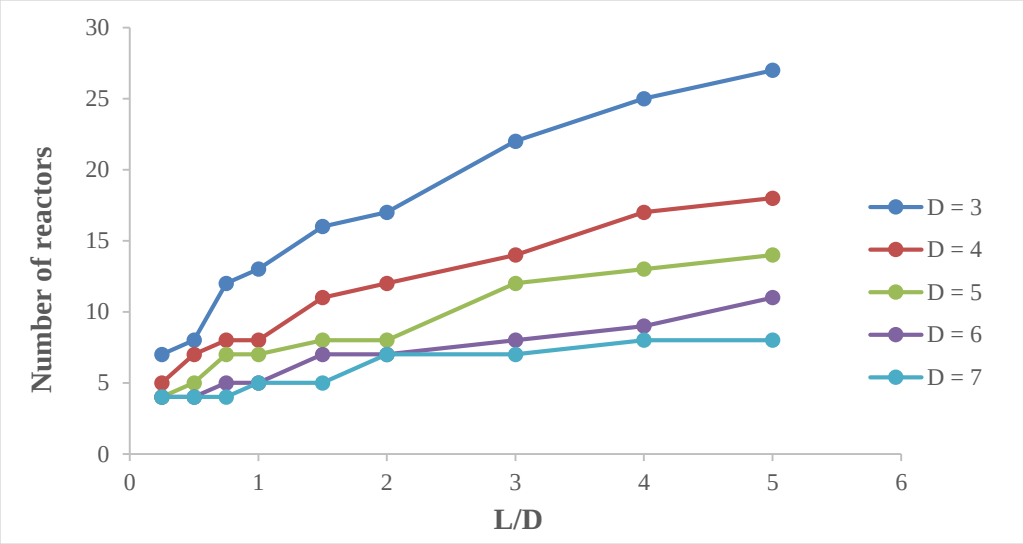

Figure 6.2: Variation of the reactors number as a function of the L/D ratio for different diameters, HR plant.

6.4.3 Purge

The addition of the purge step is of fundamental importance. In fact a purge step is needed between the phases of oxidation and reduction, in order to empty the reactor from any residual oxygen before the syngas is fed. Due to the significant presence of CO and H_2 and the high temperature of the material, there would be a sudden combustion with risks for the safety of the plant.

For this phase, an inert gas flow rate with a volume correspondent to 5 times the volume of the reactor is usually adopted. Due to the relative low flow rate required, it is possible to accomplish this phase by means of a single reactor, but at the condition that the purge duration is equal to:

$$\tau_{purge} = \frac{\tau_{oxid}}{N_{oxid}} \tag{6.8}$$

The mass flow rate of the purge, shown in Table 6.12, was therefore calculated by:

$$\dot{m}_{purge} = \frac{5\, V_{reactor} \rho_{in}}{\tau_{purge}} \tag{6.9}$$

The purge phase has to be carried out twice during a single reactor work cycle, because the oxidation and the reduction step have to be always separated by a nitrogen purge.

BASE CASE PLANT - PURGE										
	D [m]	0,25	0,5	0,75	1	1,5	2	3	4	5
τ		34	68	102	136	203	271	407	542	678
m	3	8.87	8.87	8.87	8.87	8.87	8.87	8.87	8.87	8.87
τ		80	161	241	321	482	643	964	1285	1607
m	4	8.87	8.87	8.87	8.87	8.87	8.87	8.87	8.87	8.87
τ		157	314	471	628	941	1255	1883	2510	3138
m	5	8.87	8.87	8.87	8.87	8.87	8.87	8.87	8.87	8.87
τ		271	542	813	1085	1627	2169	3254	4338	5423
m	6	8.87	8.87	8.87	8.87	8.87	8.87	8.87	8.87	8.87
τ		431	861	1292	1722	2583	3444	5167	6889	8611
m	7	8.87	8.87	8.87	8.87	8.87	8.87	8.87	8.87	8.87
HR PLANT - THE PURGE										
						L/D				
	D [m]	0,25	0,5	0,75	1	1,5	2	3	4	5
τ		9	17	26	34	51	68	102	136	170
m	3	29.73	29.73	29.73	29.73	29.73	29.73	29.73	29.73	29.73
τ		20	40	61	81	121	162	242	323	404
m	4	29.73	29.73	29.73	29.73	29.73	29.73	29.73	29.73	29.73
τ		52	105	157	210	315	420	630	840	1050
m	5	29.73	29.73	29.73	29.73	29.73	29.73	29.73	29.73	29.73
τ		68	136	204	273	409	545	818	1090	1363
m	6	29.73	29.73	29.73	29.73	29.73	29.73	29.73	29.73	29.73
τ		108	216	325	433	649	866	1298	1731	2164
m	7	29.73	29.73	29.73	29.73	29.73	29.73	29.73	29.73	29.73

Table 6.12: Mass flow rate and duration of the purge step, with the use of a single reactor.

6.4.4 The choice of geometry

To choose the best configuration among the geometries proposed, it is needed to consider some reasonable limitations. In particular:

- Reactors with very high diameter and/or height are unlikely to be used. The transportation of these components would be very difficult, and the construction on site of such structures would lead to long times and high costs. In the present analysis, it will be considered a maximum diameter and height respectively of 5.5 and 20 m.
- The reactors characterized by a very low L/D ratio (less than 1) cause very limited pressure drops and allow a reduction of beds number. But this geometry leads to a series of consequences, including:
    - The risk of fluidizing the bed due to the high flow rate in the reactors, as widely described in [8]. This is as valid as smaller is the diameter because, due to the more limited cross section, the gas velocity will be higher.

- Difficulty in feeding the reactors and in assuring a uniform gas distribution inside the beds.

From these considerations, for both the Base case plant and the HR plant, it is chosen to use reactors with a diameter of 5.5 m and a height of 11 m, which correspond to a L/D ratio equal to 2. In this way, it is possible to avoid the problems described above.
In conclusion, the main reactor parameters of each phase are shown in Table 6.133 for both the power plant configurations:

	FeO CASE			Fe CASE		
_	N,react	τ (s)	Δp/p *[%]*	N,react	τ (s)	Δp/p *[%]*
Oxid	1	420	4,06	1	1255	0,86
HR	5	2100	5,530	/	/	/
Purge	2	840	/	2	2510	/
Red	2	840	4,23	1	1255	4,78
TOTAL	10	4200		4	5020	

Table 6.13: Reactors number, pressure drop and duration of each phase. D = 5.5m and L = 11m.

6.5 Reactors operation management

For each of the two plant configurations considered it is now possible to depict the operation management of the reactors. In the following schemes Figure 6.3 and Figure 6.4 the phases of oxidation, heat removal, purge and reduction are indicated respectively with the letters O, H, P and R.

6.5.1 HR plant

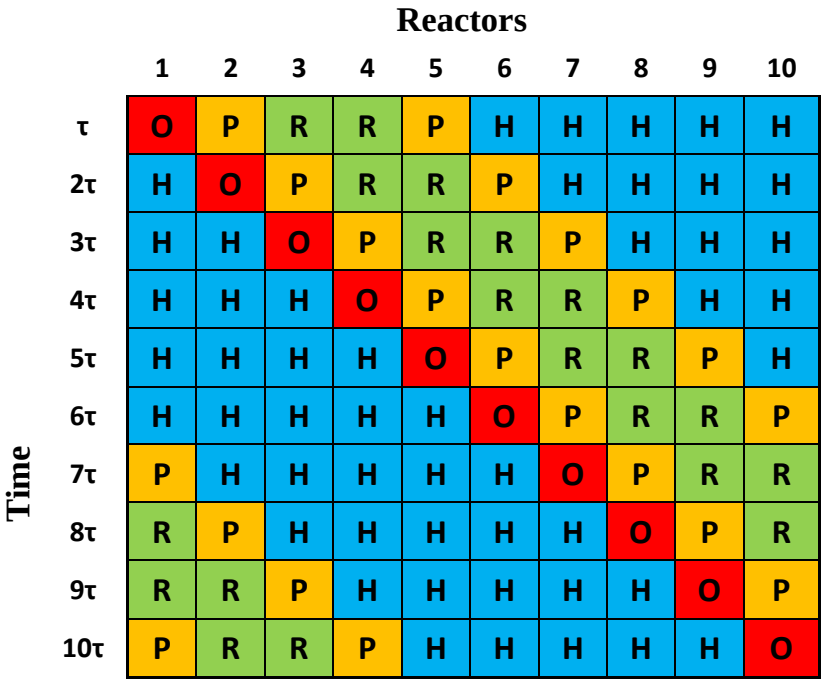

Figure 6.3: HR plant, operation management of the reactors.

It is noted that:

- At a certain instant, as example the initial time "τ", all the beds are correctly operated in the respective phases: 1 in oxidation, 2 in reduction, 2 in purge and 5 in the heat removal step.
- Considering a single reactor, as example the number 1, it can be seen how the phases are alternated:
    - Oxidation: this phase has a duration of 1τ, and all the oxidation feed (air plus steam) is fed to this reactor.
    - Heat Removal: in this step, the reactor is fed with 1/5 of the heat removal air, while the remaining 4/5 is fed to the other 4 reactors, with an adequate phase displacement.
    - Purge: all mass flow rate required is fed to this reactor for a duration equal to 1τ.This step is carried out twice per reactor work cycle.
    - Reduction: this step lasts 2τ and the reactor is fed with ½ of the total flow rate of the syngas. The remaining ½ is fed to another reactor, with an adequate phase displacement.

6.5.2 Base case plant

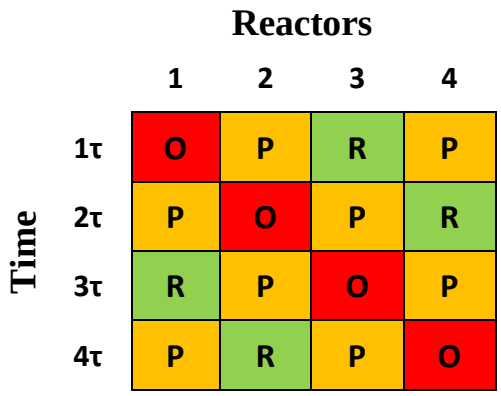

Figure 6.4: Base case plant, operation management of the reactors.

It is soon noted the significant difference with respect to the HR plant. In the Base case plant, in fact, an important reduction in the reactors number (from 10 to 4) is obtained: the heat removal step, which in the previous case required 5 beds, is not present here and the oxidation, the reduction and the purge need only one bed each.
The reason of the possibility to use one bed only in the reduction phase (with the same syngas flow rate) is that, in the base case plant, the operating pressure of the CL reactors is significantly higher than in the HR plant (36.1 bar vs. 20.5 bar).

In conclusion, the Base case plant has showed the important advantage of requiring 4 reactors only, compared to the 10 of the HR plant. Hence, in the case that the reactors and the solid material have the same price for both the plant configurations, the base case plant can potentially offer a reduction of the CL island investment costs equal to 60%.

6.5.3 Comparison of the PeCLET plants with the CLC plant

As it was said before, the direct competitor of the plant based on the PeCLET process and coal gasification, is the IG-CLC plant, which exploits the chemical looping combustion technology for feeding the downstream combined cycle. This kind of power plant was widely studied by Martelli in [8]: the same choice regarding the logic process for the evaluation of the reactors operation management was made and the same reactor geometry (D=5.5 and H=11) was used. The results of the IG-CLC presented in [8] , are here below reported:

_	N,react	τ (s)	$m_{total,in}$ *[kg/s]*	$m_{total,out}$ [kg/s]	P *[bar]*
Oxidation	3	1028	178	137	17
Purge	1	343	30	30	17
Reduction	3	1028	148	189	17
Heat Removal	7	2398	561	561	17
TOTAL	14	4797	-	-	-

Table 6.14: Results of the IG-CLC reported in [3].

It is soon noted the higher reactors number of the IG-CLC in comparison with the HR plant (PeCLET), for all the phases: oxidation, reduction and heat removal. This can be explained with the following considerations:

- The mass flow rates involved are higher in the IG-CLC, for all the reactor phases.
- The operating pressure of CL island is lower in the IG-CLC (around 17 bar).
- The maximum temperature reached in the CL island of the IG-CLC plant is much higher (1200°C):

All these factors leads to an increase of the pressure drop and, consequently, more beds are needed for keeping it below the Δp/p value of 8%.

In conclusion, the IG-PCCL (PeCLET) in the HR plant configuration leads to a reduction in the reactors number of 5 (from 14 to 10) with respect to the IG-CLC case. This potentially leads to a decrease in the investment cost of the CL of about 30%.
The Base case plant configurations (PeCLET) requires, among all the power plants presented in this work, the lowest number of reactors (3), leading to a potential investment costs saving of about 70% compared to the IG-CLC case.

Chapter 7

Conclusions

The scope of this work was to study the integration of the CL PeCLET process with an IGCC plant (IG-PCCL), to individuate the most important operating parameters and analyze their influence on the PeCLET process, as well as to propose layout schemes of the entire plant.
The most important characteristic of the PeCLET process is the production of a hydrogen rich stream that is used as fuel in the gas turbine. The hydrogen stream is produced in the oxidation reactor of the CL island, by the oxidation reaction of the metal oxide with the steam extracted from the steam turbine.
This study was mostly carried out with simulations by means of the proprietary computer code GS (Gecos, 2013).
During the simulations of the IG-PCCL the primary coal feed and the syngas produced by its gasification was kept constant in flow rate and composition. The sizes of turbo-machines used are comparable with that of a conventional IGCC cycle: the IG-PCCL considered produces a net electric power of 350 MWe with a thermal input equal to 860 MWth which results in a net electrical efficiency slightly more than 40%.
The most important operating parameters has come out to be the air-to-steam ratio in the feed of the CL oxidation reactor.
The air-to-steam ratio, whose influence was studied mostly by means of the "$\%O_2$ from air" parameter as explained in chapter 4 of this thesis, is substantially set by the choice of the Oxygen Carrier (OC) through the stoichiometry and the thermodynamics of the reactions involving the OC.
The OC is therefore a key parameter not only for the feasibility of the CL reaction system, but also for the feasibility and the design of the entire power plant.

7.1 Comparison between the Base case plant operated with Fe and the HR plant operated with FeO

In this work, two main power plant configurations were proposed: the Base case plant, result of a direct integration of the PeCLET process in the plant, and the HR plant, where a heat removal phase was added to the typical reactor work cycle. In the HR plant, in fact, an additional heat removal phase from the reactors is introduced to pre heat a large amount of air extracted from the gas turbine.
The performance of these two possible configurations were studied and the results are reported in the diagram below (**Errore. L'origine riferimento non è stata trovata.**), where the net electrical efficiency of the plants is shown as a function of the $\%O_2$ from air fed to the oxidation reactor.

From this diagram two distinct zones can be identified: the first, at low $\%O_2$ from air, where the efficiencies of the two power plants are comparable and both can be considered feasible; the latter zone, at high $\%O_2$ from air, where the choice of the HR configuration is advisable because much more competitive than the base case configuration in terms of electrical efficiency.

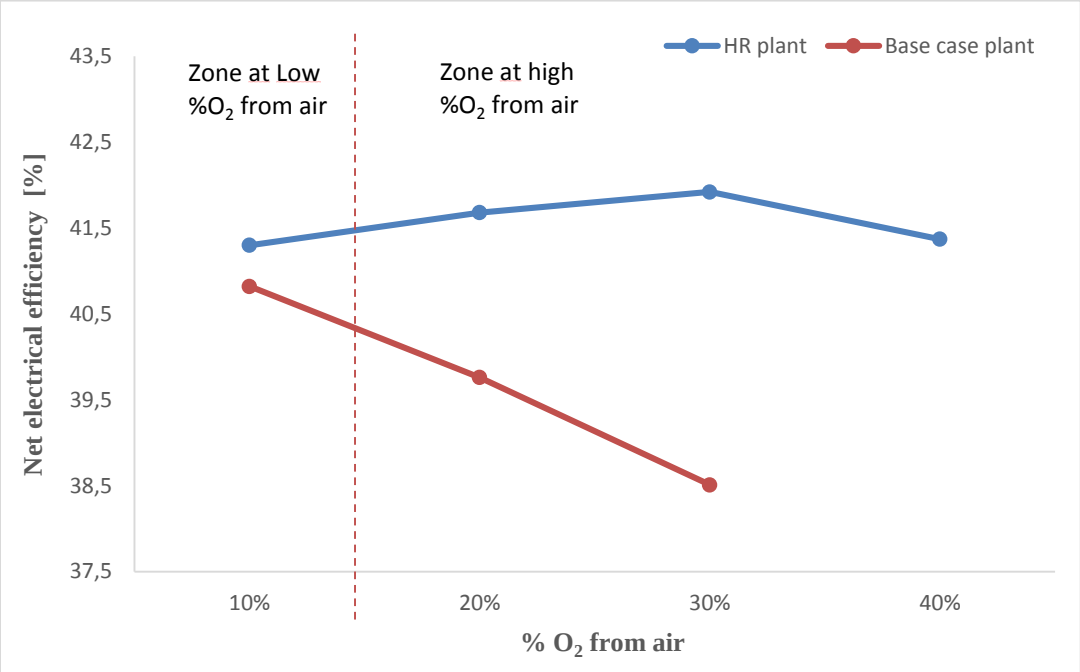

Figure 7.1: Comparison on the $\%O_2$ from air response, between the base case plant and the HR plant.

Also in the zone at low $\%O_2$ from air, the efficiency of the HR plant is slightly higher than the Base case plant, around 41.5% vs. 40.8%.
Nevertheless, the integration scheme of the Base case plant is simpler and a lower number of reactors is needed, with a significant saving in the investment cost.
Hence, from the analysis the Base case plant emerged as the preferable choice for low $\%O_2$ from air; its advantages are here below summarized:

- More simple plant integration: conceptually the PeCLET process can be inserted as it is in the IGCC plant. The syngas feeds the CL unit which, in turn, provides the hydrogen flow to the power island.
- The connection between the CL reactors and the GT is less strict (no large flow rate of air GT compressed air is fed to the reactor and then back to the turbine). As example, the operating pressure of the CL unit and of the GT can be separately optimized.
- Significant decrease in the number of reactors needed in the process. This leads to a considerable potential reduction of the plant costs.

The parameter $\%O_2$ from air is substantially set by the OC. It is important to underline that the oxygen carrier suitable for the PeCLET process, in addition to the typical material

properties needed in the CL systems, shall be able to react with the steam during the oxidation phase in order to produce a hydrogen flow.
In this work a preliminary study on iron-based oxygen carriers was also carried out. Two possible states of maximum oxidation of the iron were considered: "Fe" which low $\%O_2$ from air (11.1%) and "FeO" with a $\%O_2$ from air equal to 33.3%.
Therefore, in the case FeO is used, the HR plant is the only feasible choice; while, when the process is operated with Fe both the plant configurations are valid.
The use of Fe as most reductive state of the iron leads to the following advantages:

- The intrinsic possibility of using the Base case plant configuration.
- When the Base case plant is operated with Fe, the CL reduction reaction can be accomplished at high temperature, with the resulting advantages in the kinetics (especially for the reaction between CO and the iron-oxide).

In conclusion, the Base case plant operated with "Fe" has emerged as the better choice for the IG-PCCL plant, combining high efficiency and potentially limited investment cost.
Nevertheless all the configurations proposed in this work should be considered, since a further study on the reaction mechanism inside the reactor is needed for a complete feasibility analysis on the integration of the PeCLET process with IGCC plants.
The analyses on the OC and the PBRs carried out in this work are in fact preliminary and cover only stoichiometric and thermodynamic matters through a 0D model for the reactor. In order to accomplish a more complete feasibility study on the process, a 1D model which takes into account the kinetics is necessary. This analysis was not in the scope of the present work.
Moreover, this work suggests that the OC research direction should be addressed towards the material which can guarantee a low $\%O_2$ from air. In this way, a simpler and less expensive PeCLET process integration can be accomplished.
On the other hand, if the techno-economic feasibility of this material was not confirmed, the energy engineering would have to study carefully the plant at higher $\%O_2$ from air to find an efficient and a solution for the integration as cheap as possible.

7.2 Comparison between the PeCLET process and the CLC technology

The PeCLET process has been proved as a promising CCS technology. As typical of the CL system, the CO_2, derived from the oxidation of the carbon present in the primary fossil fuel, is captured without large penalties in the efficiency, and the correspondent SPECCA indexes reach promising value.
The PeCLET was proposed as an alternative to the CLC technology. The differences in the integration of these two concepts inserted in IGCC plants, are here below presented:

- The OC suitable for the PeCLET process has to provide fast kinetics during the reduction operation as for the CLC, but it has to be selected and designed also to

accomplish a proper conversion during the oxidation stage by reacting with O_2 and H_2O, in order to produce a hydrogen-rich flow. In the CLC the metal oxide oxidation was accomplished only by air.

- In the PeCLET process, the main energy output of the CL reactors is a diluted hydrogen stream which is used as fuel by the GT.
  The CLC technology does not provide any fuel stream, but a compressed nitrogen flow at high temperature (1200°C) which can be directly expanded in the GT expander.
- The reactors work at intermediate temperature with the following two related effects:
  - The importance in the design of the reactors, which has to accomplish the reaction processes at lower temperature than in the CLC technology. Possible problems of slow kinetics have to be managed.
  - On the other hand, the costs of the CL unit components (reactors, switching valve system and piping) can be potentially reduced.
- The operating conditions of the CL process are partly released from the gas-turbine. In the CLC technology the Turbine Inlet Temperature (TIT) was limited by the material resistance inside the reactors to 1200°C, affecting negatively the overall plant efficiency.
  In the PeCLET process, due to the hydrogen production in the CL unit, the TIT can reach higher value (the maximum achievable by the modern turbo-machines).
  The Base case plant offers an additional advantage: the lack of heat removal phase allows to optimize separately the operating pressure of the CL unit and GT compressor ratio. The CL island is therefore pressurized up to 36.1 bar, in order to reduce the consumptions of the CO_2 compression. On the other hand, the GT compressor ratio can be freely set to the value that maximizes the net electrical efficiency of the plant.

7.3 Further exploitation of the PeCLET concept

The PeCLET concept can be exploited in further processes: mainly in the ammonia synthesis and for power production with CO_2 capture through its integration with a Natural Gas Combined Cycle (NGCC).

7.3.1 PeCLET process integrated with a Natural Gas Combined Cycle

The application of the PeCLET process with a NGCC plant seems to be promising. Its potentiality will be briefly described here below.
In this work, the PeCLET process fed with syngas was studied by an equivalent system where only two kind of reaction occur: CO and H_2 oxidation reaction by air, and WGS (26). Both this reaction are exothermic and therefore the hydrogen production was always followed by a release of heat. The higher the air-to-steam ratio, the higher the production of heat instead of hydrogen. It is important to underline that the heat production is less

easily converted in an efficient way compared to the H2-rich flow (which can be directly used as fuel in the GT).
As regards the natural gas (here assumed to be composed only by CH_4), the equivalent system of the CL unit can be based on two main reactions: the oxidation of CH_4 by sub-stoichiometric air and the steam reforming:

$$CH_4 + H_2O \rightarrow CO + 3H_2 \qquad \Delta H^0_{298} = 206\ kJ/mol \tag{7.1}$$

$$CH_4 + 2O_2 \rightarrow CO_2 + 2H_2O \qquad \Delta H^0_{298} = -802\ kJ/mol \tag{7.2}$$

The steam reforming is an endothermic reaction and this leads to an important consequence: the heat (or part of the heat) released by the oxidation reaction is used in the steam reforming for the hydrogen production. Hence, the hydrogen production is maximized with respect to the production of heat.
As a result, at constant air-to-steam ratio, the PeCLET process fed by natural gas obtains higher H_2 production and less heat released compared to the syngas feed case. Hence, the base case plant (considered the preferable plant choice), could be used until higher value of the $\%O_2$ from air.
In conclusion, although for a full assessment of the NGCC plant integrated with the PeCLET process a complete thermodynamic analysis of the power cycle and a study on the reaction mechanism inside the reactor is needed, this configurations seems to offer potential advantages, due to the higher hydrogen productivity respect to the production of heat inside the CL unit.

7.3.2 Ammonia production

The PeCLET concept can be an alternative to the nowadays ammonia production with a pre-combustion CO_2 capture concept based on the use of several reactors and separation/conversion steps, which lead to efficiency penalties.
The H_2/N_2 gas mixture with the required composition, which is needed as input of this process, can be directly produced in the CL island and fed to the ammonia synthesis unit.
Using a proper steam to air ratio in the oxidation stage, it is indeed possible to produce the hydrogen flow with H/N equal to 3, as it is required for the ammonia synthesis, without any other separation/conversion step.

Index of figures

Nomenclature

Cp	Heat capacity at constant pressure [J/kg/K]
D	Diameter [m]
d_p	Particle diameter [m]
ΔH_r^0	Standard enthalpy of reaction [kJ/mol]
L	Height of the reactor [m]
M	Molecular weight [kg/kmol]
P	Pressure [bar]
T	Temperature [°C]
v	Velocity [m/s]
W_{hf}	Heat front velocity [m/s]
w_{Rrf}	Reaction front velocity [m/s]
α	Porosity
ε	Void fraction of the bed
ζ	Stoichiometric coefficient
μ	Viscosity [kg/m/s]
ρ	Density []kg/m^3]
τ	Duration of the single phase [s]
Φ	Sphericity
ω	Mass fraction

Superscript and Subscript

g	Gas phase property
s	Solid phase property
RF/HF	Reaction front/Heat front
act	Active material in the OC
in	Initial condition

Acronyms

AGR	Acid Gas Removal
AR	Air Reactor
ASU	Air Separation Unit
CCS	Carbon Capture and Storage
CGE	Cold Gas Efficiency
CLC	Chemical Looping Combustion
DEA	Di-Etanol-Ammina
FGD	Flue-Gas Desulfurization
FR	Fuel Reactor
GT	Gas Turbine
HP/IP	High/Intermediate Pressure
HR	Heat removal
HRSG	Heat Recovery Steam Generator
IGCC	Integrated Gasification Combined Cycle
LHV	Lower Heating Value
MDEA	Metil-Di-Etanol-Ammiona
NGCC	Natural Gas Combined Cycle
OR	Oxidation Reactor
PeCLET	Pre-Combustion Chemical Looping Efficient Technology
SH	Super Heater/Heated
ST	Steam Turbine
TIT	Turbine Inlet Temperature
TOT	Turbine Outlet Temperature
WGS	Water Gas Shift

Bibliography

[1] L. Treut, R. Somerville, U. Cubasch, Y. Ding, C. Mauritzen, A. Mokssit, T. Peterson, M. Prather, D. Qin, M. Manning, Z. Chen, M. Marquis, K. B. Averyt, and M. Tignor, "Historical Overview of Climate Change Science," in *Earth*, vol. Chapter 1, no. October, S. Solomon, D. Qin, M. Manning, Z. Chen, M. Marquis, K. B. Averyt, M. Tignor, and H. L. Miller, Eds. Cambridge University Press, 2007, pp. 93–127.

[2] S. Consonni, G. Lozza, G. Pelliccia, S. Rossini, and F. Saviano, "Chemical-Looping Combustion for Combined Cycles With CO2 Capture," *J. Eng. Gas Turbines Power*, vol. 128, no. 3, p. 525, 2006.

[3] R. Naqvi and O. Bolland, "Multi-stage chemical looping combustion (CLC) for combined cycles with CO2 capture," *Int. J. Greenh. Gas Control*, vol. 1, no. 1, pp. 19–30, Apr. 2007.

[4] V. Spallina, M. C. Romano, P. Chiesa, and G. Lozza, "Integration of Coal Gasification and Packed Bed CLC process for High Efficiency and Near-zero Emission Power Generation," *Energy Procedia*, vol. 37, no. 1, pp. 662–670, 2013.

[5] a. Cuadrat, a. Abad, F. García-Labiano, P. Gayán, L. F. de Diego, and J. Adánez, "Relevance of the coal rank on the performance of the in situ gasification chemical-looping combustion," *Chem. Eng. J.*, vol. 195–196, pp. 91–102, Jul. 2012.

[6] T. Mattisson, A. Lyngfelt, and H. Leion, "Chemical-looping with oxygen uncoupling for combustion of solid fuels," *Int. J. Greenh. Gas Control*, vol. 3, no. 1, pp. 11–19, Jan. 2009.

[7] J. Adánez, A. Abad, F. García-labiano, P. Gayán, and L. F. De Diego, "Progress in Combustion and Reforming Technologies . A review .," vol. 38, pp. 215–282, 2012.

[8] E. Martelli, "Dimensionamento e gestione di reattori a letto fisso per sistemi di Chemical Looping Combustion in impinati di grande taglia," 2012.

[9] M. V. S. A. V.Spallina, H.P. Hamers, F. Gallucci, "Process Intensification for Sustainable Energy Conversion, Chapter 5: Chemical Looping Combustion for Power Production,." 2014.

[10] A. Lyngfelt, T. Mattisson, B. Epple, and J. Ströhle, "Part 5 Chemical Looping for CO2 Separation," in *Efficient Carbon Capture for Coal Power Plants*, D. Stolten and V. Scherer, Eds. Weinheim: Wiley-VCH, 2011, pp. 475–524.

[11] E. Jerndal, T. Mattisson, and A. Lyngfelt, "Thermal Analysis of Chemical-Looping Combustion," *Chem. Eng. Res. Des.*, vol. 84, no. 9, pp. 795–806, Sep. 2006.

[12] H. Leion, A. Lyngfelt, M. Johansson, E. Jerndal, and T. Mattisson, “The use of ilmenite as an oxygen carrier in chemical-looping combustion,” *Chem. Eng. Res. Des.*, vol. 86, no. 9, pp. 1017–1026, Sep. 2008.

[13] L. Fan, *Chemical Looping Systems for Fossil Energy*. John WIley & Son Inc., 2010, p. 420.

[14] J. Adanez, A. Abad, F. Garcia-Labiano, P. Gayan, and L. de Diego, “Progress in Chemical-Looping Combustion and Reforming technologies,” *Prog. Energy Combust. Sci.*, vol. 38, no. 2, pp. 215–282, Apr. 2012.

[15] S. Noorman, “Packed bed reactor technology for chemical-looping combustion.” Enschede, The Netherlands, 17-Sep-2009.

[16] V. Spallina, F. Gallucci, M. C. Romano, P. Chiesa, G. Lozza, and M. van Sint Annaland, “Investigation of heat management for CLC of syngas in packed bed reactors,” *Chem. Eng. J.*, vol. 225, pp. 174–191, Jun. 2013.

[17] H. P. Hamers, M. C. Romano, V. Spallina, P. Chiesa, F. Gallucci, and M. V. S. Annaland, “Comparison on process efficiency for CLC of syngas operated in packed bed and fluidized bed reactors,” *Int. J. Greenh. Gas Control*, vol. 28, pp. 65–78, Sep. 2014.

[18] Y. Hu, *CO2 capture from oxy-fuel combustion power plants*. 2011.

[19] V. Spallina, F. Gallucci, and M. V. A. N. S. Annaland, “Pre-combustion packed bed chemical looping (PCCL) technology for high efficient H 2 -rich gas production processes,” pp. 1–12, 2014.

[20] P. Chiesa, G. Lozza, a Malandrino, M. Romano, and V. Piccolo, “Three-reactors chemical looping process for hydrogen production,” *Int. J. Hydrogen Energy*, vol. 33, no. 9, pp. 2233–2245, May 2008.

[21] A. Murugan, A. Thursfield, and I. S. Metcalfe, “A chemical looping process for hydrogen production using iron-containing perovskites,” *Energy Environ. Sci.*, vol. 4, no. 11, p. 4639, 2011.

[22] P. Chiesa, G. Lozza, and L. Mazzocchi, “Using Hydrogen as Gas Turbine Fuel,” *J. Eng. Gas Turbines Power*, vol. 127, no. 1, p. 73, 2005.

[23] M. Gazzani, P. Chiesa, E. Martelli, S. Sigali, and I. Brunetti, “Using Hydrogen as Gas Turbine Fuel: Premixed Versus Diffusive Flame Combustors,” *J. Eng. Gas Turbines Power*, vol. 136, no. 5, p. 051504, Jan. 2014.

[24] Gecos, “Gas – Steam Cycle Simulation Code http://www.gecos.polimi.it/software/gs.php.” 2013.

[25] P. Chiesa and E. Macchi, “A Thermodynamic Analysis of Different Options to Break 60% Electric Efficiency in Combined Cycle Power Plants,” *J. Eng. Gas Turbines Power*, vol. 126, no. 4, p. 770, 2004.

[26] EBTF, “European best practice guidelines for assessment of CO2 capture technologies,” 2011.

[27] IEA GHG, “Oxy Combustion Processes for CO2 Capture from Power Plant,” 2005.

[28] FP7 Democlock, “http://www.sintef.no/Projectweb/DemoClock/.” .

[29] S. Noorman and M. van Sint Annaland, “Packed Bed Reactor Technology for Chemical-Looping Combustion,” *Ind. Eng. Chem. Res.*, vol. 46, no. 12, pp. 4212–4220, Jun. 2007.

[30] W. Zhang, J. Zhang, Q. Li, Y. He, B. Tang, M. Li, Z. Zhang, and Z. Zou, “Thermodynamic analyses of iron oxides redox reactions,” in *8th Pacific Rim International Congress on Advanced Materials and Processing 2013, PRICM 8*, 2013, vol. 1, pp. 777–789.

[31] C. Liang-shih Fan, Shriniwas, “The Ohio State University, Ed., ch. 13.” .

[32] B. E. P. R. C. R. John M. Prausnitz, *The properties of gases and liquids. McGrau-Hill, 1988, ch. 9.* 1988.